7

EXPERIMENTAL GEOMAGNETISM

Experimental geomagnetism deals with experimental observations and their potential applications of palaeomagnetic and environmental magnetic investigations. Palaeomagnetism is a specialized study, which has provided positive evidence of continental drift and development of the hypothesis of plate tectonics. The other major contributions relate to understanding of the generation of EMF, palaeointensity, relative movements of continental blocks, concept of tectonostratigraphic terrains and magnetostratigraphy as a dating tool. All these varied research activities require the development and use of extremely sensitive instruments.

Palaeomagnetic studies, therefore, are of special significance to students of geology and geophysics. The deciphering of India's flight northwards is largely dependent on the acquisition of palaeomagnetic data and their interpretations. The first section covers theoretical aspects as well as experimental details of both rock magnetism and palaeomagnetism. Few examples of application of these techniques are reviewed enabling to understand apparent polar wandering path of the continents, how the magnetic minerals register the palaeolatitude and pole position and how one can de-convolute them in the laboratory.

Initially, the study of magnetism implied certain standard types of measurements such as magnetic susceptibility and remanent magnetization. With the progress in understanding of microscopic processes in natural materials of soils, sediments and rocks, the study of magnetism has considerably diversified leading to new exciting areas like the environmental geomagnetism. It is in this context that the second section of this chapter is devoted to discuss exclusively the rock and environmental geomagnetism, which constitutes one of the major subjects in modern Earth Sciences. The environmental geomagnetism, particularly for the Quaternary studies (last 2 Ma), is considered to be a powerful technique to ascertain the past climate, erosion and pollution. Results obtained from potential applications of magnetic properties or

N. Basavaiah, *Geomagnetism*

parameters through investigations of such subjects as the magnetic and chemical constitution of different rocks, sediments and waters from streams and lakes, the measurements of impurities in the atmosphere and water bodies and the reconstruction of environmental and climate change, are discussed in detail here.

7.1 PALAEOMAGNETISM AND GEOMAGNETIC FIELD IN GEOLOGICAL PAST

Even a weak Earth's magnetic field (50 μT) can make a lasting impression on rocks, baked materials and sediments. The fossil magnetism naturally present in a rock is termed the natural remanent magnetization (NRM), whose NRM directions help in recovering EMF history. This forms the subject matter of palaeomagnetism, which started to take up shape in the early 1950's. By 1960, however, it evolved into two separate disciplines referred to as rock magnetism and palaeomagnetism. By producing information about the location and orientation of continents relative to the Earth's magnetic pole, palaeomagnetism has played a significant role in understanding the Earth processes, particularly with regard to continental drift, polar wandering and the development of plate tectonics. As currently practised, palaeomagnetism includes topics related to age dating, stratigraphy and magnetic anomaly interpretation together with traditional topics like tectonics, polar wander, and historical evolutionary EMF studies.

Palaeomagnetic studies suggest EMF has frequently changed and the polarity reversals occurred 24 times during the past 4.5 Ma. It is tentatively concluded that a complete reversal of the EMF takes place in 10^3–10^4 years. The changing pattern of convection currents in the Earth's outer core is generally considered the reason for polarity reversals.

An approximate coincidence of the magnetic axis with the axis of rotation is seen to exist. Accordingly, when there is dislocation of magnetic poles, there is a change in the position of the Earth, and its outer layers with respect to the axis of rotation. Thus, the dislocation of magnetic poles takes place simultaneously with the dislocation of the geographical position, and dislocation of the geographical location influences the climatic regimes of the Earth. The slow variation of EMF at any given place, and also a slow shift in the geographical position of magnetic poles, which are roughly cyclic with a period of ~500 years, is called secular variation. By means of repeated magnetic observations from time to time made at any stations, and MOs, maps and tables can be prepared showing the annual rate of change of geomagnetic field.

I. Direct Measurements and MOs

Magnetic observatory measurements reveal EMF as a transient phenomenon. The field is subject to periodic fluctuations in direction and intensity with rates of change varying from second to thousands of years. At present, the average

annual value of the field is undergoing a regular change known as secular variation (SV), leading to a decrease in its total intensity and inclination. The first known instrumental measurement of declination was carried out by the Chinese, which was far from comprehensive. Global chain of MO measurements is used to determine EMF's past and future changes. Spherical harmonic models are created using data from MOs, satellites and ancient marine logs. There are now models based on direct measurements of geomagnetic field, e.g. London and Paris MOs that extend from ~400 yrs ago to the present (Fig. 7.1). This time span is well short of that required to obtain a valid time-averaged magnetic field, the characteristics of which must be incorporated into any valid theory for the origin of the geomagnetic field.

When SV of the geomagnetic field is averaged out over several thousand years, the field can be modelled as a geocentric axial dipole, i.e. a dipole at the centre of the Earth aligned along the Earth's rotational axis. If this was true throughout the geological past, then palaeomagnetic measurements can be related to geographic position, provided that results are averaged over a sufficiently long time range. This assumption is fundamental to the application of palaeomagnetism to geological and geophysical problems, and is therefore important to examine the characteristics of SV in the geological past and determine its effects on palaeomagnetic measurements. The two techniques, which are used to investigate the SV during pre-observational times, are: (1) archaeomagnetism and (2) palaeomagnetism.

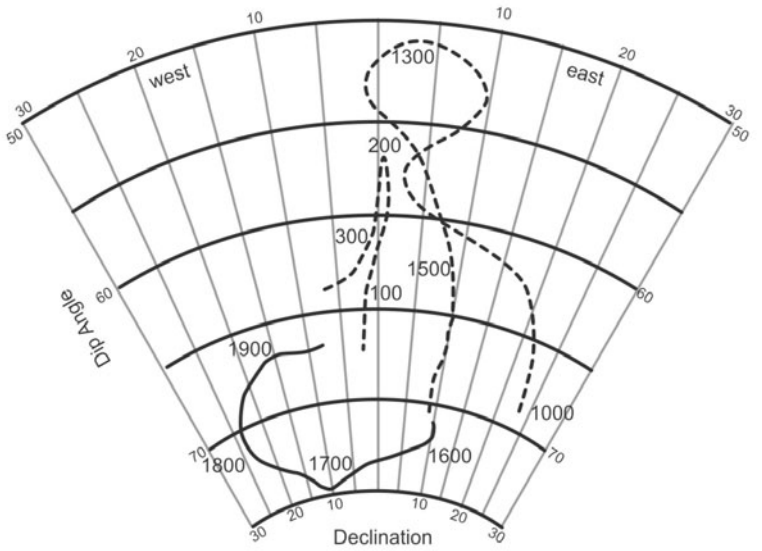

Figure 7.1. A stereographic projection of secular variation of declination and inclination since 1000 at London from observatory (solid curve) and archaeomagnetic (dashed curve) data (*courtesy:* Jacobs, v1, 1987).

II. Historical Indirect Measurements and Archaeomagnetism

As observatory studies of the geomagnetic field only extend back for 400 years, it is only relatively recent 'magnetized' material that can be dated by direct comparison with observatory record. The extension of such records over archaeological time, therefore, requires archaeomagnetic observations based on well-dated magnetized materials. Measurements of the SV during historic time are made using archaeomagnetism; the palaeomagnetism of archaeological specimens. Pottery, kilns and pots acquire thermoremanent magnetization (TRM) parallel to the geomagnetic field existing at the time they are fired. The TRM is the magnetization acquired by magnetic minerals as a result of cooling from a higher temperature ($>T_C$ of the mineral than the normal temperatures). Such magnetization is stable against mechanical, thermal and other external influences. If the objects are found at the actual position of firing, then both the declination and inclination of the palaeomagnetic field can be determined. If the objects are pottery or bricks, not in the position of firing, then only the inclination can be found. By dating the hearths, and hence the magnetizations archaeologically or by radiocarbon methods on associated material, archaeomagnetic measurements yielded results about the properties of the geomagnetic field during the last 30,000 years and a SV pattern up to ~2,000 years for southern India (Fig. 7.2).

Since archaeological materials normally record events such as firing at a specific point and time, most archaeomagnetic records are intermittent in both space and time. Over the past few thousand years, many world civilizations have produced artifacts such as kilns, helping to record the EMF at the place, and time they are baked (Fig. 7.2). However, it is not possible to extend the observations back in geological time using artifacts because such well dated materials closely spaced in time are not available.

III. Geological Past Indirect Measurements and Palaeomagnetism

The history of geomagnetic field can be extended into the geological past through the study of NRM, since natural material can record its ancient direction and intensity. If one can find such materials, reconstruct their palaeo-orientation, measure their remanent magnetization, and date the time of acquisition of the magnetization, then one can trace the geomagnetic field in the past. Palaeomagnetists have assembled a remarkable picture of the ancient geomagnetic field using such fossil remanent magnetizations from many parts of the world, and for ages ranging back to those of the very oldest rocks found on Earth. The materials studied are the youngest lava sequence, sedimentary sequence and rocks.

(i) Remanent magnetism of lava sequences: Volcanic rocks are heated well above the T_C, so the magnetization is free to align with the external magnetic

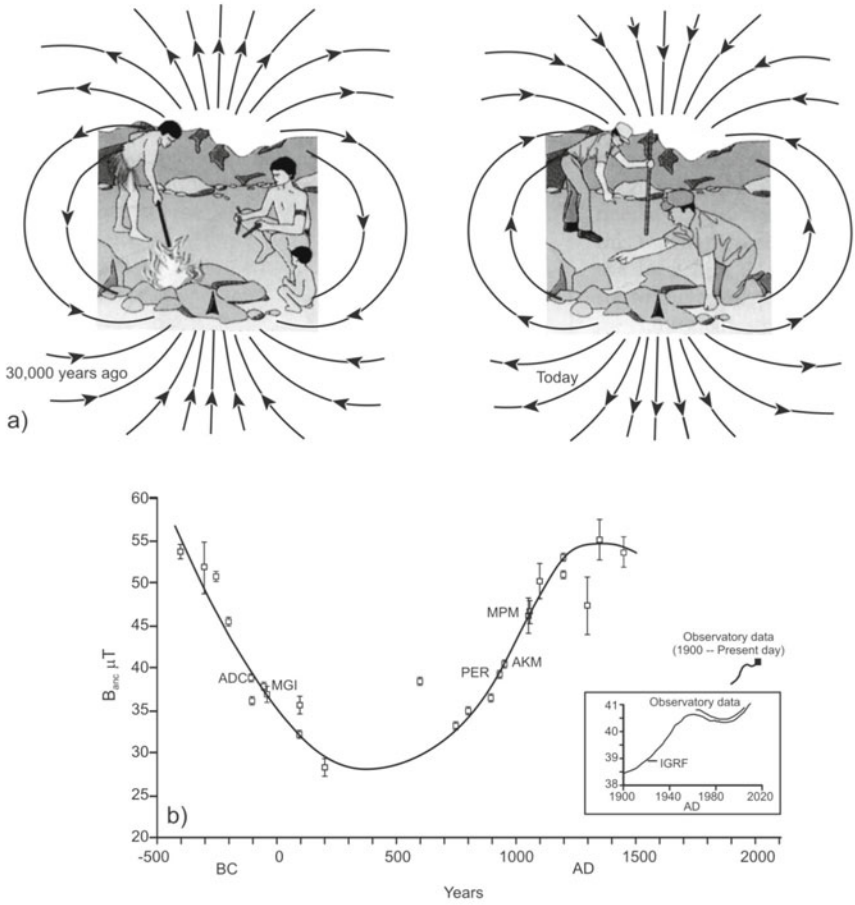

Figure 7.2. (a) Sketch showing reversed and normal patterns of Earth's magnetic field over 30 ka and present times (Press and Siever, 2002). (b) The Tamilnadu palaeointensity secular variation curve estimated using Thellier and modified Shaw methods. Error bars give the standard error of the mean for each site. Inset shows yearly mean intensity of EMF calculated from Annamalainagar and Pondicherry MOs data from 1964 to 2005 together with IGRF model since AD 1900. The horizontal dashed line indicates the present day field intensity (*courtesy:* Ramaswamy and Duraiswamy).

field, and retains it as the rock cools. The processes by which lavas become magnetized are well founded in the theory of TRM. Secular variation of the geomagnetic field may be reflected in small differences in the remanent magnetism of sequential lava flows. The results of measurements on historically dated lavas are used in conjunction with archaeomagnetism for the extension of observatory data. Dating lava flows of the remote past involve errors, which are large in comparison with the SV time scale; therefore in such cases only the sequence of geomagnetic directions can be determined.

(ii) Remanent magnetism of sediment sequences: The magnetic particles of sedimentary rocks align themselves with their magnetic axis parallel to the ambient magnetic field during their process of deposition, and give rise to detrital remanent magnetization (DRM). The magnetization acquisition process is still not well understood, and the role of the complex interplay of processes occurring during deposition, water-sediment interface processes, burial, and compaction requires further analysis (Fig. 7.3a). The magnetic polarity positions of sediments (normal and reversed) represent changes in the direction of EMF at the time of deposition of particles of the sediments. The speed of deposition of marine sediments is estimated to be 0.5 to 3.0 mm/ka. If the rate of sediment deposition is slow, then the DRM of a small sediment sample indicates the geomagnetic field at one instant on the SV timescale. If the deposition is continuous, SV may be represented by an upward variation in remanent magnetism of the sediment sequence. For most sedimentary rocks, as with lava flows, it is difficult to establish an accurate timescale. In the case of varves, however, it is generally assumed that one pair of laminae correspond to the annual deposit. Studies of lake sediments produce palaeomagnetic picture extending the historical documented observations of the geomagnetic field further back in time. The palaeomagnetic directions have discovered field reversals of SVs, possessing periods of 10 ka, and also revealed the essentially dipolar character of the geomagnetic field throughout the time span covered by the geological record. Correlation of $\delta^{18}O$ records with the marine isotopic stages can provide high-resolution age control through a reversal. Such records provide information regarding the age, timing, and duration of polarity transitions.

(iii) Remanent magnetism of rocks and origin of palaeomagnetism: Rocks of all ages with ancient fields 'fossilized' into them are significant sources of palaeomagnetism. The fact that rocks acquire the ambient magnetic field at the time of their formation was recognized by Gilbert in 1600. When solidification process passes through temperature ranges below T_C, magnetic minerals acquire permanent magnetization in the direction of the ambient field (Chapter 2). Magnetite, for instance, acquires magnetization below its T_C (Fig. 7.3b), and this is the 'spot reading' of the Earth's field. This is because the time needed for magnetic minerals to crystallize out of the magma through different temperature ranges is short compared to the time needed for significant changes to occur in the core-generated main field. A series of such extrusive rocks give a series of 'spot readings' of the field. In general, the field recorded this way is the geomagnetic field at that site, and the differences noted between individual 'spot readings' are a measure of the amount of change in the geomagnetic field.

Some researchers have inferred correlations between changes in Earth's orbital parameters, and geomagnetic field variations. The outstanding question concerns the very ancient geomagnetic field. The field is known to have existed for 3.5 Ga, suggesting it is continuously regenerated. However, polarity reversals are documented from as early as 1.5 Ga.

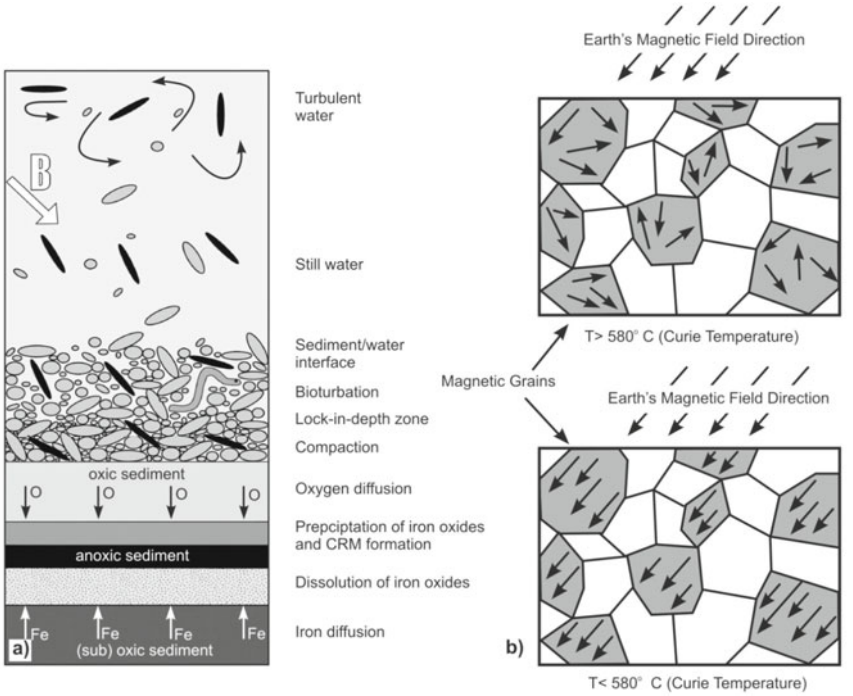

Figure 7.3. (a) Magnetization resulting from sedimentation process referred to as depositional or detrital remanent magnetization (DRM), and chemical remanent magnetization (CRM). (b) Above the Curie point (here for magnetite), atoms take random directions unlike below the Curie point in the presence of an external magnetic field, where domains line up (http://www.phys.uu.nl/~sommer/master/geopotential%20fields/).

IV. The Pioneers Who Shaped Palaeomagnetism

Humboldt was the first to describe magnetism of rocks from a serpentinite outcrop in Germany. Later in 1848, Joseph Fournet wrote a summary entitled 'Glimpses on the magnetism of ores and rocks and on the causes of some anomalies in terrestrial magnetism' providing all experimental procedures and description of magnetic ores and rocks. He prognostically suggested avoiding crystalline rocks in favour of limestone terrain to locate the MO since they affect the instruments and the readings. Delesse experimentally analyzed the magnetism of rocks and minerals, and defined for the first time in 1849, the notion of coercivity. He found coercivity depending on chemical composition, and was zero for soft iron, which increased through the addition of O, S, P, Si, and C to iron. He also deciphered shock sometimes increased magnetic power, and asserted recent lava flows are uniformly magnetized in alignment to the local EMF.

Macedonio Melloni built a very sensitive astatic magnetometer, and established permanent magnetization of 108 different species of volcanic rocks.

According to him, to study the intensity of EMF, the magnetic state of a specimen is important, and not the amount of material. He also explored the origin of TRM by heating and cooling fragments of lava to propose in 1853, 'the general law of permanent magnetization of lavas'. Later on, Sidot in 1868 announced that the direction of magnetization coincides with that of the applied field, and not the crystallographic axes of the material.

Giuseppe Folgheraiter followed Melloni, and showed that Melloni's inferences on Vesuvias lavas can be extended to other rock types also. He in 1894 was the first to distinguish between permanent and induced magnetization, and also first to recognize viscous remanent magnetization (VRM). He showed that on heating, material remagnetizes and transforms hematite to magnetite. He also laid down the foundations of archaeomagnetism by displaying the variations of inclination between 800 BC and 100 AD from Greek and Etruscan vases.

Later, Bernard Brunhes and Pierre David worked on natural bricks baked by overlying lava flow to find their magnetization to be homogeneous, but different from the recent field orientation at the site. This magnetization, they believed to be the EMF at the time when the volcanic flow transformed the clay into brick. Brunhes and David then turned their attention to lavas, since baked clays besides being rare were found to be strongly magnetic, had similar directions, and gave less homogeneous results. From a Royat quarry, they discovered two flows sandwiching a clay layer, wherein the flow at the bottom had a different direction from the overlying clay and flow layer. David also studied trachyte-made flagstones at the temple of Mercury on top of Puy-de-Dome, and found from several samples taken from the same slab dissimilar D, but identical I, helping locate the quarries from where the slabs had been extracted throwing up an archaeological application.

Brunhes discovered magnetic reversals in 1905, when he studied together: (1) an outcrop of basalt flow, and (2) baked clay under that flow near Pontfarein in Cantal, France, to find both having same negative I of –75°. The rocks collected some 100 m away from them, though had different magnetization. He reasoned that the long horizontal layer of metamorphic clay could not have turned upside down, because the lava that cooked it would have found below, and not above, leading conclusively to the concept of magnetic reversals.

Pierre Curie discovered in 1895 that magnetic susceptibility varied inversely with absolute temperature. The fact that TRM in lavas was much more intense than isothermal remanent magnetization (IRM), was discovered in 1909 by George Allen. Paul Langevin published his theory of paramagnetism in 1910, and the theory of ferromagnetism was published in 1911 by Pierre-Ernst Weiss. Further in 1926, Mercanton insisted on the stability of reversed magnetizations for past geological ages in both the hemispheres leading to the understanding of magnetic poles undergoing 'enormous displacements'. This is the first clear statement that workers in the field of palaeomagnetism could demonstrate and measure polar wander, and/or continental drift. He also described the first

magnetostratigraphic section of three reversals in Tertiary lavas. Raymond Chevallier determined SV of D in Sicily based on some 100 blocks from 10 distinct lava flows for the time-frame between 1200 and 1900 AD. Motonori Matuyama of Japan showed for samples from Manchuria and Japan that their magnetizations were arranged in two groups, a Pleistocene being normal (N), and pre-Pleistocene, reversed (R). In 1933, Johann Koenigsberger showed the importance of magnetite and maghemite as carriers of natural remanent magnetization (NRM), and proposed the first theory for TRM that led to formulation of techniques to ascertain confidence in palaeomagnetic measurements.

Emile Thellier's lasting contribution to rock and palaeomagnetic laboratory practice was the development of cleaning methods, and palaeointensity determinations which revealed the differences in behaviour of IRM versus TRM. Thellier used astatic magnetometer to measure the induced and remanent magnetization of baked and unbaked clays as far back as 1932. He also was the one to propose his famous sampling technique for large rocks or archaeomagnetic samples using a cover or 'hat' of Plaster of Paris. He also established the existence of VRM in basalts. Lake sediment studies of palaeosecular variation were undertaken by many scientists like Gustaf Ising who found SVs of 10° in D, and 20° in I when studying lake varves in Sweden dated from a period of ~350 years. Juliette Roquet, in 1954, performed the first systematic study of grain size dependence of TRM. Louis Néel wrote his first paper on ferromagnetism in 1949, and in the same year, John Graham introduced field stability tests, like fold and conglomerate tests. Along the same time, Graham and Torreson developed a very sensitive spinner magnetometer able to measure very weak magnetization.

V. Sampling, Laboratory Experiments and NRM Measurements

The palaeomagnetic method involves: (1) collecting oriented samples, (2) determining their direction of remanent magnetization, (3) confirming the stability of remanence, (4) establishing ChRM, (5) ascertaining characteristic components related to the EMF direction during rock formation, and (6) determining age of ChRM from established palaeomagnetic data with reliable radiometric absolute ages.

(i) Primary and secondary remanence: When magnetic grains alter by oxidation to, for example, hematite, or by oxidation and hydration to minerals such as goethite, the original magnetization is replaced by a later or 'secondary' magnetization in a process called remagnetization. Often, such alteration or weathering leaves some original magnetite untouched, and surrounded by younger oxides or oxyhydroxides. The resulting magnetization is now a composite of ancient ('primary'), and secondary components. In sediments, the primary remanence is usually a DRM acquired when ferromagnetic particles

are aligned in the geomagnetic field during deposition. In sedimentary rocks, dewatering during the prolonged process of lithification usually has enhanced the alignment of these grains with the geomagnetic field to produce a post-depositional detrital magnetization (PDRM). Lightning reaching the ground is capable of inducing magnetization in rocks in a very strong, essentially instantaneous magnetic field. This is called isothermal remanent magnetization (IRM), and can completely obscure the primary remanence. Meteorites are extraterrestrial samples that can acquire a secondary shock remanent magnetization (SRM), both in the event that excavated the material from the parent body, and during impact at arrival on Earth.

(ii) Isolation of NRM components using demagnetization: A major task in all palaeomagnetic investigations is to identify and separate the magnetic components in the NRM using a range of demagnetization and analysis procedures. Hence, the laboratory measurements and the Zijderveld plots arise from the need to separate these different components from each other in a process called stepwise demagnetization. Such alternating field or thermal demagnetization is done in a zero magnetic field, provided by a shielded room, lest the samples acquire a new magnetization during treatment (Fig. 7.4a,b). The MAgnetic VACuum System (MAVACS) used for thermal cleaning, which produces magnetic field free space in a 5-litre volume to an accuracy better than 2 nT is shown in Fig. 7.5. The characteristic remanent magnetization (ChRM) is the earliest acquired component of magnetization that can be isolated. Interestingly, a secondary magnetization need not be thought of as totally useless. In certain situations, a secondary magnetization's direction can be compared with known directions for the geological past, and allows one thereby to date the event that caused the rocks to acquire a secondary component of magnetization. Hence, both primary and secondary components in a rock can record geological events, e.g. the time of formation, metamorphism, or an impact

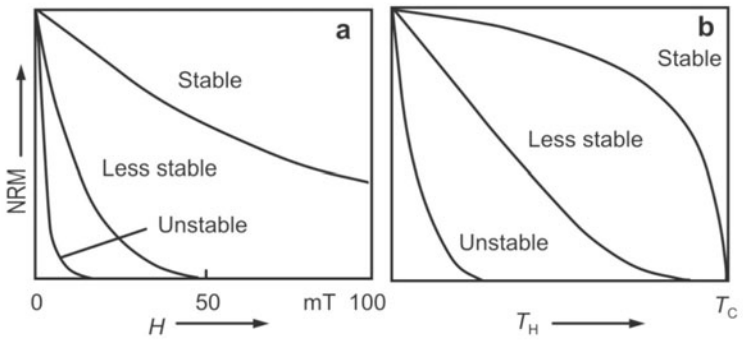

Figure 7.4. Schematic behaviour of a remanent magnetization during: (a) AF (alternating field) demagnetization, and (b) thermal demagnetization. H: maximum intensity of the alternating magnetic field, T_H: maximum heating temperature, T_C: Curie temperature (*courtesy:* Soffel).

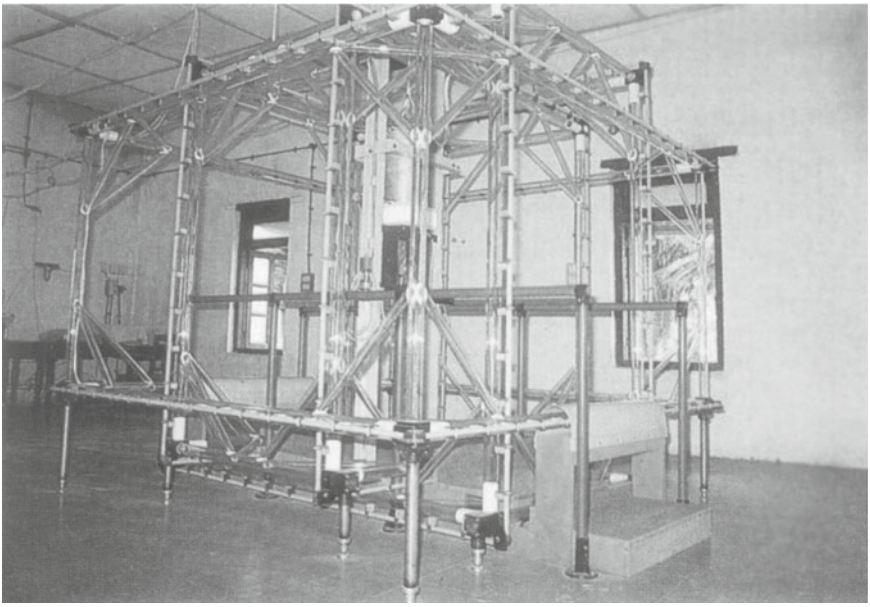

Figure 7.5. The magnetic vacuum system (MAVACS) that creates a 'magnetic vacuum' in which thermal cleaning is carried out to get at the 'primary component' to infer the direction and intensity of the ancient magnetic field.

event, and are of interest in unraveling the geological history. Depending on the intensity, and duration of the events responsible for secondary magnetizations (also known as overprints), the secondary component may partly or completely reset the primary magnetization.

Typically there is also significant effort put in to date the magnetizations so that not only the detection of the magnetic field at that particular sampling site is known, but also the time when the field was in that direction. Many of the successful applications of palaeomagnetism are derived from an effective partnership with geochronology.

(iii) Reliability and improvements in palaeomagnetic analysis: Geological processes like metamorphism during geological history of rock formation may cause remagnetization resulting in the reset of initial magnetization at younger age than the age of rock formation. This leads to erroneous age dating interpretations. A number of tests exist that can constrain the age of magnetization. If a baked contact next to an intrusion has a magnetization that is the same as that of the intrusion (because this baked margin was thermally re-magnetized at the same time as the intrusion was emplaced), and if the host rock far away from the intrusion carries a different magnetization, then this 'positive' contact test provides evidence that the magnetization of the country rock is older than the magnetization in the intrusion. Similar (fold-,

conglomerate-) tests exist in other geometrical situations, and collectively such tests provide several key poles with a high reliability factor. This factor is an invention of Van der Voo, who in the late 1980's felt the need to come up with a parameter that quantified the relative reliability of a given result. It has since become a widely used quality component.

Another assessment method involves the use of electron microscopy. Knowledge about the minerals that are potential carriers of the magnetization is tremendously important as palaeomagnetists try to decide how and when the magnetization was acquired. For magnetite, for instance, its primary nature may be revealed by its titanium content, whereas its magnetic stability can be deduced from the grain size. Grains that are larger than several micrometres (μm) are usually not able to preserve an ancient remanent magnetization. Instead, it is the fine magnetic grains of ~0.05 μm that are important. Such grains cannot be seen with an ordinary microscope, but with scanning and transmission electron microscopy, it is possible to build up the magnetization history of a large variety of rock types. Combined with modern rock magnetic research, these studies have been truly pioneering and promise to become a standard component in future studies.

VI. Palaeomagnetic Data from India

The Indian sub-continent has a northward drift, which can be understood precisely by measurement of stable remanent magnetization of well dated rocks. Palaeomagnetic study of Indian rocks was first carried out by Cleg, Deutch and Blackett. Subsequently, palaeomagnetic measurements of a few Precambrian rocks, Tertiary-Mesozoic formations (Deccan and Rajmahal traps), and Gondwana sediments were carried out. The geographical distribution of various formations studied, and the approximate sampling locations are shown in Fig. 7.6, and their palaeomagnetic data are given in Appendix 7.2.

The scarce data show that there is room for rectifying anomalies regarding: (1) Precambrian results with lack of reliable radiometric ages, (2) large gap of ~45 Ma in the Indian Cretaceous palaeomagnetic data between Rajmahal Traps (110 to 115 Ma), and the Deccan Traps (65 Ma), (3) the precise age, duration, and extent of Deccan magmatism, (4) detailed magnetostratigraphy of Cretaceous basins of the western and eastern parts of India for delineating accurate ages, (5) lack of palaeomagnetic data across different cratons of the Indian sub-continent, (6) establishing Indian sub-continent to be an amalgamation of smaller plates, or a single unit, (7) synclinal rotation of the Himalayas in the NE region, and (8) tectonic and orogenic upliftment of the Himalayas, and the effect on monsoon initiation. In order to address several neglected palaeomagnetic issues, few laboratories were established especially at Allahabad and Navi Mumbai, which are operated by IIG.

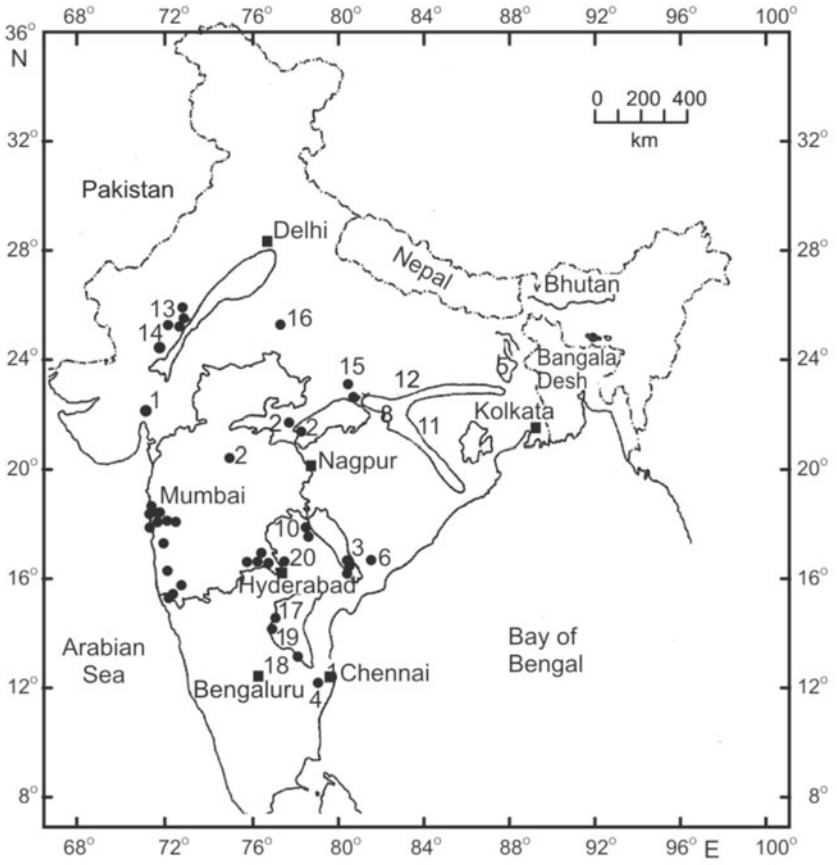

1. Pavagadh
2. Deccan traps
3. Tirupathi sandstones
4. Satyavedu sandstones
5. Rajmahal traps
6. Rajmahendri traps
7. Sylhet traps
8. Dykes from Palamau etc.
9. Parsoa sandstones
10. Kamthi sandstones
11. Himgir sandstones
12. Vindhyan sandstones
13. Malani rhyolites
14. Mundwara complex
15. B.H.Q. and B.H.J.
16. Bijwal traps
17. Veldurti hematites
18. Chitlor dykes
19. Cuddapah sandstones and shales
20. Hyderabad dyke

Figure 7.6. Geographical distribution of the various geological formations used in palaeomagnetic studies and the approximate locations of sampling sites. The sites are classified into Tertiary-Mesozoic volcanic activity, sedimentary rocks belonging to Gondwana system and Precambrian formations based on the ages of rocks studied and the dispersion in their magnetic directions shown in Appendix 7.2 (*courtesy:* Athavale and his coworkers).

7.2 PALAEOLATITUDE, POLE POSITION, APPARENT POLAR WANDER PATH

I. Geocentric Axial Dipole Hypothesis

Palaeomagnetic data analysis mainly deal with: (1) obtaining ChRM related to ancient EMF of a particular sampled rock formation, (2) gaining statistically significant data, (3) determining age of ChRM component, and (4) expressing magnetic field directions in geographical coordinates. For this purpose, some constant feature associated with the geomagnetic field is required to provide a reference system on a geological timescale. This reference system then forms the basis for comparing the palaeomagnetic results obtained from different landmasses. Based on numerous studies on rocks of ages ranging from recent to ~5.0 Ma, it has been found that EMF averaged for a period of 10 ka or more, can be assumed to be due to a geocentric axial dipole (Fig. 7.7a) coinciding with the geographical N-S axis of the Earth. Thus at any point on the surface of the Earth, the time-averaged palaeomagnetic latitude (λ) is equal to the geographic latitude (Fig. 7.7b). This is the most important assumption in palaeomagnetic studies, which enables to compare the pole position of different continental masses of a given age for the reconstruction of their relative orientations in the geological past. This assumption of the existence of geocentric dipole is in contravention to the one made in geomagnetic studies. In geomagnetic studies, the axial dipole field is known to make an angle D. Therefore, palaeomagnetic studies allow the determination of the palaeolatitude of the sampled area from inclination and orientation of the ancient pole (palaeomagnetic pole) from declination and inclination.

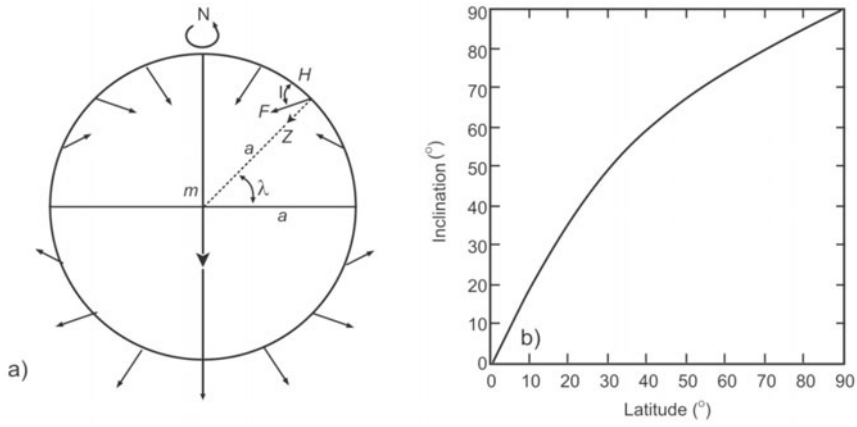

Figure 7.7. (a) The field of a geocentric axial dipole (where m - magnetic moment, a - Earth's radius, H, Z, F - horizontal, vertical components and total field at latitude λ). (b) Variation of inclination with latitude for a geocentric dipole (*courtesy:* McElhinny).

II. Palaeolatitude

The remanent magnetization acquired by either TRM of igneous, CRM of metamorphic or DRM of sediments is parallel to the ambient EMF at the time of their formation. Palaeolatitude can be calculated from the mean inclination of NRM. To find out the latitudinal location, and the polarity of geomagnetic field (N or R) at the time of rock formation (Fig. 7.7c), the equation ($\tan \lambda_s = 0.5 \tan I$) is used. In this equation, λ_s denotes palaeolatitude of the sampling site, and I is the mean inclination of the magnetization acquired in that particular rock formation.

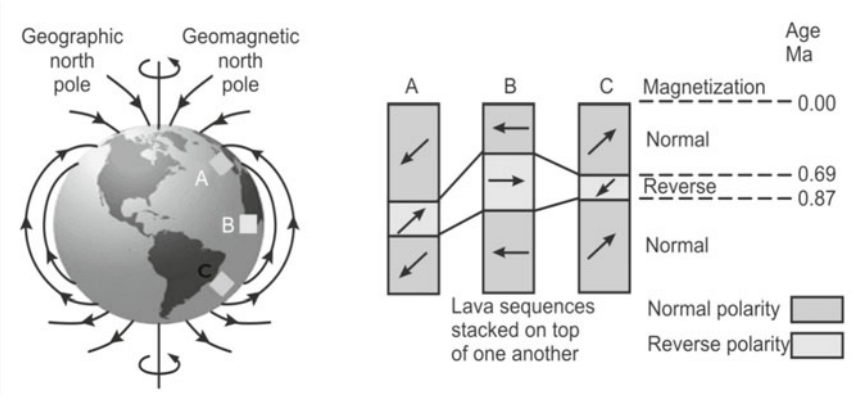

Figure 7.7c. Sketch of lavas (A-C) located at three different latitudes showing normal and reversed magnetizations (http://www.phys.uu.nl/~sommer/master/geopotential%20fields/).

By pooling together the inclination values of the remanent magnetization of Deccan rock samples with those of the dipolar field in Fig. 7.8a, the ancient geographical latitude of India can be determined. For instance, the NRM directions (D and I) of Deccan traps, particularly in terms of their mean inclinations, display variations: 64° upward in Jurassic, 60° upward in Cretaceous, 26° upward in the early Tertiary, and 17° downwards in middle Tertiary (Fig. 7.8a). It must be noted that the upward inclinations indicate the sampling site in the southern hemisphere, whereas downward inclinations suggest the site to be in the northern hemisphere with respect to the present day normal polarity, which can be related to the distribution of inclination of dipolar field at various latitudes of the Earth (Fig. 7.8a). In Fig. 7.8b, the dotted arrow represents the inclination value for Jurassic basalt in India, while the solid arrow represents that of the dipolar field. In order to make the two arrows coincide, one must place India around point *J* in the southern hemisphere. If Mumbai is taken as the reference point, which is today located at 19°N, obviously this must have been located at 40°S in the Jurassic as revealed from Fig. 7.8b. The ancient latitudes for India for four geological periods (Jurassic, Cretaceous, early Tertiary and middle Tertiary) are computed and displayed in

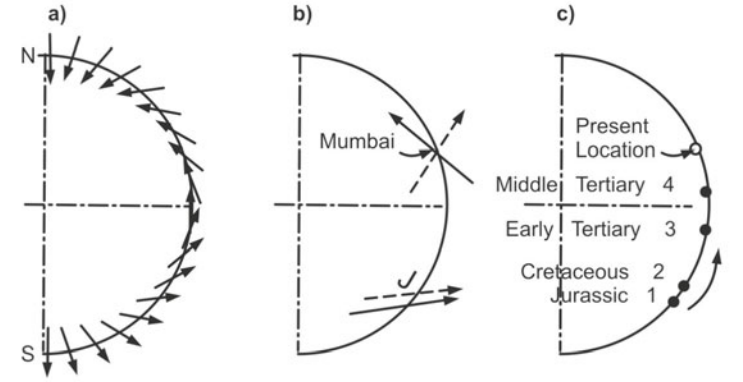

Figure 7.8. (a) Inclination values of the NRM of the dipolar field at various latitudes of the Earth. (b) The dotted arrow represents I value of the Jurassic basalt in India, while the solid arrow represents that of the dipole. In order to make the two arrows coincide, one needs to place India around point J in the southern hemisphere. If Mumbai is taken as reference point which is today located at 19°N, obviously this must have been located at 40°S in the Jurassic. (c) Ancient latitudes for India for other geological periods are computed. Mean inclinations display variations: 64° upward in Jurassic, 60° upward in Cretaceous, 26° upward in the early Tertiary and 17° downwards in middle Tertiary (*courtesy:* Deutsch).

Fig. 7.8c, which clearly shows that India moved northward for ~700 km, perhaps at the rate of a few cm/year since Jurassic.

III. Palaeomagnetic Poles and Apparent Polar Wander Path

The basic criteria for a key palaeomagnetic pole are: (1) *Age of the palaeopole:* The palaeopole should be demonstrated to be primary and the rock-unit precisely and accurately dated. (2) *Quality of the palaeopole:* The primary palaeomagnetic remanence needs properly isolated, secular variation averaged out, and where necessary, correction made for tilting. When the angles of D and I are measured, the position of the palaeomagnetic pole can be calculated (see Appendix 7.1). Table 7.1 shows formation mean directions and calculated pole positions for four sites from A to D. Palaeomagnetic measurements are made on rocks of different geological ages and continental areas with their mean pole positions given in Table 7.2. If palaeomagnetic pole positions are obtained from rocks of different ages on the same continent, these poles can be plotted. Such a plot is called an apparent polar wander path (APWP) (Fig. 7.8d-g) and shows how the magnetic pole moved relative to that continent. If such APWPs from two continents coincide, then the two continents cannot have moved relative to each other during the times shown. However, if the paths differ, there must have been relative motion between the continents. This is because these continents have drifted with respect to each other, as well as relative to the rotation axis of the Earth. Each of the several continents has its own APWP

Table 7.1 Formation mean directions (A to D) and their computed pole positions

Site ID	*Natural Remnant Magnetization (NRM)*				*Site positions*		*Pole positions*	
	Before AF demagnetization		*After AF demagnetization*		*Latitude* λ_s	*Longitude* ϕ_s	*Latitude* λ_p	*Longitude* ϕ_p
	Declination	*Inclination*	*Declination*	*Inclination*	*N*	*E*	*N*	*E*
A	151.3	51.6	155.1	48.7	16.37	73.84	38.0	281.6
B	356.9	–39.8	351.2	-52.5	15.95	74.02	40.2	263.7
C	132.9	68.1	161.8	39.1	19.25	74.83	45.0	279.0
D	317.3	–55.0	300.5	-54.7	20.91	77.86	10.4	303.6

Table 7.2 Position of the north magnetic pole in different periods as determined by palaeomagnetic studies

		North America	*Europe*	*Russian platform*	*Siberian platform*	*Africa*	*South America*	*Australia*	*India*
Tertiary	U	87N, 140E	80N, 157E	78N, 191E	66N, 234E	87N, 152E	82N, 62E	77N, 275E	
	L	85N, 197E	75N, 151E	68N, 192E	57N, 152E	85N, 186E		70N, 306E	
Cretaceous		64N, 187E	86N, 0E	66N, 166E	77N, 176E	61N, 260E	78N, 236E	53N, 329E	22N, 295E
Jurassic		76N, 142E	36N, 50E	65N, 138E		65N, 262E	84N, 256E	48N, 331E	
Triassic		62N, 100E	45N, 143E	51N, 154E	47N, 151E		80N, 71E		20N, 308E
Permian		46N, 117E	45N, 160E	44N, 162E	34N, 144E	27N, 269E	60N, 180E		7S, 304E
Carboniferous	U	37N, 126E	38N, 161E	43N, 168E		46N, 220E		46N, 315E	26S, 312E
	L			22N, 168E		26N, 206E	43N, 151E	73N, 34E	
Devonian		29N, 123E	0N, 136E	36N, 162E	28N, 151E			72N, 174E	
Silurian				28N, 149E	24N, 139E			54N, 91E	
Ordovician		28N, 192E	10N, 176E		25S, 131E	24S, 165E	11S, 143E	2N, 188E	
Cambrian		7N, 140E	22N, 167E	8N, 189E	36S, 127E				28N, 212E

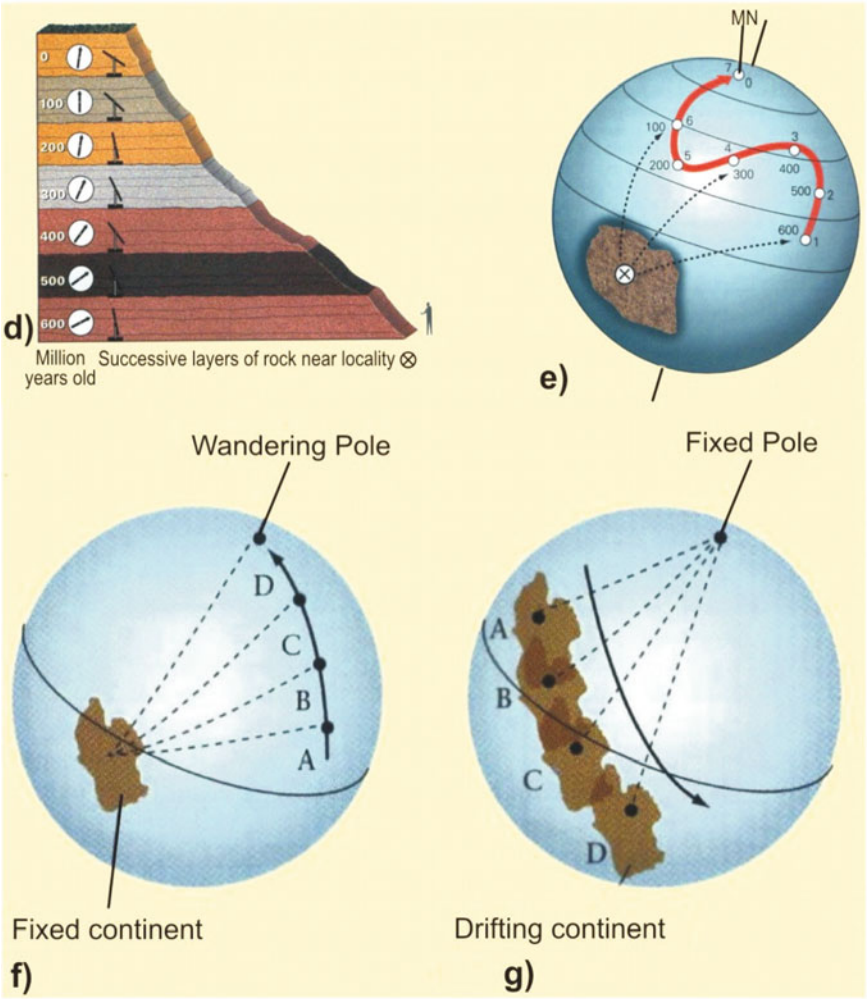

Figure 7.8. (d) Successive rock layers. (e) Movement of poles from 600 Ma to present. (f) APWP derived fixing the continent. (g) Continental drift keeping pole position fixed (http://www.phys.uu.nl/ ~sommer/master/geopotential%20fields/).

curve altogether different from that of other continents, but all converging at the present-day pole. The only plausible alternative, therefore, is that the continents have migrated their position during the geological period. Comparison of APWPs from different continents enables observation of their ancient juxtaposition. Their reconstructions can be compared and improved using palaeontological, geochronological, geomorphological and structural data.

IV. Plate Tectonics

Plate tectonics views the whole Earth as a dynamic system in which internal heat drives lithospheric plates in relative motion with respect to each other

(Chapter 2). Palaeomagnetism enables to view continental movements in the past, viz. changes in latitude and orientation relative to the geographic poles. The worldwide efforts led to the discovery of polarity reversals of the EMF over geological history and thus the realization that the seafloor acts as a tape recorder of the Earth's magnetic reversals and polar wandering (Chapter 2). In particular, the polar wandering is the interpretation given to the observation that the magnetic pole (and the geographic pole) has moved extensively in the geologic past.

According to the GAD model, when averaged over time, magnetic north is geographic north. There are simple relationships between the geographic latitude and the angle I of the EMF, which are applied to plate reconstruction and palaeogeography. Palaeomagnetic data can be used to find latitude and N-S orientation of the palaeocontinents. Palaeolatitude changes calculated from palaeomagnetic data are consistent with palaeoclimatic changes; the distribution of various palaeoclimatic indicators is latitude dependent. Although it is not possible to assign longitudinal position to the palaeocontinents, the relative positions of the continents around the globe can often be pieced together by matching the shapes of APWPs.

There are two principal ways of summarizing palaeomagnetic data for a given region. One approach is to construct palaeogeographic maps of the region for different geologic periods. A much simpler way is to plot successive positions of palaeomagnetic pole for a given continent from epoch to epoch on present latitude-longitude grid. By careful gathering the available palaeomagnetic, geological and geophysical data and integrating them, Earth scientists are testing new hypotheses about smaller scale, intracontinental deformation. It is important to realize the crucial role that palaeomagnetic studies have played in providing the tectonic framework that guides geological investigation and interpretation.

7.3 MAGNETOCHRONOLOGY

Palaeomagnetic dating and graphic correlation methods take advantage of the fact that the EMF varies over time and this variation is recorded by the rocks. The magnetic field has two stages, normal and reversed. One of the most fascinating characteristics of the EMF is that the dipole undergoes complete polarity reversals a few times every million years on average. The intervals between reversals have a stable normal or reversed polarity and are called subchrons, chrons, and superchrons, depending on their duration. Analysis of rocks of increasing age allows to trace the history of the magnetic field and palaeomagnetism can be used as a chronological tool: the polarity, direction and intensity are compared with reference curves and the rock's relative age is derived. Methods and techniques differ according to the age and thus the time resolution needed as described below.

I. Secular Variation Magnetostratigraphy

Earth's field can be divided on a broad spectrum of time variations as shown in Fig. 7.9a. The horizontal scale represents a temporal change, whereas the vertical line height gives relative magnitudes of each type of magnetic field contribution. These temporal intensity and directional changes are due to internal and external sources of field (details in Chapters 1 and 3). Changes in geomagnetic direction useful for dating are of two types; generally assumed to be caused by fluid motion in the core reflecting antiparallel directions (180° of D and opposite sign of I). The first type relates to polarity reversals having periods on the order of 10^6 years, and these polarity intervals are called chrons. There are also short N and R intervals, whose duration lies between 10^4 and 10^5 years, called subchrons. During a polarity reversal, the intensity of the field drops to ~10 to 20%, then increases again. The last one occured ~780 ka ago (Chapter 2, Fig. 7.12). The second type is called secular changes, whose periods are from 10^2 to 10^3 years. These are minor (fleeting) changes in the nondipole part of the field, whose D and I changes to the extent of ~30°, and are recognizable over regions of 'continental extent'.

SV master curves provide rapid means of dating sediment sequences by matching the fluctuations with a previously dated SV record. This approach, however, is much more difficult to apply than that of polarity reversals because: (1) geomagnetic secular variations are not uniformily global, (2) SV records are generally based on lake sediments, which are exceedingly difficult to date

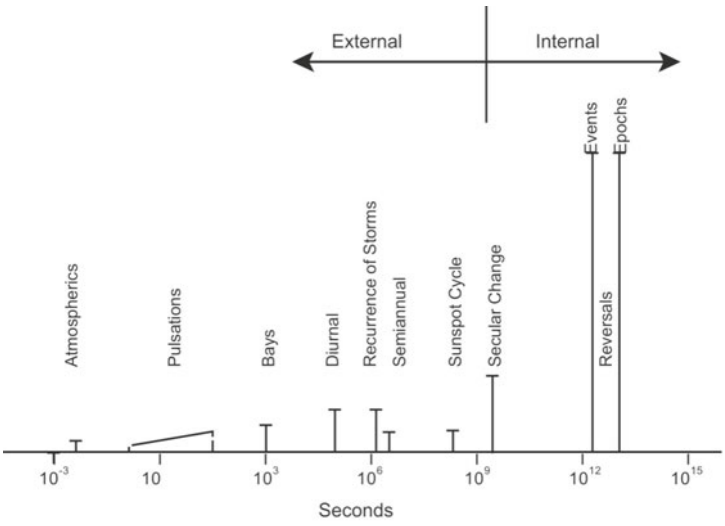

Figure 7.9a. Internal and external temporal changes in the magnetic field observed on the surface of the Earth are represented in this figure. The amplitudes of the shorter-period changes are exaggerated relative to the secular change and reversals (http://www.grisda.org/origins/10018.htm).

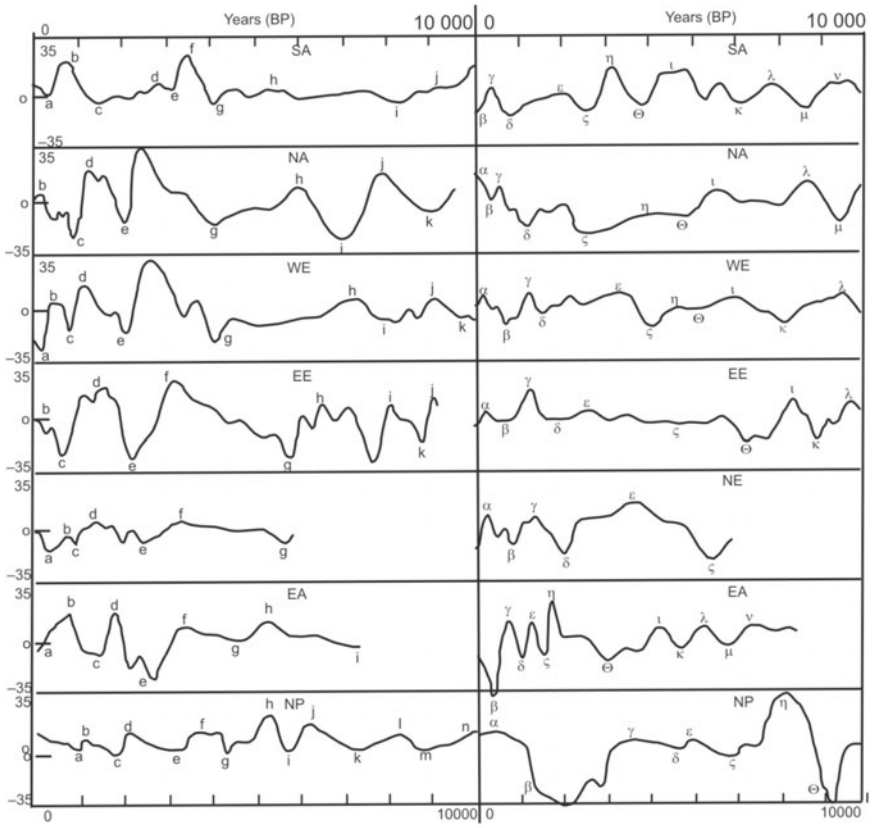

Figure 7.9b. Regional Holocene declination and inclination master curves for South Australia, SA; North America, NA; western Europe, WE; eastern Europe, EE; Near East, NE; East Asia, EA and north Pacific, NP. Curves based on data from different sources given in Thompson and Oldfield, 1986.

with better than 10% accuracy, and (3) SV patterns with amplitudes of ~20° are more susceptible to noise than polarity changes of 180°. Secular I fluctuations are large and significant at low latitudes, whereas secular D changes are prominent at high latitudes, hence are used for dating purposes in the respective regions (Fig. 7.9b, Table 7.3). The SV records of both D and I from seven regions of the world (Fig. 7.3b) are useful for dating applications of magnetostratigraphy within the past 10 ka. These patterns of SV can be used as master curves for dating newly acquired palaeomagnetic records.

Sediments and volcanic rock record several types of magnetic archive of interest to palaeolimnologists. At the longest timescales, a record of polarity reversals is preserved and identified in lake deposits, providing absolute age information. However, the binary nature of magnetic reversals (N or R) implies that some independent means need to be employed to infer polarity transition in a particular sequence of lake beds. In practice, this is usually done by cross-

correlation with some other source of age information such as biostratigraphical or radiometric dates (Table 7.3).

Table 7.3. Ages of magnetostratigraphic features (Thompson and Oldfield, 1986)

	*SA**	*NA*	*WE*	*EE*	*NE*	*EA*	*NP*
Declination							
a[Ψ]	300	-	140	160	220	0	900
b	680	100	450	300	700	700	1100
c	1300	750	600	600	850	1200	1800
d	2000	1200	1000	1400	1300	1650	2150
e	2800	2000	2000	2200	1900	2200	3200
f	3500	2400	2600	3100	2100	3100	3900
g	4500	4000	4900	5700	2400	4400	4400
h	5500	5900	7100	6500	3200	5100	5300
i	8300	7000	8300	7600	5600	7300	5600
j	9000	7900	9100	8000	-	-	6000
k	-	9000	10000	8700	-	-	8350
l	-	-	-	9000	-	-	8900
Inclination							
α	-	50	240	300	300	-	200
β	-	420	650	600	550	400	2150
γ	400	750	1150	1300	700	760	3500
δ	900	1200	1650	1900	900	1000	4700
ε	1900	2300	3100	2600	1400	1300	5100
ς	2600	2900	3800	4600	2000	1550	5800
η	3200	3700	4300	5500	3600	1750	7000
θ	3600	4400	5000	6400	5300	2800	8200
ι	4600	5300	6000	7200	-	4100	8950
κ	6000	6600	7100	7800	-	4600	9800
λ	6800	7700	8300	8600	-	5100	-
μ	7900	8400	8800	-	-	5600	-
ν	8600	9600	9700	-	-	6600	-
ξ	10000	-	-	-	-	-	-

* SA South Australia (35°S 140°E) based on Barton and McElhinny (1981)
NA North America (45°N 90°W) based on Banerjee et al. (1979)
WE Western Europe (55°N 05°W) based on Turner and Thompson (1981)
EE Eastern Europe (60°N 30°E) based on Huttunen and Stober (1980)
NE Near East (30°N 35°E) based on Thompson et al. (1985)
EA Eastern Asia (35°N 140°E) based on Horie et al. (1980)
NP North Pacific (20°N 155°W) based on McWilliams et al. (1982)

[Ψ] a to l declination turning points. α to ξ inclination turning points. Ages tabulated in calibrated ^{14}C years BP. The EA ages are rather poorly known, based here on a linear interpolation between the basal tephra layer and the archaeomagnetic features preserved in the upper sediments. Errors in ^{14}C ages at all the sites possibly amount to several hundred years. Labelling of the palaeomagnetic features is purely for convenience of reference. Any likenesses in ages or in shapes of similarly labelled features are probably chance occurrences, unlikely to be duplicated in other parts of the world.

II. Magnetostratigraphy and Geomagnetic Polarity Timescale (GPTS)

Magnetostratigraphy refers to the description, correlation, and dating of rock sequences by means of magnetic polarity reversals. Remanent magnetic moments measured on field-oriented rock specimens along sedimentary strata enable to determine polarity reversals of EMF during the time interval of deposition of those particular sedimentary strata called magnetostratigraphy. One of the most fascinating characteristics of the EMF is that the dipole undergoes complete polarity reversals a few times every million years on average. The intervals between reversals have a stable normal or reversed polarity and are called subchrons, chrons, and superchrons, depending on their duration. They define characteristic pattern of polarity zones through time and, as such, form a fundamental tool for dating of the geological record: the geomagnetic polarity time scale (GPTS).

In a sequence of rock formations, each polarity intervals are called magnetozones. Magnetozones of alternating polarity yield magnetic polarity stratigraphy. This form of magnetostratigraphy plays an important role in the construction of GPTS. The association of radiometric ages with key biostratigraphic stage boundaries, which are correlated by magnetostratigraphy to the marine polarity record, yields a dated GPTS.

Exact stratigraphic correlation of normally, and reversely magnetized strata from all over the world assumes significance. The potassium-argon (K-Ar) technique has made it possible to precisely date volcanic rocks of known polarities helping to compare polarity patterns in a stratigraphic column to define its age. This is therefore an indirect dating method, since recognition of polarity reversals alone does not provide an estimate of age. Palaeontological analyses based on ammonites, foraminifera, or nanofossils define a biostratigraphy that is tied to the magnetostratigraphy.

Since continental volcanic activity is essentially an intermittent process, a continuous sequence of the entire history of polarity changes is not possible. However, marine magnetic anomalies at the mid-oceanic ridges give a continuous pattern, and order of polarity reversals from Mesozoic (~200 Ma) to the present. The age of polarity reversals is determined from the sea-floor spreading model, and age of marine magnetic anomalies on the basis of hypothesis of Vine and Matthews. The extrapolation of this timescale enables isochrons to be drawn on the ocean floor up to 2000 to 3000 km from the ridge axis. This permits correlation of anomalies of specific number, and age from one ocean to the other helping to erect a Mesozoic-Cenozoic polarity timescale.

Microfossils also help in establishing polarity timescale. For example, to test the polarity chron 25 (this pertains to marine magnetic anomaly numbering system) of early Palaeocene age, a core is drilled through the sediment containing marine magnetic anomaly 25. This core when studied should contain microfossils of the same age (early Paleocene) as determined from magnetic

anomalies. Palaeontological dating of deep sea sediment cores puts a strong constraint on the polarity timescale. A polarity superchron for Phanerozoic and Proterozoic is given in Fig. 7.10.

To use a geomagnetic timescale to date the oceanic plates, it is necessary to recognize specific anomalies. The prominent anomalies up to age 83 Ma are numbered from one to thirty-three. For ages 125-162 Ma, they are labelled with the prefix M (M standing for Mesozoic). Particularly prominent is the long magnetic quiet zone in the Cretaceous (83-124 Ma numbered C34), during which no reversals occurred. Information for construction of GPTS is lacking for older periods (oldest oceanic crust that still exists is ~200 Ma), and hence determination of polarity timescale beyond 200 Ma has to be done through palaeomagnetic studies from the continental rocks alone. Nevertheless, several attempts have been made to set up polarity timescales of earlier periods including the Precambrian. The best known features of the polarity timescale for the Paleozoic are the Permo-Carboniferous R-superchron, R-superchron in the Devonian, and N-superchron in the late Ordovician and early Silurian (Fig. 7.10). Schmidt and Embeleton recognize that a common APWP can be drawn

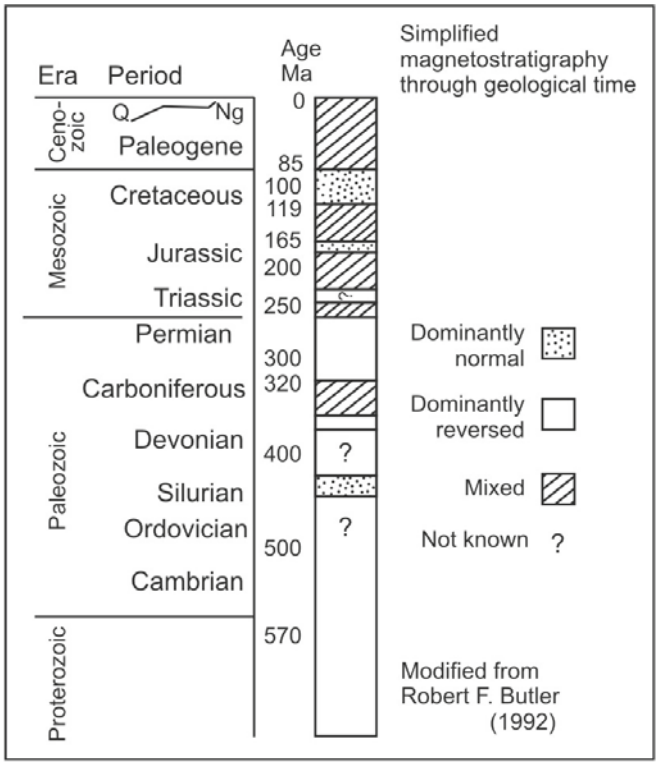

Figure 7.10. Simplified magnetostratigraphy through geological time scale modified from Butler, 1992. This is used to understand the pattern of polarity reversals from the Paleozoic and Proterozoic eras.

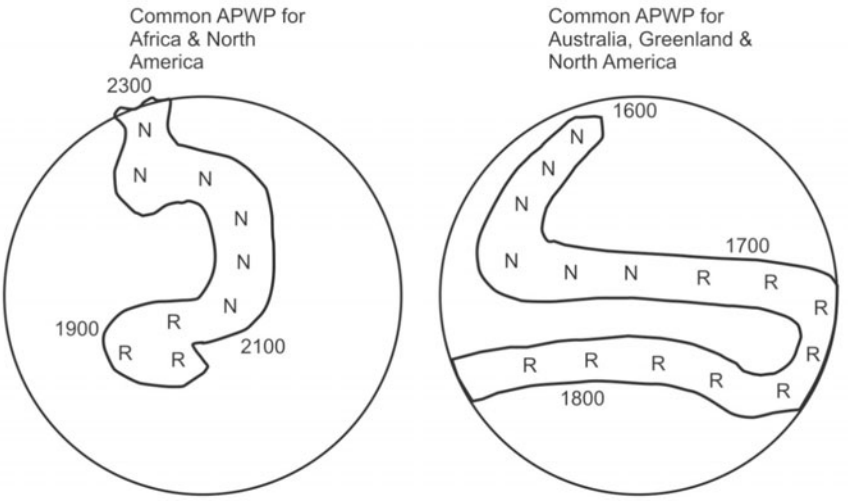

Figure 7.11. Simplified figure from Schmidt and Embleton (1981). N-poles with normal polarity, R-poles with reversed polarity.

for Africa, Australia, Greenland and north America. They have shown that the N-polarities predominate from 2300 Ma to ~2100 Ma (Fig. 7.11). From 2100 to ~1650 Ma, the R-polarities are common. N-polarities again become the norm from 1650 Ma onwards. Halls in 1991 reported from Matachewa dyke swarm of Canada, the oldest known magnetic reversal to have occurred at 2452 Ma ago.

III. Application of GPTS for the past 6.0 Ma

The polarity timescale of the last ~5.0 Ma has been established by compiling palaeomagnetic data of known K-Ar or biostratigraphic ages. Allan Cox and Richard Doell have built a well defined polarity timescale comprising epochs and events (Fig. 7.12). The optimum GPTS is the CK95 timescale, which adjusts for Earth's orbital variations and climatic responses published in 1995 by Cande and Kent. Significant periods of time marked by consistent orientations of the EMF are called epochs (it is the same term used for the smallest division of the geological timescale, e.g. Pliocene epoch). Epochs come in two states (Fig. 7.11) of N and R. Unfortunately, it is impossible to extend the polarity timescale beyond 4.5 Ma, because of inaccurate dating. Within the Brunhes normal polarity epoch, which began 0.78 Ma ago, many have identified temporary reversals and major polarity fluctuations, termed excursions such as 272 ka (Biwa II), 187–192 ka (Biwa I), 110–120 ka (Blake), 40–45 ka (Laschamp), 25–30 ka (Mono lake), 10 to 12 ka (Gothenburg) and ~2.8 ka (Starno). Short-term variations of the magnetic field are also used for dating during the last few hundred ka.

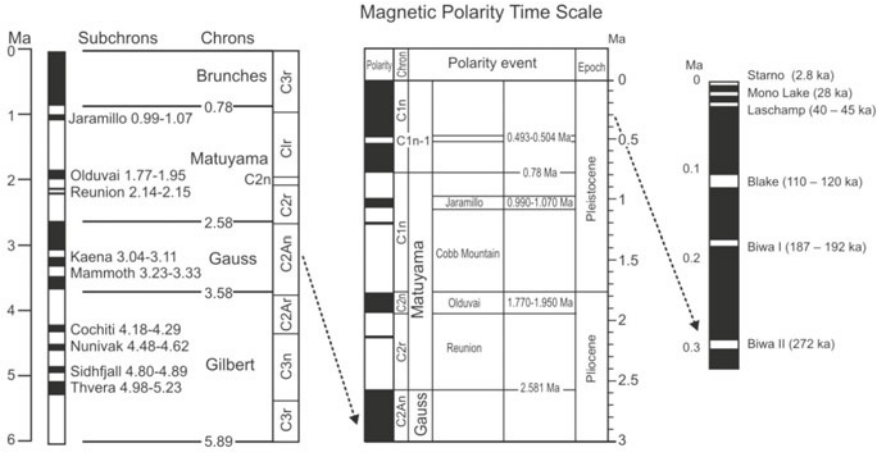

Figure 7.12. Details of the recent reversals of the Earth's magnetic field as determined from detailed radiometric dating of continental and oceanic island lavas and palaeomagnetism of marine sediments. Simplified geomagnetic polarity time scale with focus on Quaternary magnetostratigraphy (Cande and Kent, 1995). Epochs (chrons) have been named after prominent scientists (e.g. Gilbert, Gauss, Bruhnes, Gauss) and events (subchrons) are named after their location found (e.g. Olduvai George, Tanzania, the site of early hominid discoveries of Leakey; Mammoth, California, USA and Jaramilo creek, New Mexico, USA). This scale may not yet be completed; many short events remain to be firmly established.

7.4 IMPLICATIONS OF PALAEOMAGNETIC RESULTS

Study Areas: Palaeomagnetic studies have been carried out (on): (1) dyke swarms of the Deccan volcanic province (~65 Ma) in the Dhule district of Maharashtra, (2) magmatic rocks occurring in Kutch rift basin, Gujarat, (3) middle to upper Cretaceous (~100 Ma) sediments of the Bagh group in the Man valley of Madhya Pradesh, (4) dolerite dykes and Closepet granite in the Archaean terrain of south India, (5) Eocene (~55 Ma) sediments of the Tapti river section in the Cambay basin of the Gujarat, and (6) magnetostratigraphy of Tertiary sequence of Machhial-Neri river section, Himachal Pradesh. Magnetostratigraphic screening of sedimentary formations covering the entire Cretaceous period in the western part of Narmada basin infers their magnetization/remagnetization ages, and related tectonic and geophysical implications. The salient features of the studies are as follows:

I. Dyke Swarms of Deccan Volcanic Province

Dykes present south of Narmada river and Mumbai region have yielded pole positions similar to the Deccan Super Pole (40°N, 79°W) shown in Fig. 7.13a. These intrusions are affiliated to the massive Deccan extrusion that took place ~65 Ma ago, which spanned a short duration of just <0.5 Ma. The studies also

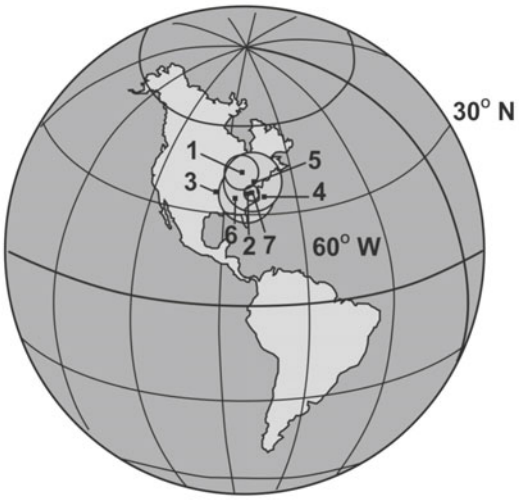

Figure 7.13a. Palaeomagnetic pole positions of the Deccan trap related dykes and the Deccan Super Pole. Note dyke intrusions are affiliated to the Deccan extrusion, which spanned a short duration of just <0.5 Ma. (1) Murud dykes, (2) Dhadgaon dykes, (3) and (4) Mandaleshwar dykes, (5) Goa dykes, (6) North Kerala dykes and (7) Deccan Super Pole.

indicate post-trappean dyke swarms which possibly coincide with the opening of Arabian sea, and rifting of the Seychelles-Mascarene oceanic plateau.

II. Tholeiites and Alkali Basalts of the Kutch Rift Basin

Palaeomagnetic results of 30 magmatic bodies of Kutch, Gujarat yielded a VGP pole at 33.7°N and 81.2°W (d_P/d_m= 5.81/9.18), which is statistically concordant with that of the Deccan Super Pole (36.9°N and 78.7°W). The magmatic rocks of the Kutch basin are broadly contemporaneous straddling 30N-29R-29N chrons. It is suggested that the magmatic rocks of Kutch were generated by the impact of the Reunion plume on the Kutch lithosphere under extensional setting (Fig. 7.13b).

III. Cretaceous Bagh Group Sediments: Pervasive Deccan Remagnetization

The mid to upper Cretaceous intra-trappean Bagh sediments in the Man river valley of Narmada basin in Dhar District, Madhya Pradesh have their pole position near the late Cretaceous segment of the Indian APWP (Fig. 7.14a). It is concordant with other poles reported from the Deccan basalt flows, and also with dated deep sea cores of the Indian ocean. The study has further revealed that these sediments were subjected to large scale remagnetization due to igneous activity of Deccan basalt effusion. Since Andaman sediments are far away

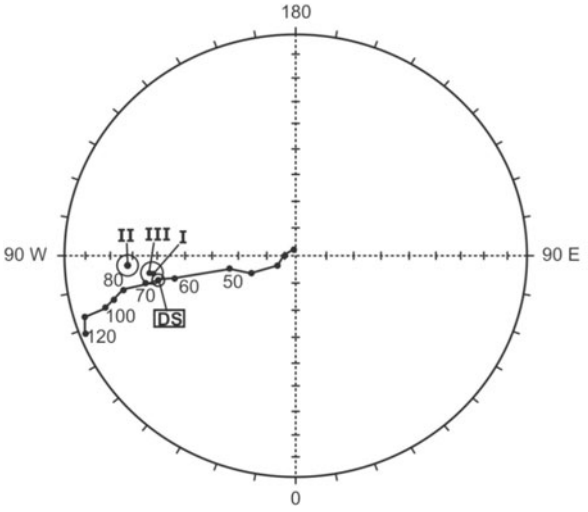

Figure 7.13b. Groups I, II and III Kutch magmatic bodies, and Deccan Super pole (DS) virtual geomagnetic poles (VGP) are plotted along with synthetic APWP for India. Group I: Tholeiites and gabbroic dykes of Kutch mainland, Group II: Alkali basalt plugs of Kutch mainland and Group III: Magmatic rocks of northern Island belt (*courtesy:* Paul et al.).

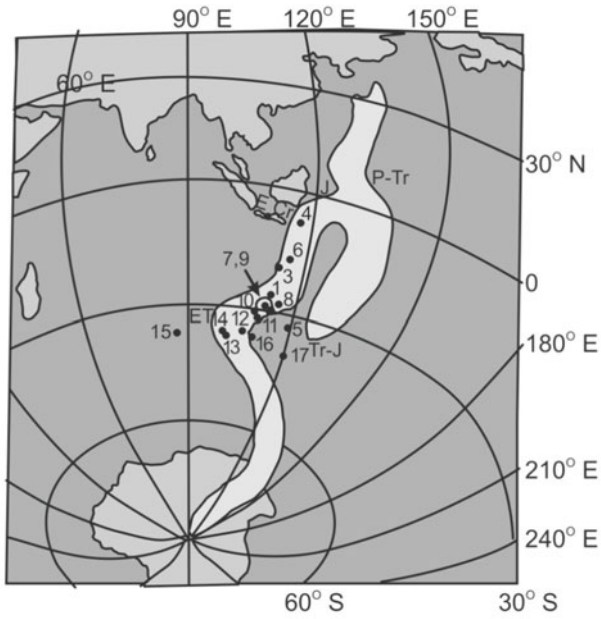

Figure 7.14a. Palaeopoles obtained for different rocks of Cretaceous age. The swath, in greyish white, is the APWP suggested for India and Pakistan (*courtesy:* Prasad et al.).

from the Deccan influence, Bagh sediments can give reliable palaeomagnetic and magnetostratigraphic results in Cretaceous period for the Indian subcontinent. The results also revealed that the Indian subcontinent experienced counterclockwise rotation by 13°±3° and a latitudinal northward drift by 3°±3° during Deccan volcanism.

IV. Eocene Sediments of the Cambay Basin

The middle to upper Eocene sediments of Tapti river section near the village of Bodhan (21°18′ N; 73°3′ E), in Gujarat showed a mismatch with Tertiary part of the standard APWP. Two pole positions are displaced east of the APWP, which suggests a clockwise rotation of ~65° of the sampled area. The two rotated poles are almost coincident, and agree reasonably well with the APWP, the displacement being 10° towards the younger side of the polar path. The discrepancy arises due to steeper inclinations observed in the rock samples, than was expected at the sampling locality according to the relevant portion of the APWP.

V. Proterozoic Dykes of the South Indian Granulite Terrain

Palaeomagnetic results on Proterozoic dolerite dykes from the granite greenstone terrain (GGT) are similar to the adjacent Tiruvannamalai dykes from the adjoining south Indian granulite terrain (SIGT). Thus, there was no relative movement, at least since 1600 Ma ago, between the GGT and SIGT. The palaeomagnetic directions of basement rocks to these dykes showed an age of ~1100-1000 Ma due to partial remagnetization/streaking that occurred probably during eastern ghats orogeny (EGO). Anorthosite rocks at Oddanchatram from SIGT have yielded two magnetic components: (1) corresponding to ~1100 to 1000 Ma reflecting the vestiges of EGO, and (2) ~550 Ma corresponding to the Pan-African thermal event that has prominently affected part of the SIGT.

VI. Magnetostratigraphy of the Tertiary Sequence

The magnetostratigraphic investigations on the ~5-km thick sedimentary sequence of Himachal Pradesh Machhial-Neri section yielded 12-N and 12-R polarity magnetozones. The graphical comparison of prepared magnetic polarity scale (MPS) is compared with standard GPTS within chrons 5AAr to 6r. The sediment deposition is found to have occurred within a span of ~7-Ma, ranging in age from 20 to ~13 Ma with an average sedimentation rate of ~63 cm kyr^{-1}.

VII. Magnetostratigraphy of the Karewa Palaeolake Sediments

The Karewa (in Kashmir) lake deposits are in the northwest Himalaya, which is an intermontane basin presently experiencing rapid uplift along its southwestern margin. Karewa sediment profile contains a unique climatic record

of a series of climatic oscillations, comprising glacials, interglacials and interstadials. Rock magnetic studies reveal titanomagnetite, magnetite and hematite are the main carrier of characteristic remanent magnetization.

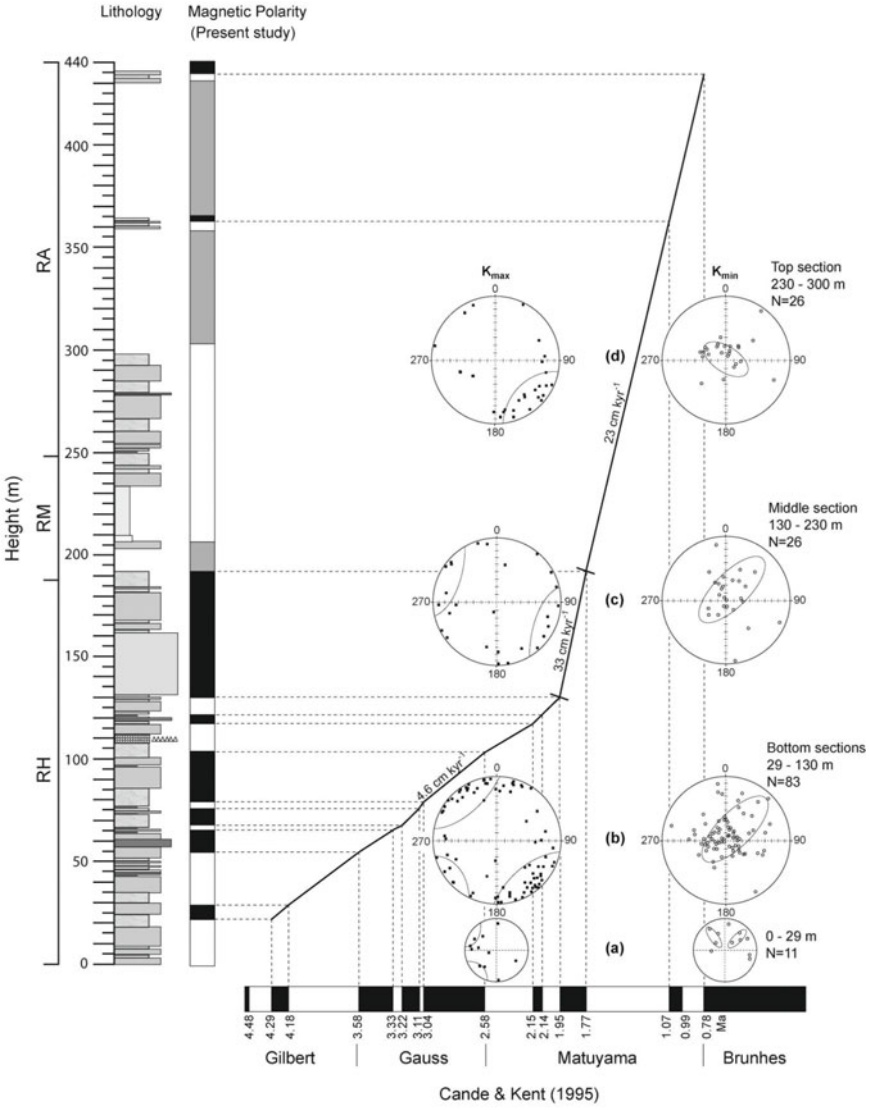

Figure 7.14b. Age vs. stratigraphic thickness plot of Kashmir paleolake sediments showing the sediment accumulation rate (SAR) deduced from polarity sequence and anisotropy of magnetic susceptibility (AMS). Note an increase in sedimentation rate from 4.6 cm/kyr to 33 cm/kyr at Plio-Pleistocene boundary coinciding the onset of westerlies in the Kashmir valley, thereby reducing the influence of SW monsoon (Basavaiah et al., 2010).

Detailed magnetostratigraphy has been investigated from 250 sites collected at 435 m thick Romushi section of lower Karewa deposits, which records a chronometrically constrained volcanic ash. The ChRM directions obtained through AF demagnetization procedure are used to calculate the virtual geomagnetic pole (VGP) positions. VGP latitudes were plotted against the stratigraphic level to obtain the magnetic polarity time scale (MPTS). A total of eight normal and eight reverse polarities are deciphered in Romushi sediments. MPTS of Romushi formation is well correlated with standard GPTS (Fig. 7.12). The samples collected from Romushi river section gave an age of 0.79 to 4.68 Ma and sediment accumulation rates (SAR) range from 32 to 4.6 cm kyr^{-1}. The revised magnetostratigraphy delineates chronological depositional processes influenced by both climatic and tectonic factors. For example, the low SAR of 4.6 cm kyr^{-1} indicates a calm sedimentation regime prevailed until the Pliocene/Pleistocene boundary. The rapid increase in SAR after ~2.0 Ma, is either due to local or regional tectonic event, or by strengthening of the monsoon reported for ~2.6 Ma.

7.5 ENVIRONMENTAL GEOMAGNETISM

Rocks, baked materials and sediments owe their magnetization/magnetic properties to Fe oxides, oxyhydroxides, sulfides and solid solution components present in them. Recent developments in electronics and computing have helped manufacture sensitive instruments for magnetic measurements, enhancing/establishing a now familiar study area called environmental geomagnetism (also called mineral magnetism). The rock magnetic techniques investigate nondirectional magnetic properties of natural and synthetic materials to delineate environmental or climatic controls on accumulation of the parent material (rocks, glacial till, eolian and alluvial deposits), and its microstructural and chemical alteration (pedogenesis) with time. Basically, environmental geomagnetism employs the experimental approach to identify/characterize the mineralogy, concentration, grain size, morphology and composition of the magnetic mineral phases present.

Magnetic grains with their distinctive assemblages are virtually omnipresent and their type, size and concentration change relative to their source and depositional history. The sensitivity and detection of magnetic attributes (even in ppm to ppb concentration ranges) by environmental instrumentation make the methodology relatively inexpensive, easy, and rapid compared with other types of mineralogical analysis. This methodology has a nondestructive trait, wherein the same samples can be used for any additional and complementary investigations. In multidisciplinary studies, one small diameter core is generally sampled for pollen, diatom, ostracode, isotope, geochemistry, mineral magnetism, carbon, radiocarbon, lead isotope and amino acid dating. Consequently, the researchers run out of sample before they run out of ways to examine it. Thus, the nondestructive method of environmental geomagnetism

stands to be a great asset. Most importantly, it enables comparison of different records across thousands of kilometres. Magnetic analyses thus help a great deal in producing spatial as well as temporal record of ambient climatic, environmental and post depositional processes. Environmental magnetists use the magnetic properties to isolate natural and human-induced changes in climate and environment on both spatial (site-specific and regional scales) and temporal (contemporary and geological timescales) level.

7.6 ENVIRONMENTAL GEOMAGNETISM VS. PALAEOMAGNETISM

Environmental geomagnetism is a distinct scientific entity, which studies intrinsic magnetic characteristics of the mineral types within nonoriented samples such as magnetic susceptibility (χ), frequency dependent susceptibility (χ_{FD}), anhysteretic remanent magnetization (ARM) and isothermal remanent magnetization (IRM). Some of these properties (χ and χ_{FD}) are measured in the field, while others are measured as a remanent response to a series of externally applied and artificially induced magnetizing fields of different kinds (AC, DC) and magnitudes (ARM, 0.1 T and IRM up to ~9 T) in the laboratory. The magnetic properties of sediments are entirely independent of the EMF and are largely a function of mineralogy and grain size that provide insights into the mode of transport, deposition and changes in their properties caused by different processes of iron mineral authigenesis, diagenesis and dissolution. Thus, this branch is independent of palaeomagnetism, which primarily determines the directional nature of remanent geomagnetic field, wherein oriented samples are an absolute necessity. In mineral magnetic research, however, samples are not required to be measured in situ or to have their original orientation noted. It involves measuring 'bulk' magnetic properties complementing other techniques such as geochemical or micropalaeontological studies, to name just a few.

Environmental geomagnetism also has palaeomagnetic applications which focus on: (1) correlation of palaeomagnetic signals in sediment cores, (2) development of astronomically calibrated age model, (3) testing the hypothesis of orbital forcing of the EMF, and (4) determining the origin of the palaeomagnetic signal. In essence, environmental magnetic measurements allow detection of quantitative as well as qualitative variations in magnetic minerals as an aid to environmental data interpretation, rather than the geomagnetic directional properties. Thus, palaeo and rock magnetists use magnetic measurements to identify which magnetic minerals are responsible for acquiring a record of the Earth's magnetic polarity at their time of formation. Environmental geomagnetists seek to identify causal links between magnetic properties and climatic and environmental histories/origins.

7.7 ENVIRONMENTAL MAGNETISM: OBJECTIVES AND EVOLUTION

Environmental magnetism largely relies on the sensitivity of Fe compounds to physicochemical changes, and on their tendency to persist as diagnostic 'tracers' over long periods of time. Magnetic properties of the natural materials are largely connected with the element Fe, its valency, concentration, and partitioning. This methodology can be applied to many areas of study such as soil forming processes, slope and evolution, basin erosion/sedimentation, sediment source tracing, historical/contemporary particulate pollution, differentiation of atmospheric dusts/aerosols, stratigraphic correlation of a wide range of temporal/spatial/depositional sites, archaeological studies of pottery/soils, interpretation of palaeoclimatic records, diagenetic changes and authigenic sulphide formation. Besides, the growth of biomagnetism as a major field has run parallel to the above developments.

Environmental magnetism has evolved on three principal objectives: (1) characterizing spatial variability in physical properties of the shallow subsurface (soils, sedimentary sequences) environment, wherein the information is used to model palaeoclimate and palaeoenvironment, (2) environment pollution characterization based on the fact that atmospherically transported magnetic particulate material makes a significant contribution to the iron (hydr)oxide particle content of many sedimentary deposits/soils and (3) biomagnetism, where the research programme aims to provide information about the environmental control variables (temperature, rainfall, pH, as well as microbial type and concentration) for the process of Fe^{3+} to Fe^{2+} reduction and challenges posed by environmental magnetic observations of biomineralized nanophase (1–100 nm) materials. The most fascinating examples of investigation come from magnetotactic bacteria found in diverse environments playing a role in fine magnetic particle (submicron size) studies.

I. The Beginnings

Gustav Ising first used magnetic minerals as a proxy in 1926. He collected annually laminated glacial lake sediments from Sweden and measured their χ and NRM, which varied seasonally and with distance from the source. He found lake sediments deposited in the spring time were more magnetic than those deposited in winter. He interpreted it in terms of detrital input and higher density of magnetic minerals. Forty years later, John Mackereth used magnetic measurements on lake sediments from Windermere to investigate the magnetic mineral source.

In 1950s, the study of soil magnetism was pioneered by Le Borgne, who unraveled the phenomenon of magnetic 'enhancement' (increased χ) in natural top soils (humus rich horizons), and ascribed it to in situ conversion of a proportion of the weakly magnetic forms of iron (hydr)oxide to a strongly magnetic form of secondary ferrimagnetic oxides (maghemite, magnetite). But

the process controlling the enhancement of χ was then poorly understood. Thompson and Oldfield later invoked a mechanism based on Mullin's hypothesis to explain the postulated formation of microcrystalline maghemite or magnetite from weakly magnetic iron (hydr)oxides through the redox cycles, which occur under normal pedogenic conditions. An alternate hypothesis proposes soil bacteria to grow small chains of stable single domain (SSD) magnetite crystals within their cells resulting into the enhancement observed as normal part of pedogenesis.

Frank Oldfield, in the mid 1970s, was inspired by a demonstration by Mackereth of the use of palaeomagnetic secular D measurements for dating Holocene lake sediments. He found χ had striking similarity between cores of the Lough Neagh sediments, which became the first attempt of core correlation. He and his coworkers in late 1970s put forward the concept of using magnetic properties as proxy parameters. Thompson and his team's article in '*Science*' in 1980 formally announced environmental magnetism to be a sub-discipline, and extended the use of rock magnetic methods in soil, sediment, peat and atmospheric dust studies. It has now become a rapidly expanding research methodology (see review articles and books by King and his associates, Thompson and Oldfield, Oldfield, Maher and Thompson, Walden and his associates, Evans and Heller and Basavaiah and Khadkikar).

II. Environmental Impacts on Magnetic Minerals

In an environmental system, the magnetic minerals found in descending order are iron oxides (hematite, magnetite, maghemite), iron oxyhydroxides (ferrihydrite, goethite, lepidocrocite), iron sulphides (greigite, pyrrhotite) and manganese (rhodochrosite, vivianite) minerals (Chapter 2), which are commonly scattered within the nonmagnetic matrix of the natural materials.

The nature of Fe compounds, their presence, environmental sensitivity and variable stability make magnetic measurements widely adaptable to many environmental fields. For instance, majority of magnetic minerals, which cycle in environmental systems, originate from the Earth's crust and pass through the atmosphere, hydrosphere and biosphere in varied ways (Fig. 7.15). Only a small part of atmospheric magnetic dust is derived directly from the Earth's interior, via volcanic eruption, whereas extra-terrestrial inputs are found to be very limited. Magnetic minerals in unweathered parent rock material or those which survive largely unaltered in weathered contexts are characterized as primary minerals. Those formed by chemical/physical processes or biogenic effects associated with weathering, pedogenesis, diagenesis or authigenesis are secondary. Human intervention also leads to some of these processes such as fossil fuel combustion and soil erosion (Fig. 7.15).

Chemical transformation can lead to Fe conversions among paramagnetic, ferrimagnetic and antiferromagnetic forms giving rise to environmental 'finger prints', which become significant indicators in environmental tracing investigation. Also, fire and soil forming processes enhance top soil magnetic

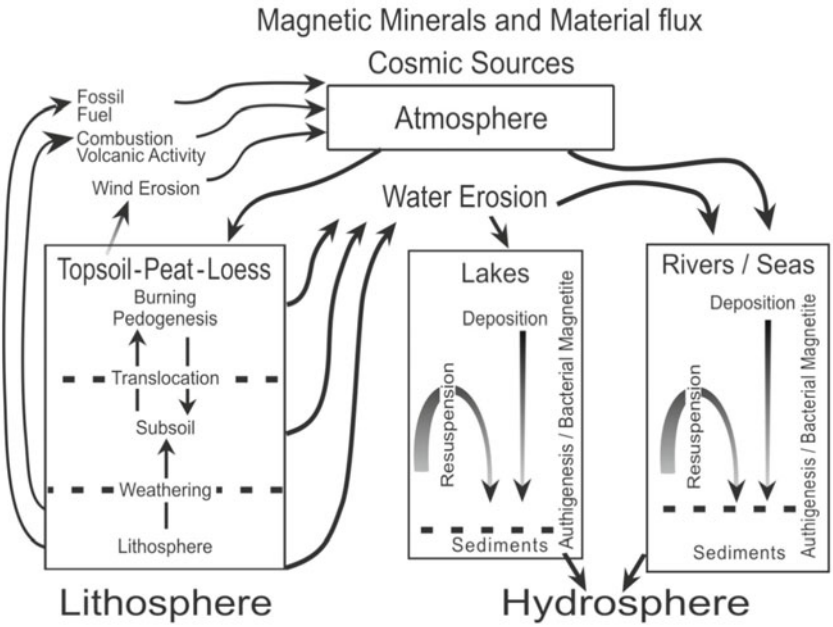

Figure 7.15. Major sources and cycles of magnetic minerals within the environment. Magnetic minerals can be produced, modified, transported and deposited by a range of environmental and anthropogenic processes. Environmental geomagnetism can be applied to identify/differentiate/characterize principal sources of magnetic minerals displaying ferromagnetic behaviour within the environment of soils and sediments. These include detrital minerals derived from rocks, sediments or soils (transported by water or wind), authigenic/diagenetic production, volcanic ash, in-situ pedogenic processes, cosmic sources (important near sites of meteor impacts), anthropogenic pollution and magnetic bacteria. Examples of major areas of application of environmental geomagnetism include environmental change, past climates, sediment sourcing and mapping of particulate pollution (Thompson and Oldfield, 1986).

material by converting nonferrimagnetic minerals to fine ferrimagnetic grains. These secondary magnetic oxides differ, both in crystal form and size, from the primary magnetic oxides present in the underlying substrates; both of primary and secondary minerals are eroded and incorporated in river and lake sediments. Thus, differences in primary and secondary magnetic minerals form the basis for sediment source identification. Alternatively, chemical transformation can make the environmental interpretation of magnetic data more difficult. Diagenesis or authigenesis, for example, may distort the magnetic 'signals' from source materials preserved in sediments, which can mislead the analysts.

Physical processes usually perform the function of simply removing and redepositing magnetic mineral assemblages. These processes are relatively conservative of magnetic minerals, but the magnetic properties can still be

affected through the following mechanisms: (1) magnetic grain size reductions and crystal shape changes, (2) regrouping of mineral assemblages, and (3) vertical rearranging of magnetic assemblages. However, these minerals are found to persist unaltered in a wide range of transport and deposition contexts. Hence, appropriate mechanism needs to be taken into consideration, when specific EMM study is finalized. For instance, particle size based magnetic study should be harnessed to reduce the effect of sorting in sediment source tracing. Sediment source identification can be established in a catchment system (if) (1) some weathering and soil formation have taken place and the types of source materials can be characterized by magnetic measurements, (2) the timescale over which erosion and sedimentation are being studied is substantially shorter than the rate at which the assemblage of metastable Fe oxides is being transformed in the potentially eroding soil and (3) sediment diagenesis or authigenesis have not affected the magnetic properties of the sediments.

III. Magnetic Mineralogy as a Proxy

Natural as well as anthropogenic influenced climatic and environmental changes have occurred innumerable times in the past. In a fundamental sense, the discernment of past changes (and future ones) requires a database that goes long back in time and space. This information is contained in historical records of meteorological observatories, ship-logs, personal records, etc., as also in religious texts and epics which volunteer detailed descriptions of floods, droughts and such other natural disasters. They are, however, allegedly considered short on reliability. But, the 'proxy' indicators of climatic alteration, unlike historical records, go a long way back in time (Ma), and their distinguishing feature is their ability to characterize the natural system, or part thereof in an approximate manner. They are also easily and quickly 'measured' at a competitive cost, enabling rapid measurement of large number of samples; a key advantage in obtaining high-resolution spatial and temporal environmental data.

Climate proxies are generally used as signs of past climatic processes, which include physicochemical properties and isotopic compositions of minerals, fluids or gases. The other contenders are the anatomical assemblages of certain fossil plants, animals, and presence (or absence) of index fossils. On land, climatic variables used as proxies include temperature, precipitation and evaporation. In the ocean, the key variables include currents, temperature, salinity, nutrient availability, productivity and redox chemistry. Biodiversity patterns, continental weathering rates, winds and storms also come in handy as climatic proxies.

The use and reliability of different proxies are established by comparing the present day values with some record of the past, e.g. the tree-ring thickness or the isotopic composition of water. Here, the present is used as a key to the past. When scientists understand how tree rings change their thickness in recent

wet and dry periods, the information (or an assumption) gained is then extrapolated back in time to make a reliable (nearer to truth) estimate of a climate or an environmental change. The assumptions, however, involve some amount of uncertainty. The conjecture that under different climatic conditions, a marine organism grew most vigorously during the same season and at the same water depth as in the modern environment, has a tinge of chaos and uncertainty to it. To circumvent this problem, multiple proxies, about whom few suppositions are made, are used in the decision making process to increase the reliability of palaeoclimate reconstruction. The physical proxies like old air extracted from bubbles in ice cores, old water from pore spaces in seabed sediments or continental rocks, concentration of noble gases found dissolved in old groundwater provide direct evidence of past climatic compositions. In the category of direct evidences are also included sand dunes, and glacially polished bedrock.

Many cross checks are used when interpreting proxies for climate changes. Marine isotopic stages (MIS) deduced from alternate warm and cool period of the Earth's past climate are used as one of the tallies. Based on carbon and oxygen isotopes from the marine sediments/organisms, these stages are chronologically arranged as MIS1, 2, 3, 4, etc. (Fig. 7.16). It is based on the fact that physical and chemical characteristics of atoms of differing isotopic mass increase with decreasing temperature of the medium. For example, the carbonate shells growing in water typically favouring isotopically heavy oxygen tend to become isotopically heavier at lower temperatures. The growth of ice sheets removes isotopically light water (ordinary water) from the ocean, forcing the organism to use isotopically heavy oxygen from water in their carbonate shells, which then provide information on the presence (or absence) of ice sheets over time. To quote another example, a few chemicals are always common in the environment, but the organism may use only a typical 'favoured' isotope. A shortage of this chemical may force it to use another 'less favoured' isotope. Also, marine photosynthesis increasingly favours a lighter isotope of carbon as CO_2 becomes more abundant. This allows estimation of changes in CO_2 concentration from the isotopic composition of organic matter in oceanic sediments. The change in ocean isotopic composition can be estimated independently from the composition of pore waters in sediments, whereas the change in temperature can be estimated from both the abundance of cold or warm loving shells in sediments. Concentrations of noncarbonate ions substituted into calcium carbonate shells provide further information. Reversals of the EMF have helped to provide a timescale for changes in oxygen isotopes, giving it a chronology that could be used to understand the frequency of glaciations and rates of change (Fig. 7.16).

It is important to consider the quantum of time when interpreting climatic change. Four major timescales are generally considered, which include: Long-term (hundreds of Ma), medium-term (one Ma), short-term (~160 ka), and modern period (hundreds of year). This is important because climate has both

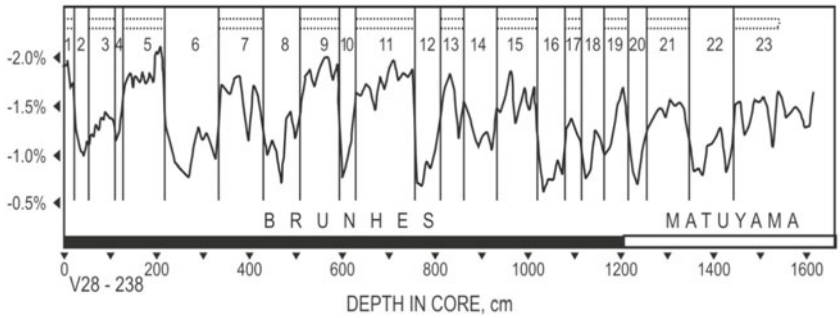

Figure 7.16. Climatic oscillations during the last 870 ka based on oxygen isotopic measurements of marine foraminifera from the sea core V28-238 (*courtesy:* Emiliani).

long-term trends and short-term variability. Long-term datasets provide the observer with a sense of 'big picture' of the climatic trends, when major shifts such as ice ages are easily recognizable. Short-term variations like a colder than average month, can exist within longer pattern of warming trend. The coexistence of short and long-term trends complicates the climate change signal. But, the magnetic proxy is able to tackle and discern the complex trends in a far better and cogent way than the other proxies.

The oceanic sediments are a mix of terrestrial and atmospheric constituents. The rivers of the Himalayas and the peninsular India drain tonnes of detrital material into the Bay of Bengal and the Arabian Sea, where the typical rate of sedimentation is much higher for the former than the latter. Lake sediments, on the other hand, have the potential of yielding high-resolution palaeoclimatic fluctuations, especially from proglacial lakes, which may have annual laminations (varves) that are deposited in the higher central Himalayas. The time resolution achievable from these lakes depends on sedimentation rate, sampling interval, and methods of dating. In general the temporal resolution is ca. 100 years. For high resolution in time, cores are retrieved from areas, where sedimentation rate is higher, but for a longer history with poorer temporal resolution sedimentary cores are raised from regions where sedimentation rate is slower. These sediments are studied for understanding long-term dynamics of the monsoon and climatic fluctuations. However, the chemical and biological proxies are limited in spread and strongly depend on the local climatic and environmental conditions. Index fossils thrive in particular locations and particular climatic umbrella only (their growth is also a function of a number of other variables). Hence, their use in tying up loose ends connected to climate, environment, stratigraphy and correlation remains equivocal.

Magnetic proxy parameters do not have this limitation, and so reliable results can be obtained from them. To begin with, relationships are found to exist between χ and oxygen isotope ratios, elemental constituents, and foraminifera instilling confidence in using it as a quantified and calibrated proxy. The carriers of magnetic properties of samples generally result from the

uppermost layer of crust (sediments), which is prone to many physical (erosion, weathering) and chemical (oxidation, reduction) processes governed by atmospheric, oceanic and terrestrial system changes (Fig. 7.15). Precipitation, in excess or deficit, has some chemical (change in redox environment) and physical (increased or decreased detrital input) influence on the lake, ocean and terrestrial sediments. In case of terrestrial sediments, the variable degree of water saturation alters the redox states leading to the formation of magnetite during periods of enhanced rainfall, whereas the formation of hematite/goethite is made possible through oxidative processes during periods of reduced rainfall. This interpretation has been experimentally verified and established. Fe-oxide system is found to be capable of carrying out a few interconversions between its different phases. In favourable conditions, almost every Fe-oxide can be converted into at least two others. Under oxic conditions, goethite and hematite are found to be the end members of many transformation routes, since thermodynamically, they are the most stable compounds. Although thermodynamically unstable (in the presence of oxygen), magnetite and maghemite are widespread in the environment. It is seen that at RT, magnetite very slowly oxidizes to maghemite. But at higher temperatures, magnetite metamorphoses to hematite. The oxidation of magnetite to maghemite is thus a significant environmental process, and is a topotactic reaction in which the original particle morphology is maintained throughout. Experiments have also shown ultrafine magnetite crystals (100 to 300 nm) to change to maghemite at RT, but in some cases, small particle sizes, of a couple of hundred nm, failed to initiate oxidation even after one year. Some experiments show that for ~9 nm nanocrystals at 24°C in water, oxidation is detectable after a few hours and completed in ~3 months.

These experimental reactions are replicated in natural environment. In an actual environmental setting, thermal transformation of magnetic polymorphs caused by natural or man made fires is seen to be widespread. The frequent occurrence of maghemite in surface soils of the tropics and at localized burning sites around the world, is due to the presence of organic matter which directs the transformation of goethite or ferrihydrite during heating to maghemite, whereas in the absence of organic matter, hematite is formed. Reductants such as zinc powder or elemental sulphur lead to maghemite formation, and it is assumed that the transformation proceeds via magnetite. In fact with higher amounts of reductant, e.g. sucrose, and/or lower O_2 supply, magnetite is formed instead of maghemite.

This establishes the veracity of magnetic proxy evidences for palaeoenvironmental interpretation. Palaeoclimatic history from magnetic properties is reconstructed by determining the magnetic framework of the sedimentary material. The next step involves ascertaining the basic aspect of the climate (physical-chemical), which predominantly has control over the magnetic signature. Finally, the magnetic measurements reveal the parameters (especially χ, ARM) most sensitive to climate change. In all this, it becomes

essential to identify space and time characteristics of climate/environment and magnetic minerals and ascertain their relationship with each other. However, in some situations, this magnetic proxy can be nonunique and noisy, to circumvent which independent and complementary analyses are adopted to compare the magnetic data with other environmental proxies, e.g. pollen, carbon isotopes or geochemistry.

IV. Mineral Magnetic Data of Resolving Ambiguity

In studies of environmental magnetism, often the recourse is to use only magnetic properties as analytical probes. In such cases, data interpretation becomes difficult since measurements are of bulk properties, comprising contributions from the entire gamut of magnetic minerals, rendering it to be nonunique. Hence, their scales are generally utilized in a relative sense. To get around this problem, many a times, ratios of several parameters are used to reduce nonuniqueness. In the process, interpretation of a ratio may change depending on the absolute values of numerator and denominator. Hence, the analysis may vary from one depositional environment to another or sometimes within similar kinds of environment as well. Proper comprehension of a mineral magnetic dataset, therefore, requires expert training and a feel for potential variability in the databank. The compilation of existing theoretical and experimental data derived from known sample sets enables to narrow down the ambiguity in interpretation and also reveals several ways of plotting the results. As a consequence, the inferences of sample 'interrogation' can be related to all the information available for the samples enabling to search causes of variability of magnetic properties. In the light of this, mineral magnetic data is interpreted confidently without resorting to use of other proxy data. Also, the results enumerated ahead and compiled from different sources can indicate the type of information obtained from the qualitative study of the magnetic and complementary parameters. The rock magnetic components listed in Appendix 7.3 provide an overview of the measurements undertaken in rock and environmental magnetism research.

V. Mineral Magnetism: Theory and Measurement

All substances demonstrate some degree of magnetic behaviour determined by: (1) interactions between electron spins, and (2) nature of their alignment in B_{ext}. In order to allow interpretations of bulk magnetic measurements, the phenomenon of magnetism is usually discussed on the subatomic scale, and then in ascending scales of reference in terms of atoms, subgrains, grains and grain assemblages (Fig. 7.17).

Basic magnetism: Minerals consisting of ions without an intrinsic magnetic moment are diamagnetic (Chapter 2). Minerals with an intrinsic magnetic moment are either ferro-, ferri- or antiferro-magnetic, where there exists exchange interaction between these ions, or paramagnetic, when there is no

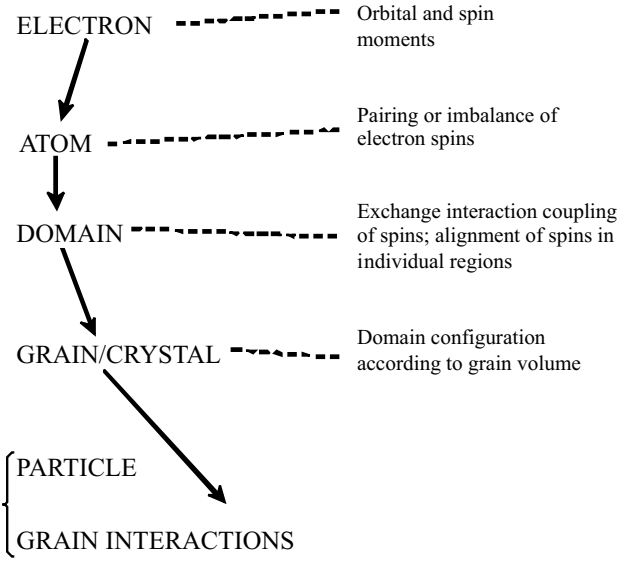

Figure 7.17. Scales of magnetic order.

interaction. For the existence of an intrinsic magnetic moment in an ion, presence of unpaired electrons in the electron's outer shell is necessary. Different magnetic measurement techniques respond to different properties of a mineral assemblage, e.g. paramagnetic and diamagnetic minerals have an effect on only the susceptibility measurements, but SIRM measurement reacts to minerals, which retain remanent magnetism. Table 7.4 summarizes the magnetization and remanence characteristics of main types of magnetic behaviour.

Magnetic granulometry is the determination of the effective grain-size of magnetic materials, based on the discrimination between magnetic relaxation effects (SP and SD particles) and domain processes (MD grains). In rock magnetism, magnetic grains are divided into SP, SD (stable SD), PSD and MD according to their magnetic properties, and domain states (Chapter 2, Fig. 7.18). The approximate magnetic grain size (distinct from sediment particle size) boundaries for magnetite are: SP (20–25 nm), SD (25–80 nm), PSD (80 to ~10–15 nm), and MD grains (>10–15 μm) (Chapter 2). Basically, there are two types of magnetic parameters that are strongly dependent on grain size: (1) magnetic hysteresis and (2) remanence properties. Also it is based on measuring some of these same magnetic parameters as a function of temperature either low temperature or high temperature, below or above RT. Figure 7.18 illustrates relationships between the magnetic parameters and the mineral grain size.

An approximate method, known as the Lowrie-Fuller test, compares the AF demagnetization spectra of ARM and SIRM to distinguish fine grains

Table 7.4 Main types of magnetic behaviour.

Substance	*Ferrimagnetic*	*Antiferromagnetic*	*Paramagnetic*	*Diamagnetic*
Definition	These substances are strongly attracted by the magnet		These substances are weakly attracted by the magnet	These substances are repelled by the magnet
Nature of alignment	Part of the atoms line up in one direction, the other part oppositely with net moment	Electron spins alternate atom by atom, thus cancelling out each generated moment	Align with the applied field	Align in opposite direction to the applied field
Field	+	+	+	-
Susceptibility (χ)	Large and positive	Small and positive	Small and positive	Small and negative
Magnetization	Strong	Weak	Weak	Very weak
Remanence	High	Low	None	None
Temperature effect	$\chi \propto 1/T$	$\chi \propto 1/T$	$\chi \propto 1/T$	Independent of temperature
Examples	Magnetite Maghemite Greigite	Hematite Goethite	Ferrihydrite Lepidocrocite	Quartz Calcite

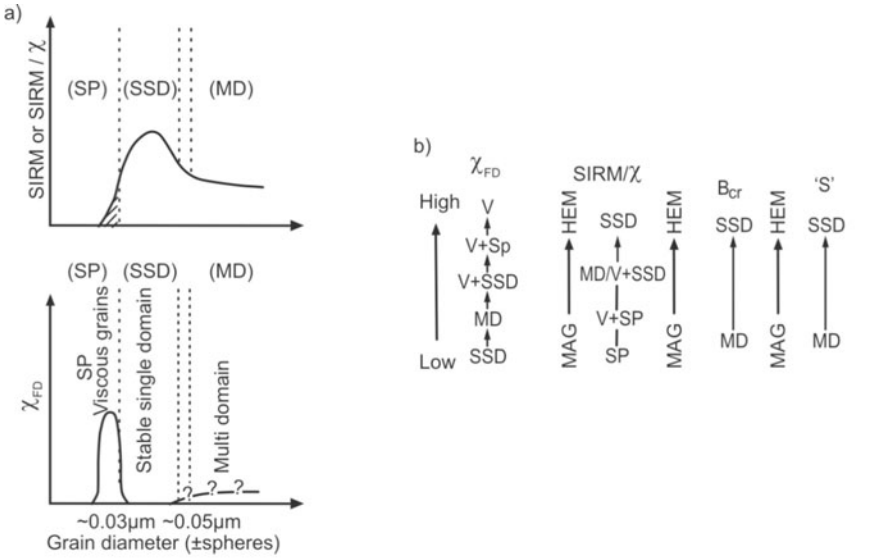

Figure 7.18. (a) The relationships between SIRM (SIRM/χ) and χ, and mineral grain size, showing approximate ranges of miltidomain, SSD and viscous grains. (b) A summary of the general influences on χ, SIRM/χ, B_{Cr} and S ratios of mineral grain size (MD, SSD, SP) and mineral type: magnetite (MAG) and hematite (HEM) (*courtesy:* Dearing and his coworkers).

(<20 μm) from coarse grains (>20 μm). Banerjee and his coworkers in 1981 argued that the ratio of anhysteretic susceptibility (χ_{arm}) to magnetic susceptibility (χ) can be used as a proxy for grain-size changes in magnetite. This reasoning is based on the fact that ARM is enhanced in the fine-grained SD fraction, whereas χ is relatively independent for the coarse grained PSD and MD fractions. The ratio, therefore, varies inversely with grain size. Furthermore, as pointed out by King and his coworkers in 1982, χ_{arm} is a strong function of concentration, so caution is warranted. Nonetheless, it is clear that susceptibility is virtually independent of grain-size, while χ_{arm} is a strong function of grain size, so changes in χ_{arm} normalized by χ in fact reflect changes in grain-size. Later, Maher and Oldfield have proposed variations of this method using χ_{arm}/SIRM or χ_{arm}/χ_{FD} to discriminate SP from MD particles.

Application of magnetic granulometry: The determination of effective grain sizes is useful for various geological and geophysical problems such as detection of climatic and cultural signatures left in natural sedimentary materials and formation/erosion of soil on bed rock. Grain size determinations are extremely valuable to identify origins of the various components in environmental samples. Since the data have contributions from all magnetic grain sizes, including detrital/pedogenic components, some magnetic properties, particularly coercivity and remanence, vary greatly with particle size. It is therefore possible

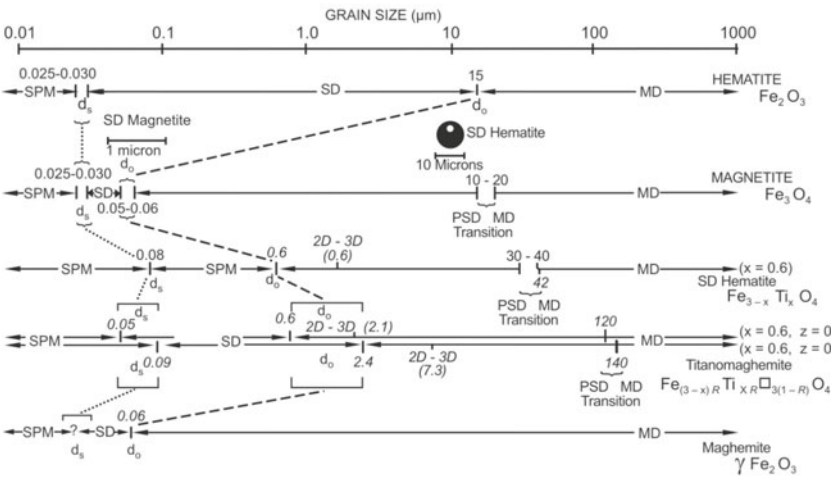

Figure 7.19. Theoretical and experimentally determined critical grain size transitions in some common iron oxide minerals (*courtesy:* Dunlop).

to categorize grain-size by the study of remanence. It is widely accepted that the coarse MD fraction is predominantly detrital (eolian), while the ultrafine SP grains are mainly authigenic or pedogenic in origin. An increasing body of evidence supports the dominance of in situ formation of ultrafine magnetic minerals, which enhance the susceptibility of soil layers. The critical grain size boundaries, which divide the various types of size-dependent magnetic behaviour are shown in Fig. 7.19. Moving from the finest to coarsest grain sizes, the boundaries d_s and d_0 separate those particles, which display SP to SSD and to PSD through MD behaviour.

7.8 PRIMARY MAGNETIC MEASUREMENTS—MAGNETIC PROPERTIES

Magnetic measurements do not just reveal the nature of magnetic material, but also signify its structure through anisotropy and its history through palaeomagnetism. To comprehend the relationship between magnetic parameters, and distinctive features of magnetic grains (e.g. chemistry, size, shape, defects and origin), a number of smart and effective techniques have been developed. To bring out the practical facets, and its realistic applications, a brief description of magnetic parameters and the basis that lies behind the methodology and interpretation of data is described.

I. Low-field Magnetic Susceptibility (χ)

This type of susceptibility is the ability of a given substance to get magnetized, i.e. it grows an induced magnetization that dissipates after the external field is

removed. There are several valid definitions in vogue, but the one given by Encyclopedia Britannica defines magnetic susceptibility as 'a quantitative measure of the extent to which a material may be magnetized in relation to a given applied magnetic field'. Thus χ is studied by applying magnetic field (H) and measuring the magnetization (M) induced in the material. There exists a relation connecting M and H: $M = \chi_V H$, which yields $\chi_V = M/H$, where v denotes 'volume'. χ is specified either by volume (κ) or mass (χ) ($=\kappa/\rho$, here κ is replaced by χ_V and ρ is density). Thus, χ is used to classify materials in terms of their response to B_{ext} as diamagnetic, paramagnetic and ferro(i)magnetic, making it an attractive magnetic characterization tool.

If ultrafine SP particles are present, the frequency of applied AC field has significant effect in terms of applied magnetic field. At higher frequencies, energy of thermal fluctuations reduces the alignment effect of the applied field, and consequently χ measured at higher frequencies is always equal or lower than that measured at lower frequencies. By measuring at different frequencies, the frequency dependent of magnetic susceptibility $\chi_{FD\%}$ can be expressed as (Fig. 7.18a):

$$\chi_{FD\%} = (\chi_{LF} - \chi_{HF}/\chi_{LF}) \times 100$$

χ_{FD} is particularly sensitive to grain sizes spanning the SSD to SP boundary, often referred to as fine viscous (Fig. 7.18a), because these grains show a degree of time dependent loss of remanence. Hence, this is a proxy for the relative amount of SP grains. It has strong implications with regard to delineating source type, since mineral assemblage exhibiting χ_{FD} is rare in unweathered rocks, volcanic ashes or fossil fuel derived sediments, but is characteristic of soils in which secondary magnetic minerals form as a result of pedogenesis and fire. Thus, natural susceptibility of sediment needs to be measured at two or more different frequencies to gain information about the amount and grain size of magnetite. For instance, while ultrafine magnetite (<0.03 μm) is formed in soils giving high (>8%, <16%) χ_{FD} percentages, relatively larger magnetite (MD ranges) is usually eroded out of rocks. While χ_{FD} depends on grain size, χ itself depends mostly on magnetic mineralogy and its concentration.

Pedogenesis and/or intense weathering induce hematite-magnetite transformation and reduction in effective grain size. This change is reflected in χ and χ_{FD}, which display higher susceptibility for magnetite. Simultaneous χ and χ_{FD} measurement discriminates active enhancement of ferrimagnetic minerals during pedogenesis from the passive enhancement caused by the leaching away of nonmagnetic components in the humus-rich horizon. Thus, a parallel increase of χ as well as χ_{FD} points to secondary origin, whereas variations of χ not associated with corresponding variation of χ_{FD} indicate contribution of ferrimagnetic minerals of primary origin. Therefore, χ and its frequency dependence are used to determine the intensity of weathering, and hence climatic changes in different environments.

High-field magnetic susceptibility: Hysteresis loop is used to determine χ at fields higher than the EMF. The field strength H_{MAX} relating to χ_{MAX} is practically independent of the percentage magnetite, but is connected with the grain size. The greater the grain size, the smaller is H_{MAX}. For pure crystals of magnetite, H_{MAX} will be 2 mT or even smaller. The ratio of χ_{MAX} to χ at the EMF does not appear to vary with the grain size, but is dependent on the percentage of magnetite by volume. Generally, the reversible high field susceptibility (χ_{HIGH}) is measured as the gradient of the magnetization slope between 800 and 1000 mT, indicating paramagnetic and antiferromagnetic component of a material minus the diamagnetic component.

Factors affecting susceptibility: Magnetic susceptibility is influenced by the type of magnetic minerals, their shape, size and the geological history. It decreases as a rule with decreasing grain size. Layered rocks always exhibit magnetic anisotropy, i.e. the susceptibility ($\chi_{||}$) along the layers is greater than the susceptibility across the layers ($\chi_{\perp}$). The magnetic anisotropy of a rock is defined by the ratio $\chi_{||}/\chi_{\perp}$. This ratio can be as high as 3.0 and is dependent on the percentage of magnetite content. This observation does not, however, apply to the susceptibilities obtained in situ. One of the main interests in the determination of the low field anisotropy of magnetic susceptibility (AMS) is its value as a petrofabric indicator. In magnetite, for example, shape anisotropy is dominant, as crystalline anisotropy is weak. Thus, for an elongate (nonspherical) magnetite grain, susceptibility measured in a magnetic field parallel to the grain's long axis would be greater than the susceptibility measured in the same field if that field is applied normal to the grain's long axis. AMS studies are useful in delineating individual flow directions of Deccan basalts, tectonic and metamorphic events of south Indian highly deformed rocks.

Curie temperature susceptibility, χ-T graphs: Low-field susceptibility is controlled by the internal forces acting in a grain. These in turn are determined by mineralogy, crystal structure, shape, and size of the grains. These parameters may vary with temperature as thermal energy of the system is increased or decreased. Magnetocrystalline anisotropy is particularly sensitive to temperature, and is dependent on crystal structure and composition only. High-temperature (high-T) and low- temperature (low-T) susceptibility were studied from liquid nitrogen temperature (–196°C) to 700°C. Measurements on natural and synthetically produced magnetites of known sizes have helped to define the major changes in χ with crystal size and domain, which are shown in Fig. 7.20.

The presence of minerals and domains is detected from the shapes of the χ-T curves and distinctive transition points. Figure 7.20 summarizes the more common features in low-T and high-T curves. The lack of irreversible change and the presence of several diagnostic transitions mean that low-T curves are easier to interpret than their high-T counterparts.

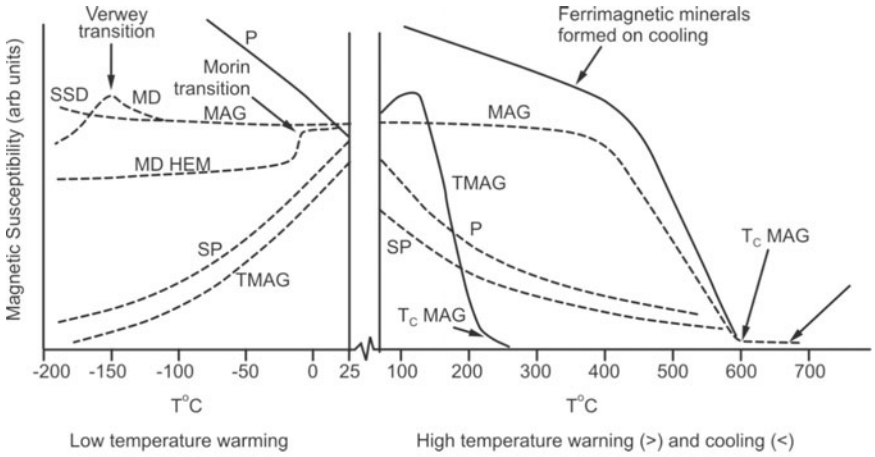

Figure 7.20. Schematic trends and transitions of κ_{lf} values from -196°C (liquid nitrogen) to 700°C for different minerals and domains; SP, SSD, MD, paramagnetic (P), magnetite (MAG: T_C 580°C), titanomagnetite (TMAG: T_C 250°C) and hematite (HEM). Susceptibility axis not to scale (*courtesy:* Dearing).

II. Anhysteretic Remanent Magnetization (ARM)

This parameter, independent of hysteresis effects, is measured by subjecting a sample to an increasing, then decreasing alternating field in the presence of a weak DC bias field, which serves to impart a magnetization in a known direction. Typical values for the peak alternating field (H_{AC}) are 100-300 mT, whereas the bias field varies between 30 and 100 μT. All ferrimagnetic minerals with a coercivity ≤ H_{AC} are remagnetized.

The ARM intensity is a function of the bias field, for low bias fields (<100 μT), it scales linearly. Hence by dividing the ARM intensity by the bias field value, a field-independent parameter is created, referred to as anhysteretic susceptibility (χ_{ARM}) through its analogy with χ. Some instruments allow the field to sense particular coercivity windows and such ARMs are referred to as partial ARM (pARM). ARM is considered to be a good analog of TRM created by cooling through the T_C in a small magnetic field. In particular, stable SD domain grains are sensed by ARM.

Anhysteretic remanence shows grain-size-dependence in magnetite (Fig. 7.21), such that SSD to PSD grains (0.02 to 0.1 μm) have a higher remanence than larger MD grains. It is suggested that IRM_{20mT}/χ_{ARM} ratios provide a simple way to discriminate between a ferrimagnetic mineral assemblage dominated by SSD or MD grain sizes (ca. >1 μm), aiding to clarify the dominant control upon χ_{ARM}. Also, the effects of SP or large MD grains which can dominate the χ are minimized. Ultrafine grains ranging from SSD to SP of ferrimagnetic minerals formed by pedogenesis give rise to characteristic χ_{ARM} and χ_{FD}.

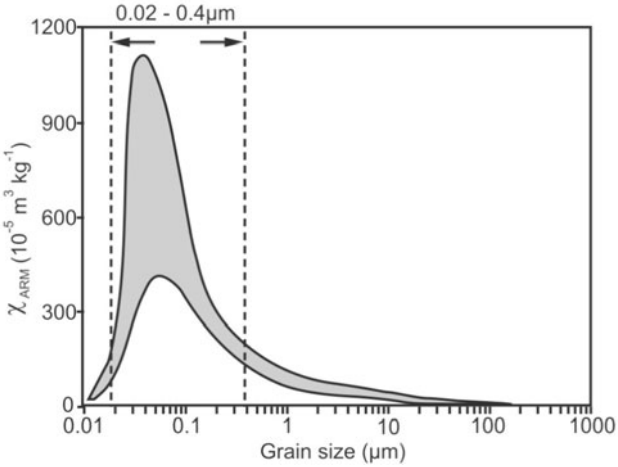

Figure 7.21. Variation of χ_{ARM} values with magnetic grain size in the 0.02–0.4 μm range for magnetite. With ferromagnetic grain sizes both above and below this range χ_{ARM} values drop quite dramatically (*courtesy:* Maher).

ARM is used in a variety of applications: (1) estimate absolute palaeointensity from igneous rocks, and relative palaeointensity from lake and marine sediments, (2) characterize magnetic carriers, and determine domain state/grain size, (3) detect magnetic fabrics in rocks/sediments, and (4) study the fundamental aspect of magnetism.

III. Isothermal Remanent Magnetization (IRM)

As indicated by the name, IRM is a remanent magnetization acquired without the aid of changes in temperature. The term IRM denotes a remanence resulting from the application and subsequent removal of a pulsed DC field. Beyond the threshold of χ measurements, magnetic substances magnetized in a direct field (H_{IRM}, generally >10 mT) follow a magnetization acquisition curve to a point of saturation (Fig. 7.22b). All ferro(i)magnetic grains with a coercivity ≤ H_{IRM} are remagnetized in the applied field direction. Since IRM is a strong-field remanence, the imparted magnetization is not linearly related to H_{IRM}.

Saturating IRM (SIRM) is the maximum IRM a sample can obtain, and is determined by recording IRM in progressively higher magnetic fields (Fig. 7.22b). On reaching saturation, IRM does not increase further regardless of strength (high) of the magnetic field. The saturation field depends strongly on the type and to some degree on the grain size distribution of magnetic mineral(s). For minerals such as hematite and goethite, magnetic fields larger than a few Tesla are required for saturation. Nevertheless, some laboratories with limited magnetic 'power' at their disposal still call IRM_{1T} as SIRM. Figure 7.23a shows grain-size dependence of SIRM for (titano-)magnetite, hematite and pyrrhotite. Thus, magnetite and hematite give out characteristic 'curves' when subjected

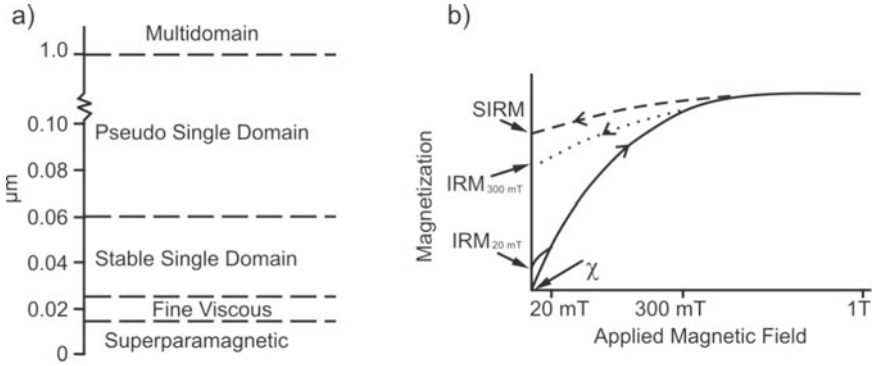

Figure 7.22. A sketch of: (a) Magnetic grain size boundaries and (b) IRM acquisition curve (*courtesy:* Oldfield).

to the entire spectrum of IRMs with an increase in induced field (Figs 7.24 and 7.25).

Low-field IRMs are not fully representative, because they are mainly influenced by magnetically 'soft' ferrimagnetic grain sizes. But, IRMs imparted in fields >300 mT reflect signatures of all remanence holding minerals, including canted antiferromagnetic and 'hard' and 'soft' ferrimagnetic minerals. A general linear relationship between SIRM and χ (Fig. 7.23b) can also be used to characterize the maximum possible range of magnetic mineral assemblages.

Further, a combination of magnetic parameters including the forward IRM acquisition curve, SIRM, coercivity, B_{CR}, IRM demagnetization curve and S-ratio are used to determine sediment sources.

IRM acquisition in forward and back-fields: Recently, researchers have started to measure IRM acquisition curve (remanence vs. log of the applied

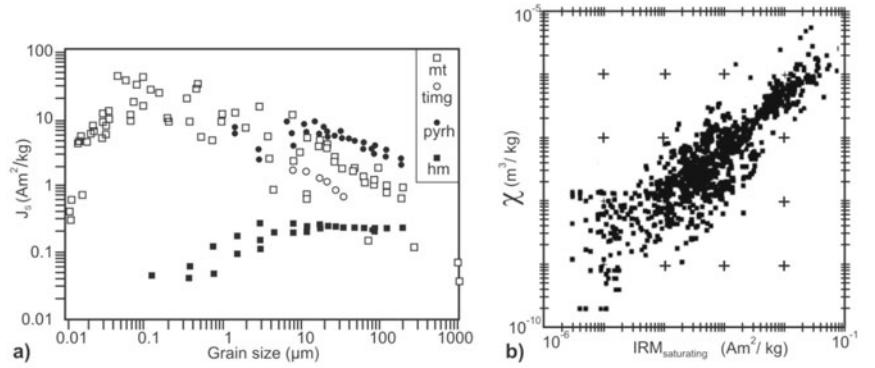

Figure 7.23. (a) Variation in intensity of Saturation IRM in different magnetic minerals as a function of grain size (*courtesy:* Jackson, 1991). (b) Log-log plot of 1000 natural samples (Thompson and Oldfield, 1986). The IRM is imparted in a magnetizing field strong enough to saturate magnetite.

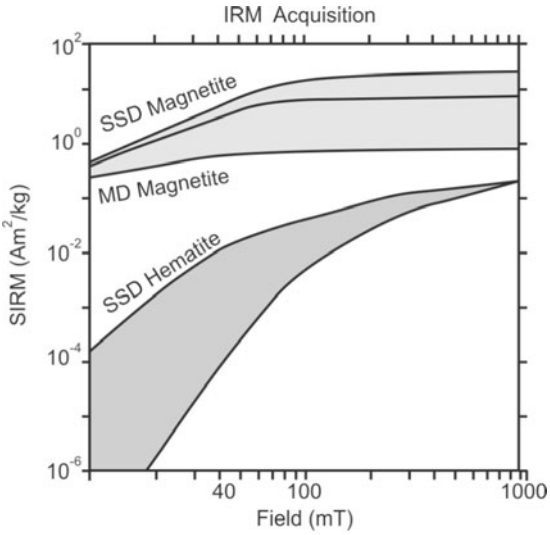

Figure 7.24. Acquisition of isothermal remanent magnetisation with increase in inducing field strength. Magnetite crystals have curves of acquired remanence that plot in the stippled area, whereas hematite crystals plot in the cross-hatched area (*courtesy:* Thompson).

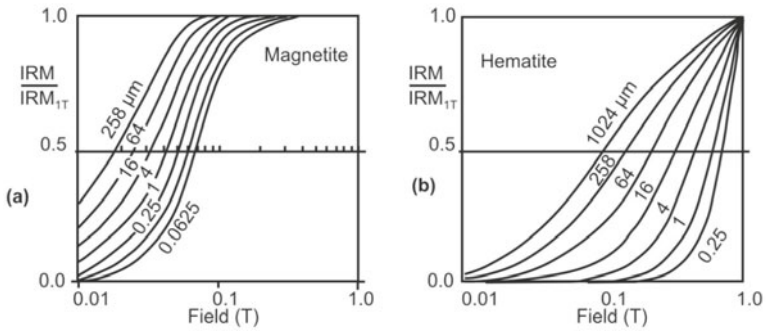

Figure 7.25. Empirically derived, idealized, normalized acquisition of isothermal remanent magnetization curves for magnetite (a) and hematite (b) of different grain sizes (*courtesy:* Thompson).

field); the gradient of this curve is the IRM coercivity spectra. In this process, a sample is demagnetized after ARM measurement, and then exposed initially to small fields (~20 mT), later on subjecting to a set of increasing magnetic fields, say in the range 0–4 T. All these fields are applied in the same direction and are commonly referred to as 'forward' fields. After each field is applied, the sample magnetization is measured. These values represent total combined vector for each field and can be termed as the 'raw' data. A typical IRM acquisition analysis requires a selection of a series of the following forward fields (all in mT): 20, 40, 60, 80, 100, 200, 300, 500, 600, 800 and 1000.

Such a progressive field produces IRM acquisition data, which can easily be compared with theoretically derived IRM acquisition data (Figs 7.24 and 7.25). Also, once the sample is saturated, a number of backfields may be used; the following set of fields is sufficient (all in mT): 20, 40, 100 and 300.

To understand/appreciate the form of raw data, a sequence of hypothetical measurements for four samples is listed out in Table 7.5. Note the data for samples 1 and 2. This is considered to be a 'good' one, since for the forward fields the remanence acquired becomes gradually greater and is always positive. It reaches a maximum at 1000 mT, and thereon when the backfields are applied (–20, –40, –100 and –300 mT), the SIRM at 1000 mT goes on reducing to eventually become negative. The data for samples 3 and 4, show errors at 300 and 100 mT forward reading, respectively. The 1000 mT forward field reading for sample 3 is slightly smaller than the 800 mT forward field reading. Also, for sample 4, the 300 mT backfield reading is in error, since it is larger than the saturation achieved by 1000 mT forward field. For possible errors in measurements, there are a number of explanations: (1) small calibration errors, (2) small differences in the orientation of the sample within the magnetometer, (3) movement of grains within the sample pot, and (4) delay between magnetization in the pulse magnetizer and the remanence measurement in the magnetometer.

Partial IRMs: Partial IRMs and their ratios are widely used for sediment characterization in environmental (rock) magnetism. For example, the hard fraction, HIRM, is determined by substracting the IRM acquired in 300 mT (IRM_{300}) from SIRM, to estimate the contribution of antiferromagnetic minerals (e.g. hematite and goethite) to the saturation remanence. HIRM is an absolute

Table 7.5 Hypothetical raw data for four samples generated using the combination of pulse magnetizer and magnetometer

Fields		*Sample 1*	*Sample 2*	*Sample 3*	*Sample 4*
20	forward (mT)	65.3	3.3	190.2	65.3
40		140.6	19.5	260.2	160.6
100		1025.7	70.6	792.4	–1095.7
300		1534.0	140.3	62.5	1634.0
500		1601.1	166.4	4112.3	1701.1
600		1606.3	185.3	4263.5	1706.3
800		1607.3	190.2	4302.6	1707.3
1000		1608.5	195.4	4296.5	1708.5
20	back (mT)	1200.6	140.3	2200.7	1300.6
40		800.6	26.4	–3.9	600.6
100		–792.3	–95.2	–1024.4	–992.3
300		–1554.6	–165.0	–2684.9	–1754.6

Values represent total combined vector taken from the magnetometer for each field (*courtesy:* Walden)

concentration-dependent parameter. The soft fraction is quantified in relative terms through S-ratios, calculated from measurements of SIRM and of the IRM subsequently acquired in backfields of 100 mT (IRM_{-100}) or 300 mT (IRM_{-300}): $S_{100} = -IRM_{-100}/SIRM$ and $S_{300} = -IRM_{-300}/SIRM$. These ratios range from –1 for samples containing only hard antiferromagnets to +1 for samples dominated by soft ferrimagnets. These parameters are frequently used in palaeoceanographic and environmental applications because they are sensitive to changes in magnetic mineralogy. Table 7.6 shows a hypothetical example of this process for an individual sample. In effect, it normalizes the data for each sample for its overall concentration of magnetic minerals, as indicated by SIRM. The advantage of this exercise is that it aids in comparing different samples and exhibits the proportion of remanence acquired by each one of them at relatively low or high fields helping to identify the relative proportions of magnetically 'soft' and 'hard' mineral species.

Component analysis of IRM coercivity spectra: In contrast to magnetic susceptibility, the remanent magnetization is carried only by ferro(i)magnetic minerals. The ability to retain a remanent magnetization is a coercivity parameter and is dependent on grain size, temperature, and an applied field. Information about the remanence carriers can be obtained by analyzing IRM coercivity spectra. The coercivity of grains is governed by their volume, shape, stress, oxidation state and impurity content. Therefore, an attempt can be made to separate and quantify different magnetic components according to their coercivities. Another way to quantify mixed magnetic mineralogy is the IRM component analysis, the decomposition of a measured IRM acquisition curve into several components with the use of model analysis. Initially, cumulative log-Gaussian curves are used to closely conform to measured IRM acquisition

Table 7.6 Processing of a raw data set to produce mass specific IRM data for each forward field and IRM/SIRM ratios for both the forward and back fields

Sample weight = 10.09 g			*Forward field only*	*All fields*
Field used		*Raw data (total combined vector × 1.29)*	*Mass specific IRM*	*IRM/SIRM ratio*
20	forward (mT)	57.7	5.72	0.25
500		199.3	19.75	0.86
600		217.8	21.59	0.94
1000		230.7	22.86	1.00
20	back (mT)	83.9		0.36
100		–143.6		–0.26
300		–204.8		–0.89

Hypothetical data for an individual sample. The raw data values represent the total combined vector taken from the magnetometer (*courtesy:* Walden)

curves. Recently Kruiver and her coworkers proposed the use of the F-test (and t-test) to judge upon the number of coercivity fractions required for the optimal fit.

IV. Demagnetization Parameters

Demagnetization techniques test the stability of the magnetic minerals that carry the remanent magnetization, and provide information on their properties. Starting from the SIRM state, application of successively larger backfields causes the net remanence first to decrease, and then to grow in the reverse direction eventually reaching the negative SIRM state. This process is often termed DC demagnetization (Figs 7.26 and 7.27), and is similar to a part of the isothermal remanent hysteresis cycle.

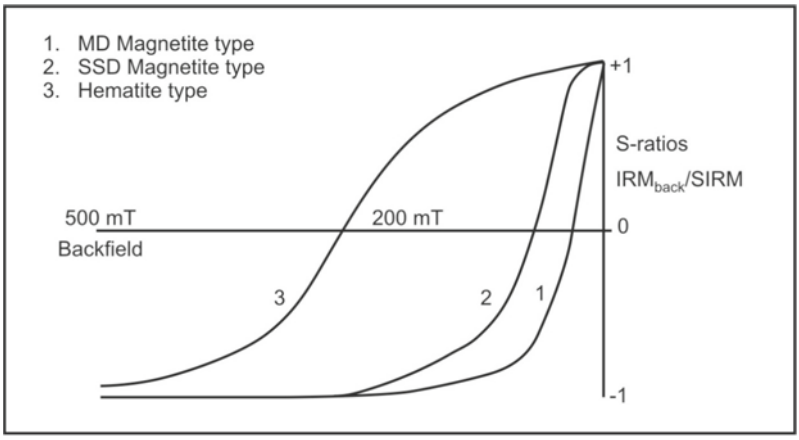

Figure 7.26. Typical coercivity spectra plots for MD magnetite, SSD magnetite and hematite.

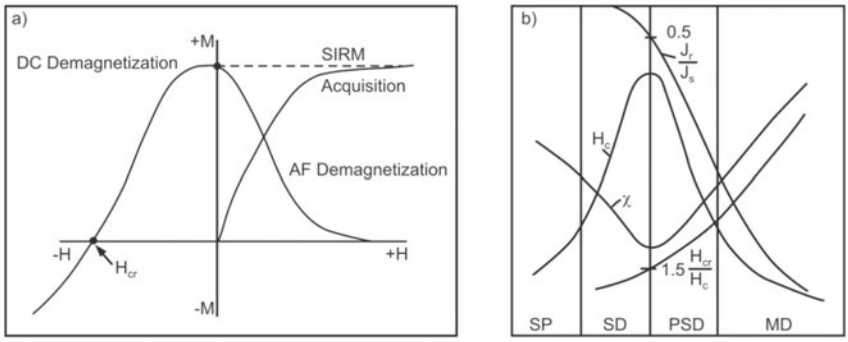

Figure 7.27. (a) Comparison of DC demagnetization, IRM acquisition and AF demagnetization. (b) Magnetic properties of small particles: H_c coercive force, χ susceptibility, M_{rs}/M_s and H_{cr}/H_c (*courtesy:* Soffel).

Assemblages dominated by MD and SP grains exhibit 'soft' demagnetization behaviour, because they easily relinquish the induced alignment of their moments, through domain relocation and thermal disordering. Characteristically, concave demagnetization curves result with low H_{CR} (backfield at which the IRM equals zero) values and reverse saturation attained in low field strengths (Fig. 7.27b). A slightly more resistant curve arises from the harder response of SSD grains, giving a convexity in the upper part of the curve due to initial resistance in the lower fields before realigning at slightly higher intensities. Coercivity curves derived from canted antiferromagnetic minerals contrast with those typically characterizing ferrimagnetic minerals (Fig. 7.26), e.g. convexity of the curve indicates the extreme magnetic 'hardness' of the material giving high (>60 mT) values of H_{CR}, which only attain reverse saturation at maximum backfield intensities. Coercivity is thus seen to sensitively discriminate between natural samples, even where the curves are composite results of mineral and grain size mixtures.

The two parameters of the coercivity spectra, simplified S-ratios ($IRM_{-0.1T}/IRM_{1T}$) and Y-percentages [$(IRM_{-0.3T}/IRM_{1T} \times 2) \times 100$], are useful to discriminate between 'hard' and 'soft' magnetic minerals (Fig. 7.26). A sample's coercivity spectrum is estimated by plotting the ratio of IRM to $IRM_{0.8T}$ for a range of backfields (5–500 mT). High H_{CR} suggests 'hard' or 'hematite type' behaviour. Intermediate and low values indicate SSD and MD 'magnetite type' behaviour, respectively.

With AF demagnetization, the peak AF is increased until magnetic minerals with the highest coercivity are demagnetized (Fig. 7.27a). It is important to note that coercive force values are concentration-independent. To a first-order description, this is warranted in many natural situations. Under this condition, values of magnetizations and various remanences scale linear with the concentration of the magnetic minerals. By dividing two concentration-dependent parameters, a concentration-independent ratio is obtained that contains information on grain size or the oxidation degree of the magnetic mineral.

V. Hysteresis and Remanence Coercivity

Most of the fundamental magnetic properties used in environmental magnetism studies can be illustrated and defined with reference to a hypothetical hysteresis loop (Fig. 7.28) for an assemblage of randomly oriented ferro(i)magnetic grains ranging in size from MD through to SSD and SP.

The induced magnetization rises (shown by [a] on the apparent curve) when a small magnetic field is applied (Fig. 7.28). On removal, however, the magnetization intensity returns to 'pre-magnetized' state. This linear and reversible response is produced by the combined reactions of the constituent magnetic grains: (1) in MD grains, reversible movement of domain walls causes enlargement of domains, whose moments are aligned closest to the field direction. Conversely, slight rotation of the nonaligned moments also takes

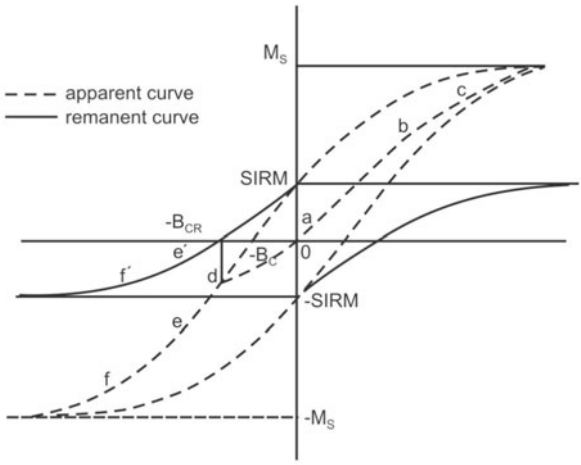

Figure 7.28. The hysteresis loop of a magnetic material. Various symbols are explained in the text (*courtesy:* Dankers).

place, (2) in SSD grains, there is slight domain rotation towards the field direction, whereas (3) SP grains spend a proportionally longer time aligned within the field. The gradient of the curve (a) gives the χ of the sample. The χ is the magnetization observed in low field, which is equivalent to the Earth's field (50–100 μT).

Subsequently, when the applied field intensity is increased, magnetization again increases, but now non-linearly (part [b] of the apparent curve), and the process is no longer reversible. When the applied field is removed, the induced magnetization does not return to its origin, but merely relaxes towards a level of remanent intensity defined as IRM. This non-reversible magnetization process is produced by contributions from MD and SSD grains. In MD grains, it is caused due to irreversible domain wall movements, while in SSD it is by irreversible flipping or rotating of the previous easy axes of magnetization. SP grains do not contribute to remanence, since their in-field alignment is lost through thermal disordering immediately upon removal from the field. Further increase in applied field intensity induces increased in-field and remanent magnetization. But, a point is reached where no further in-field magnetization is attained despite continued field increase. This point represents the largest magnetization the assemblage can attain with maximum alignment of: (1) the domains of the larger grains (achieved through energized wall movement), (2) the individual domains of the small grains (which have all been flipped and/or rotated), and (3) the individual SP grains. This maximum magnetization is termed the saturation magnetization (M_S on the apparent curve), which relaxes to the saturation IRM (SIRM, on the remanent curve). M_S is measured in the laboratory by applying a magnetic field over 1 to 2 T.

The amount of viscous magnetization loss undergone by a sample from its M_S to its SIRM is dependent on the grain sizes present with the moments of

MD and to a lesser extent SSD grains. These tend to readjust and relax towards their inherent easy axes of magnetization, while the SP grains totally lose their imposed in-field magnetic order. The ratio of SIRM to M_s for an assemblage of randomly oriented SSD grains has been theoretically calculated as 0.5 for magnetite and Ti-magnetite, PSD grains give a ratio between 0.1 and 0.3 for magnetite and 0.05 for Ti-magnetite, and MD and SP grains tend towards a ratio of zero. Thus, the viscous loss is greatest for SP and MD grains and least for the SSD configuration (Figs 7.29, 7.30 and Table 7.7).

Having attained forward saturation of the sample, a series of fields is then applied in the opposite direction to identify DC demagnetization behaviour of mineralogy and grain volume. This is attained by verifying the degree of ease (or difficulty) with which the induced forward magnetization can be reduced and then reversed. The point (d) on the remanent curve reveals the SIRM to have been reduced to zero. The field intensity required to achieve this is the parameter of remanent coercivity (B_{CR}). At this point, half of the remanent magnetization is directed opposite to the original remanent saturation direction.

Table 7.7 Magnetic hysteresis properties of some pure samples of known narrow grain size

Sample	*Domain state*	M_S 10^{-6} *A m*^{2}	M_{RS} 10^{-6} *A m*^{2}	M_{RS}/M_S	B_C *mT*	B_{CR} *mT*	B_{CR}/B_C
Magnetite	fine PSD	2.32	0.92	0.397	38.4	57.7	1.5
Magnetite	PSD	1.80	0.29	0.162	8.7	18.6	2.1
Magnetite	MD	9.07	0.08	0.008	1.2	14.4	12.0
Magnetite	MD	7.67	0.09	0.011	1.4	12.0	8.8
Hematite	SD	1.98	1.19	0.602	150	230	1.5
Greigite	SD	0.81	0.45	0.557	53.8	69.4	1.3

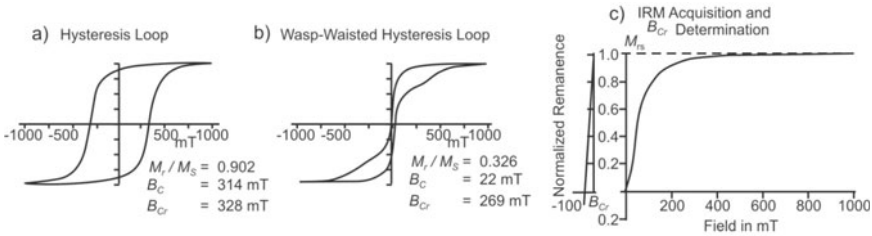

Figure 7.29. Examples of magnetic hysteresis loops (a, b). (a) Hysteresis loop of an ensemble of SSD, characterized by square hysteresis loops; loops of PSD and MD are increasingly slender and have inclined slopes hysteresis loop for hematite. (b) Example 'wasp-waisted' hysteresis loop. The central section is smaller than the outer parts. Wasp-waisted loops are typically of mixed phases with contrasting coercivities: either a mixture of two magnetic minerals (magnetite and hematite in the present case) or a mixture of SP and MD of the same mineral. (c) Determination of an IRM acquisition curve and the remanent coercive force (*courtesy:* Dekkers).

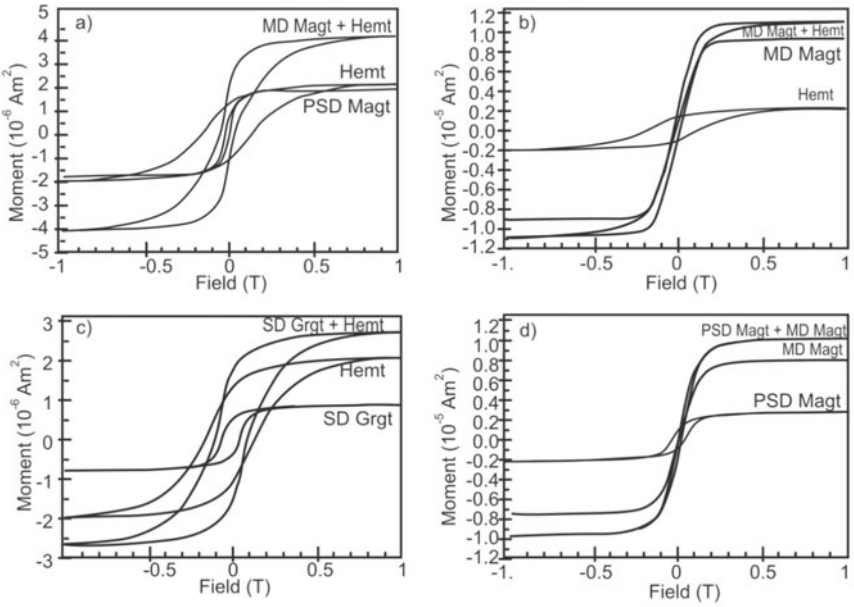

Figure 7.30. Hysteresis loops for two pure samples of known grain size, shown with the composite loop obtained by measuring both samples together. Loops are listed from lowest to highest moment: (a) PSD magnetite, hematite, PSD magnetite + hematite; (b) hematite, MD magnetite, MD magnetite + hematite; (c) SD greigite, hematite, SD greigite + hematite; and (d) PSD magnetite, MD magnetite, PSD + MD magnetite. The hysteresis parameters for these samples are listed in Table 7.7 and can be matched by comparing M_s values (*courtesy:* Roberts).

These two directional moments being 'equal but opposing' cancel each other thereby producing a zero net moment. On the apparent curve, the coercive force B_C (Fig. 7.28) occurs, where in-field forward and reverse magnetizations are 'equal and balanced'. Continued increased intensity of the reverse fields past the B_C and B_{CR} points causes the induced magnetization to follow the paths (e) to (f) and (e') to (f') on the apparent and remanent curves, respectively. The cycle of hysteresis is then completed with the attainment of reverse saturation and remanent magnetizations (M_S and –SIRM). A reverse field of 300 mT corresponding to point (f) on the curve, denoted by IRM_{-300} is given by (Of'). The ratio IRM/SIRM at a specific reverse field is denoted by [S-ratio] (Fig. 7.28). For hematite, B_{CR} is >0.2 T; for magnetite it is ~0.05 T. Values of S–ratio (~IRM_{-300}/SIRM) of ~1 indicate a high proportion of magnetite, whereas the lower values indicate an increasing proportion of hematite and goethite.

Day plot and hysteresis loops: If there is only one magnetic mineral, and it is known to be magnetite or titanomagnetite, the grain size can often be estimated from the plot of two ratios between magnetization (M_{rs}/M_s), and coercivity (H_{cr}/H_c). It is called the Day plot obtained from bulk hysteresis parameters.

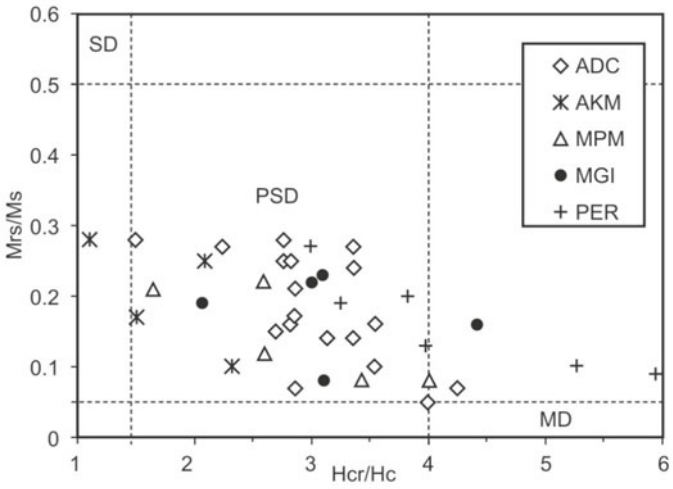

Figure 7.31. The data of Indian archaeological samples as shown on 'Day plot'. ADC - Adhichanallur, AKM - Azhagankulam, MGI - Mangudi, MPM - Mamallapuram and PER - Perur. M_S = saturation magnetization, M_{rS} = saturation remanent magnetization, H_c = coercivity, H_{cr} = remanent coercive force. The plot is usually divided into regions: SD for $M_{rS}/M_S > 0.5$ and $H_{Cr}/H_C < 1.5$, MD for $M_{rS}/M_S < 0.05$ and $H_{Cr}/H_C > 4$ and PSD.

Figure 7.31 illustrates how SSD, PSD and MD grains can be recognized through their magnetization and coercivity ratios in the Indian archaeological samples, where identification of SSD magnetic grains is important in absolute paleointensity studies.

7.9 SECONDARY MAGNETIC PARAMETERS: INTERPARAMETRIC RATIOS

Concentration independent parameters: These reflect relative proportions of magnetic minerals of different types and/or grain sizes and are thus mainly unaffected by bulk concentration of magnetic material in a sample. These are inter-paramagnetic quotients (or ratios) primarily influenced by either the mineralogical or granulometric composition of the sample's magnetic assemblage rather than its bulk concentration. The most important concentration-independent parameters include S-ratio, SIRM/χ, χ_{arm}/χ, χ_{arm}/SIRM, χ_{fd}%, HIRM%, SIRM/M_S, B_{CR}/B_C and M_{RS}/M_S.

Rock magnetic parameters and their ratios: In routine environmental studies, about a dozen magnetic parameters and ratios are used to characterize magnetic materials, which basically relate to four main aspects of mineral magnetic properties (Table 7.8). These are: (i) the concentration of magnetic minerals, (ii) the stability of the magnetization (measured by the hysteresis loop width; goethite and hematite have high stabilities, hence low S-ratios), (iii) the

squareness of the hysteresis loop (related to steepest gradient of the hysteresis loop; goethite and hematite show square loops that can be identified by IRM/χ ratio), and (iv) the type of magnetic interactions between crystals as chains (Table 7.8).

Table 7.8 Four important mineral magnetic properties

Characteristic	*Hysteresis loop*	*Remanence*
Concentration	Height	IRMs
Stability	Width	S ratios or ARM demag
Ease of magnetization	Squareness	SIRM/χ or ARM/χ
Grain interactions	Steepness	ARM/SIRM

Figure 7.32 presents a flowchart which shows how a few magnetic measurements can be used to discriminate between the major magnetic constituents. The flowchart uses magnetic ratios rather than individual magnetic properties, because individual remanence or magnetization measurements predominantly reflect just magnetic concentration, and not magnetic mineralogy. In the flow chart, four types of magnetic ratio have been listed to aid in mineral discrimination. They are: (i) S-ratios which relate to IRM acquisition, (ii) IRM/χ and ARM/χ ratios, measure of the shape/squareness of hysteresis loop, (iii) ratio A_{-40}, a measure of the stability of the anhysteretic remanence and (iv) ratio ARM/SIRM, which is related to the strength of grain interactions. Table 7.9 summarizes typical values of these four types of ratio for a range of natural magnetic minerals. A biplot of magnetic stability against squareness (Fig. 7.33) graphically reveals these differences for a range of magnetic minerals, grain sizes and morphologies.

Table 7.9 Typical magnetic ratios of natural minerals (*courtesy:* Maher and Thompson)

Mineral	*SIRM/χ (kA m^{-1})*	*S_{40}*	*S_{100}*	*A_{-40}*	*A/S*	*ARM/χ (kA m^{-1})*
Magnetite (soft)	1.6	0.83	0.97	0.001	0.02	0.03
Magnetite (hard)	55	0.26	0.85	0.5	0.005	0.3
Titanomagnetite (soft)	10	0.5	0.82	0.24	0.004	0.5
Titanomagnetite (hard)	60	0.08	0.34	0.9	0.04	2.4
Hematite	400	0.005	0.003	Low	0.001	0.01
Ilmenohematite	320	0.02	0.13	0.9	0.004	19.0
Greigite	92	0.03	0.38	0.8	0.01	0.9
Pyrrhotite (soft)	90	0.8	0.95	0.04	0.018	1.6
Goethite	70	0.005	0.02	Low	0.01	1.0
Iron	40	0.4	0.8	0.5	0.01	0.4

S_{40}: proportion of SIRM grown in a forward DC field of 40 mT
S_{100}: proportion of SIRM grown in a forward DC field of 100 mT
A_{-40}: proportion of ARM remaining after partial demagnetization in a peak alternating field of 40 mT
A/S: ratio of ARM to SIRM

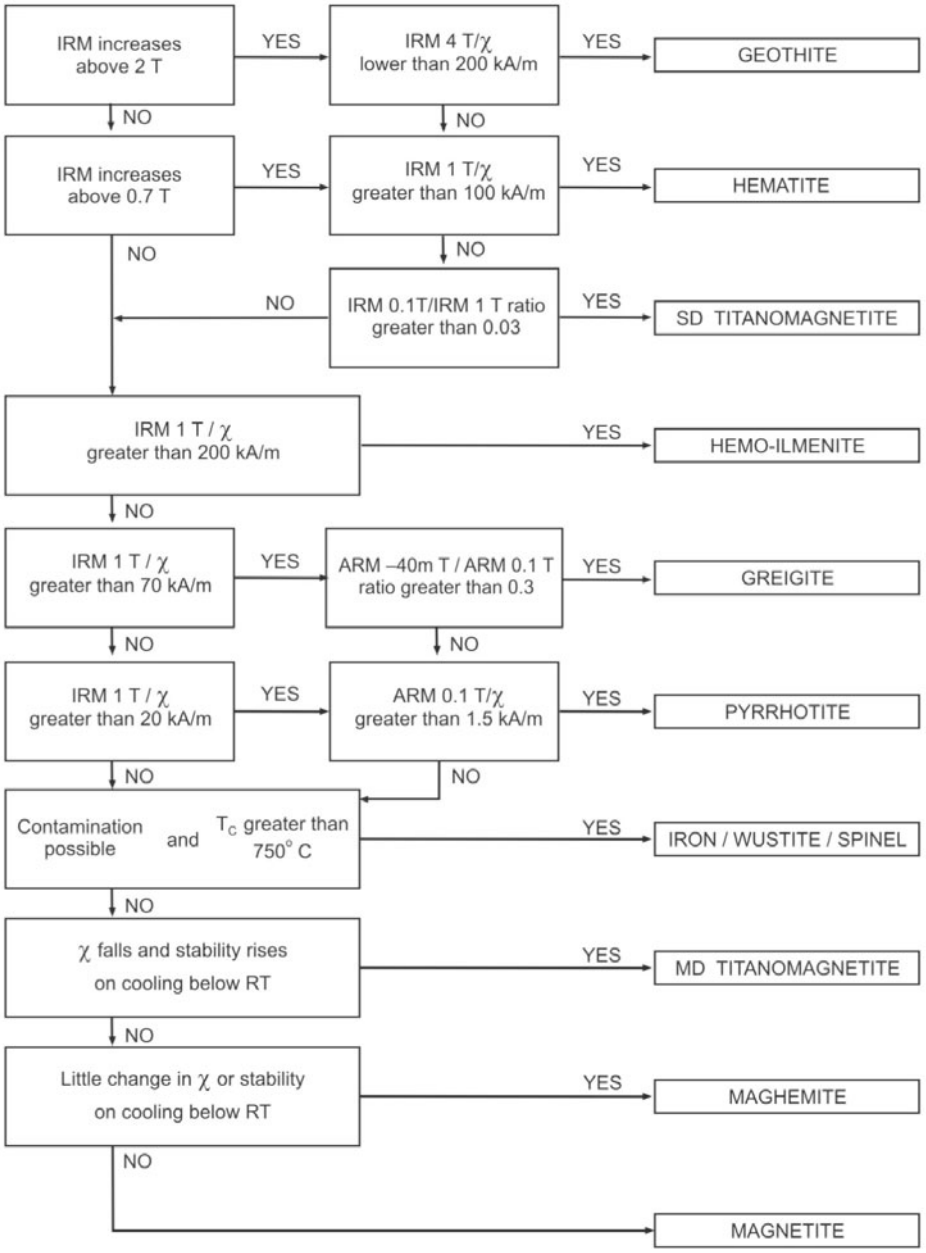

Figure 7.32. A flowchart indicating utility of few magnetic measurements to discriminate between the major magnetic minerals found in environmental samples. Note few magnetic measurements are sufficient to identify major magnetic constituents in the samples (Maher and Thompson, 1999).

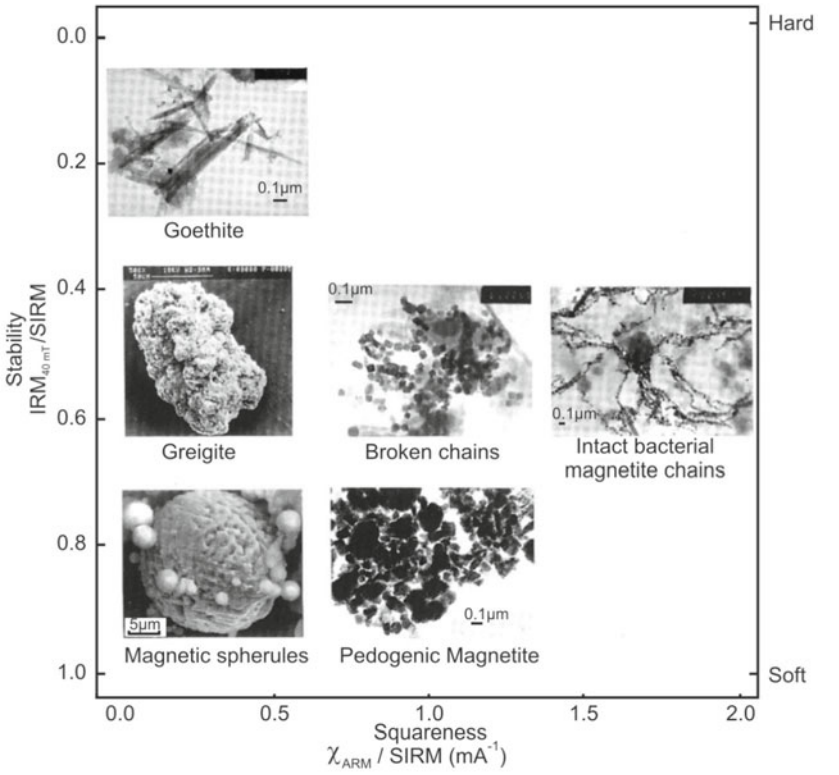

Figure 7.33. A biplot of magnetic stability vs. squareness showing six examples of different magnetic minerals, grain sizes and morphologies (*courtesy:* Maher and Thompson).

7.10 MAGNETIC STUDIES, COMPLEX ISSUES

Magnetic method is a powerful tool to reconstruct environmental history, though it is restricted in its application by the potential complexity of relationship between sediment sources and sinks. A catchment has several magnetically distinguishable sources, because of which determining relative source contributions become mathematically and statistically complicated.

A significant impediment to use of lake and marine sediment records is the post-depositional chemical changes in magnetic mineralogy. Dissolution is a diagenetic process that involves initial loss of the finest magnetic fraction and later on the coarser magnetic minerals. In such cases, the assumption of an entirely detrital origin becomes erroneous, because it requires the presumption that magnetic properties are conserved during transport from the source to the sink.

Apart from the chemical reduction of magnetite, marine and freshwater bacterium are also found capable of dissolving and reducing magnetite. Iron sulfides such as greigite, and fine grained (SSD) biogenic magnetite are reported

to have authigenically grown in lacustrine and marine sediments. These minerals are produced intracellularly and to some extent extracellularly. Magnetic bacteria have also been found in soils as well. Thus, biogenic ferrimagnetic minerals can make a contribution to the assemblage of magnetic minerals in sediments, although this contribution is likely to be more significant in depositional environments that favour the growth of magnetotactic bacteria.

An important issue associated with sediment transportation processes is the complex relationship between sediment particle size and magnetic properties. The highest χ values occur in the <125 μm fraction of river bed sediment, implying downstream increase in particle sorting, which makes the sediment progressively finer. However, this relatively simple setting is complicated by other processes that come into play in the form of abrasion, particle breakage or the selective deposition of heavy minerals that contain a high proportion of magnetic minerals (like magnetite). To reduce ambiguity associated with sediment transport, it thus becomes necessary to conduct tracing studies on well defined (laboratory sorted) particle size fractions. This may, however, not eliminate magnetic mineral dilution or enrichment by fluvial sorting processes.

I. The Mixing and Unmixing Problem

Rocks and sediments inevitably contain mixtures of magnetic minerals of different grain sizes and weathering states. Most environmental (rock) magnetic techniques rely on a set of parameters, designed to interpret in terms of mineralogy, concentration and domain state of magnetic minerals. In some cases, however, such interpretation of natural samples can be misleading. A more reliable approach to magnetic mineralogy models is based on the analysis of magnetization curves, which are decomposed into a set of elementary contributions characterizing specific set of magnetic grains with unimodal distribution (component analysis) of physical and chemical properties. Magnetic components are then related to specific biogeochemical signatures, not characterized as just SSD magnetite. This unconventional approach opens up a direct link to the interpretation of natural processes on a multidisciplinary level. Despite these advantages, component analysis has not yet come into wide use for three reasons: (1) lack of quantitative magnetic models for natural, non-ideal magnetic grains, and/or the statistical distribution of their properties, (2) intrinsic mathematical complexity of unmixing problems, and (3) need of accurate measurements that are beyond the usual standards.

Since magnetic components rarely occur alone in natural samples, unmixing techniques and rock magnetic models are interdependent. Recently, efforts have been initiated to verify the basic properties of magnetization curves, and obtain useful/reliable solutions to the unmixing problem. It has already resulted in collection of a few hundred magnetic components from various natural environments. The properties of these components are controlled by their biogeochemical history, regardless of the provenance of the hosting sediment.

For example, the coercivity of all detrital magnetites is tuned by the transport mechanism (air/water) and the ARM of biogenic magnetites is controlled by their (paleo)redox condition. The consistency of these results supports the linear additivity principle upon which all current magnetic unmixing methods are based. Once the rock magnetic properties of individual components and their statistical distribution are known, the solution of unmixing problems provides important benefits. One of the major benefits pertains to making the whole process simple, thereby making it accessible to even the non-specialized users. Simplified unmixing algorithms are robust, and are capable of delivering reliable results based on relatively fast measurements.

II. Ternary Diagram and Thermomagnetic Curves

In the context of mineral magnetic studies, it is those minerals spanning the solid solution series between magnetite (Fe_3O_4) and maghemite (γFe_2O_3), which are most important. In addition, the various Ti substituted compositions of these two minerals called titanomagnetite and titanomaghemite often dominate much of the magnetic information gained from the bulk sample measurements.

Three solid solution series on Fig. 7.34 have a characteristic crystal form, but vary in their composition, especially the Fe/Ti ratio (Chapter 2). As the material oxidizes, it moves across a constant Ti/Fe ratio line signifying increase in its oxygen concentration. The titanomagnetites solid solution series are usually found in basic igneous rocks with a movement towards the magnetite end of the series as rocks become more acidic. The ilmenite-hematite solid solution series are usually found in more oxygen-rich environments. For example, hematite can be formed by the oxidation of titanomagnetites or by inversion of maghematite (>350°C). The minerals of pseudo-brookite solid solution series are all paramagnetic above liquid oxygen temperature (Chapter 2). At low latitudes, weathering in the form of low temperature oxidation (LTO) of titanomagnetites yields ferro(i)magnetic mineral as a product through the process of maghemitization. Pyrrhotite (FeS_{1+x}, $0<x<0.15$) when present also contributes to LTO.

Thermomagnetic analysis determines the compositional diagnostic T_C for different minerals by monitoring high-field magnetization M_S-T, and low-field susceptibility (χ-T) during heating to a maximum of 700°C (Figs 7.20 and 7.34). This together with results of chemical analyses plotted on ternary diagram, can be diagnostic of the chemistry of magnetic minerals. Two points in the ternary diagram represent chemical composition of the magnetic mineral between Fe-Ti oxides. Curie temperatures change with oxidation degree of the magnetic mineral according to its position in ternary diagram and Ti content. Thermal alteration frequently occurs, when the magnetic mineral is heated. Alteration temperatures and thermomagnetic behaviour of the alteration products provide further information as to the initial mineralogy of the sample. Use of magnetic measurements at cryogenic temperatures for characterizing magnetic mineralogy is becoming a valuable new tool in rock magnetic and

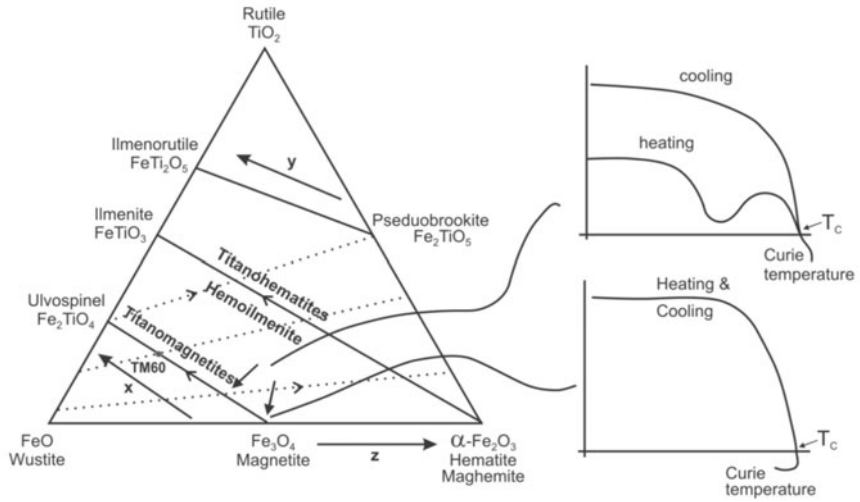

Figure 7.34. Ternary diagram for iron oxides. Solid lines are solid solution series with increasing titanium concentration (x). The dashed lines with arrow indicate the direction of oxidation (z). Two typical examples show compositional relationships (*x* or *y*) and Curie temperatures of Fe-Ti oxide minerals (http://magician.ucsd.edu/Essentials/WebBook162x.png).

environmental magnetic investigations. This is because low-T magnetometry has the potential to complement conventional high-T methods, while offering an advantage of avoiding chemical alteration in magnetic mineralogy during heating.

The various enviromagnetic parameters and their combinations discussed here are employed for the purpose of answering three broad questions: (1) Composition (i.e. which magnetic minerals are present?), (2) Concentration (i.e. how much of each one is present?), and (3) Granulometry (i.e. what are the dominant grain sizes present?).

7.11 ENVIRONMENTAL MAGNETISM—ITS APPLICATION TO THE INDIAN DEPOSITIONAL SETTINGS

Mineral magnetic variations, depending on the environmental context, are used as an aid towards elucidation of a diversity of problems. Several Indian research groups are working diligently to reconstruct palaeoclimate over the subcontinent, and its contiguous oceanic realm. These studies offer considerable potential to correlate marine and terrestrial sequences. However, only a few investigators have used rock magnetic and environmental magnetic properties to extract palaeoclimatic and palaeoceanographic information, which has been presented in the next sections.

Depositional environments under investigation: Indian subcontinent has many sedimentary basins, which are investigated for a complete perception of

the sources and processes to understand subcontinental environmental and climatic changes. In this attempt, use of other techniques such as X-ray diffraction (XRD), scanning electron microscope (SEM), and transmission electron microscope (TEM) is undertaken to confirm rock magnetic interpretation.

Mineral magnetic measurements have been performed on core and hand specimens collected from India encompassing depositional environments of varying type and provenance, viz. ~>4.0 Ma Kashmir Karewa palaeolake sequence; ~10 ka to ~30 ka old palaeolake sequences in the central higher Himalayas at Goting, Pipalkoti, Burfu and Garbayang; ~12 ka shallow playa lakes of Thar desert in Rajasthan; Nalsarovar lake in Gujarat, which is almost ~6.0 ka; ~5.0 ka Mastani lake near Pune; ~500 years old Powai and Tulsi lakes in Mumbai city; near shore deltaic/estuarine environments like those of Godavari, Krishna, Cauvery and Iskapalli situated on east coast and Mandovi on west coast; ~25 ka Himalayan loess deposits, ~25 ka, ~50 ka and ~120 ka terra rossae palaeosols of Saurashtra, and beach samples of Maharashtra, Karnataka and Goa. Figure 7.35 shows the locations, from where sedimentary samples have been collected for environmental magnetic investigations.

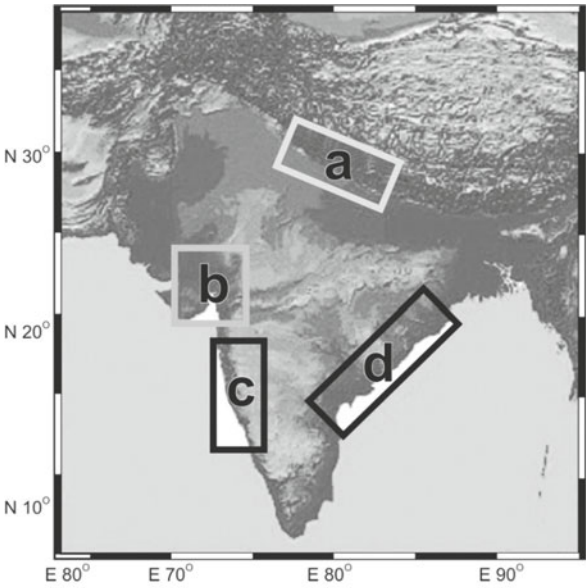

Figure 7.35. Location map of the samples collected for environmental mineral magnetic studies. Digital elevation model based on 1-arc sec resolution (~0.03 km) GTOPO30 data. (a) Proglacial lake deposits from central higher Himalayas, (b) Thar desert lakes and playas, Gulf of Kutch coastal deposits and continental deposits in Mainland Gujarat, (c) Mumbai lakes and Konkan belts covering estuaries in Goa and mangroves along the west coast and (d) East coast deltas, viz. Mahanadi, Krishna, Godavari, Cauvery and Pennar. In these regions stress is being given on mangrove deposits as they are ideal sites for using the mineral magnetic approach.

7.12 MAGNETIC SUSCEPTIBILITY AND DEPOSITIONAL ENVIRONMENTS

How stable are Fe oxides in a given set of environmental conditions, and modify with a change in chemical and physical ambience are discussed earlier. Since they have the diagnostic ability at interconversions between different phases, magnetic minerals are used as a quantified and calibrated proxy. The premise is based on the fact that magnetic mineralogy reflects the course of environmental (climate) changes by recording evidence of associated modifications in sedimentation, weathering and pedogenic regimes. In all, magnetic susceptibility is found to be a valuable tool that accurately plays back the original signals entrenched in the sediments.

I. Magnetic Susceptibility and Mangrove Sediments

In India, mangroves are unevenly distributed along the east and west coast regions. Because of major deltas along the east coast, the mangroves here are better and well developed compared to those along the west coast. Factors such as geomorphology, climate, tidal amplitude/duration and quantity of freshwater inflow determine the mangrove distribution, wherein the sedimentation is influenced by interaction between the mangrove root systems and sediment laden tidal waters.

Indian climate is dominated by two monsoon seasons, and the rate of rainfall varies considerably from one place to the other. Holocene monsoonal and environmental changes are stored in mangrove swamps, where high rate of sediment accumulation takes place. Accordingly, the mangrove swamps develop into good storage sites with a huge pile of fine black clays and silts ideally suited for high-resolution palaeoclimatic study. Natural events and man-made changes have significant impact on the climate, which in turn affects the vegetation, and these signatures are reflected in the subsurface sediments of mangroves. As of now, there is hardly any input of environmental magnetism from the mangrove swamp sediments of India, and hence there is tremendous scope to utilize this technique.

In sediments of Deccan basalts, the magnetization is due mainly to large-grained (titano)magnetite grains of high χ. But, when the rock or sediment weathers by the passage of water through cracks, it results in oxidized grains such as hematite that has a much lower χ. The core logs of χ are used for two studies: (1) to see if different outcrops could be characterized for their similar or dissimilar origins and (2) to use weathering profiles to differentiate diverse depositional sequences.

The transition or variation in χ is governed by a change in the depositional environment. For example, the characteristic feature of mangrove sediments is the display of very low and consistently invariant χ values, which discriminate these deposits from others (Figs 7.36 and 7.37). The section from the base to 40 cm depth, where there is a change in environment, is dominated by very

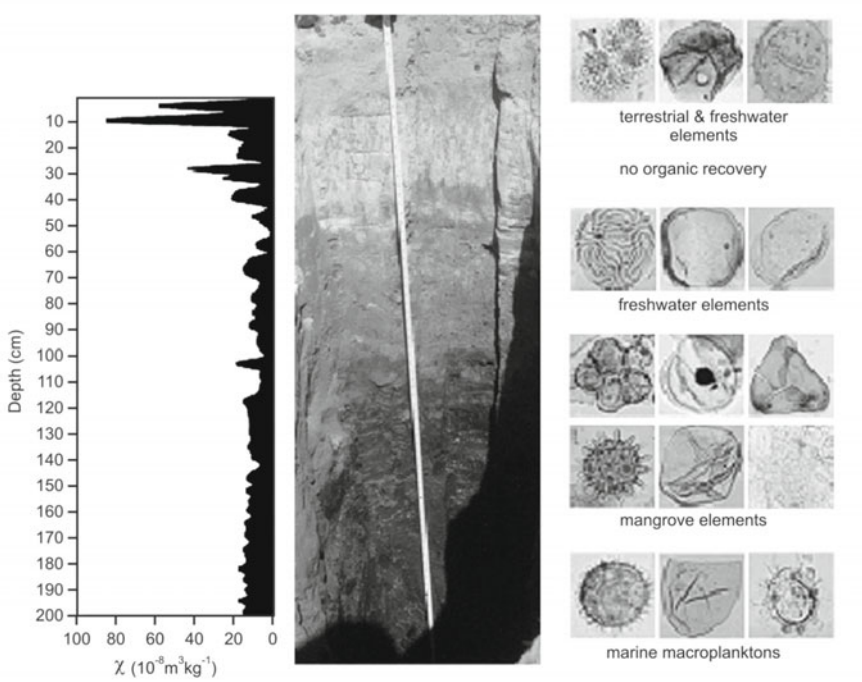

Figure 7.36. The Hadi mangrove sediment core with representative microfossil assemblages at different species and corresponding magnetic susceptibility curve. The low and invariant χ values correspond to the dark clays of mangrove origin. Magnetic susceptibility together with palynoflora enables to recognize marine, estuarine, freshwater aquatics, sandy beach and terrestrial or hinterland ecological complexes (Kumaran et al., 2004).

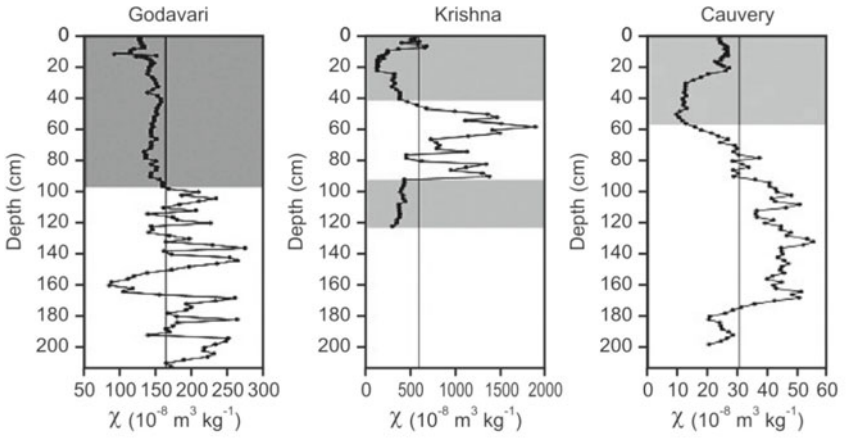

Figure 7.37. The mangrove sediments from east coast deltaic vibra-cores exhibit low and invariant magnetic susceptibility values. The χ logs across three major east coast deltaic basins distinguish depositional mangrove environments from non-depositional ones in a relatively more reliable and inexpensive manner (Seetharamaiah et al., 2004).

low χ variation reflecting mangrove elements (Fig. 7.36). The terrestrial and freshwater sediment input increase χ values significantly towards the top.

The major peninsular rivers like Godavari, Krishna and Cauvery have built large deltas on the eastern coast of India over a total area of ~19,187 sq km. The initiation of these modern deltas is believed to have begun ~8.5–6.5 ka and the rivers bring in a total sediment load of 28×10^9 tonnes annually to the Bay of Bengal. These deltas are characterized by the presence of extensive mangrove swamps along their seaward margins. Low χ variation of the shaded portion (Fig. 7.37) is the repository of mangrove sediments, whereas the highly fluctuating χ indicates more vigorous detrital environment from eastern India deltaic environments of Godavari, Krishna and Cauvery. The ^{14}C ages obtained are: Godavari mangrove delta (2.1 to 1.7 cal ka at 83 cm depth), Krishna mangrove (4.3 to 3.7 cal ka at 95 cm), and Cauvery mangrove (2.3 to 2.0 cal ka at 126 cm).

Generally, sediments from various environments have different χ values. But, the mangrove results indicate that even in a similar environment, ferrimagnetic mineral concentrations vary vertically from one delta to another. The χ values range between 10 and 2000 with the highest ferrimagnetic mineral concentrations in Krishna mangrove swamp followed by Godavari and Cauvery. In the upper part of the cores, there is a steady decrease in χ. High fluctuations in χ occur below 100 cm depth in Godavari, and ~40 to 60 cm depth in Krishna and Cauvery delta mangroves, indicating a change in sequence evolution of deltaic environments during the late Holocene in these regions. It is argued that fluctuations in Holocene χ records reflect climatic change in sediment provenance areas.

II. Magnetic Susceptibility and Flood Plain Sediments

Floods are usually local, short-lived events that happen suddenly across a part of moving or still water body because of intense precipitation that produces more runoff than an area can store or a stream can carry within its normal channel. Rivers can also flood when dams fail, when ice jams or landslides temporarily block a channel or when snow melts rapidly depositing detrital components in the nearby areas giving rise to flood plains. In a broader sense, normally dry lands can be flooded by high lake levels, by high tides or by waves driven ashore by strong winds. Thus, these sediments contain history of climatic changes in the form of flooding and nonflooding events.

The sediments of the Mahi floodplain cover a considerable part of western India, which were formed within the time span of 30 to 10 ka. Rapid oscillations in the intensity of SW monsoon during the last glacial phase have been deciphered from magnetic and calcrete proxy records. Alternating strong and weak monsoon events identified from Mahi river basin in Gujarat, suggest impact of glaciation and glacier melting to have occurred on regional and global scale.

The values of χ and χ_{FD}% vary from 12 to 21 SI and from 0 to 1.2%, respectively. Here both allogenic and authigenic processes (pedogenesis and early diagenesis) occurred together, to differentiate which χ records were compared with opaque magnetic heavy mineral percentages. As can be seen from Fig. 7.38, increase in χ_{FD}% follows an increase in opaque magnetic heavy mineral concentration pointing to heavy detrital input on account of flooding. As opposed to this phenomenon, when there is an increase in χ_{FD}% accompanied by a decrease in opaque magnetic heavy minerals, it is suggestive of pedogenesis. The secondary enrichment of ferrous/ferric Fe due to pedogenesis is captured by simultaneous converging or diverging trends in χ_{FD}% and magnetic heavy mineral concentration. Based on these two collective parameters, four pedogenic horizons are delineated. Seven flood and non-flood periods are also identified, reflecting strong and weak monsoonal phases at a time scale of a few thousand years.

III. Mineral Magnetism and Foraminiferal Assemblage in Mudflat Sediments

Mudflat is an intertidal sedimentary area formed by deposition in low energy coastal environment, like an estuary, whose sediment consists mostly of silts and clays with a high organic content. It is also characterized by high biological productivity and abundance of organisms, but has low diversity with few rare species.

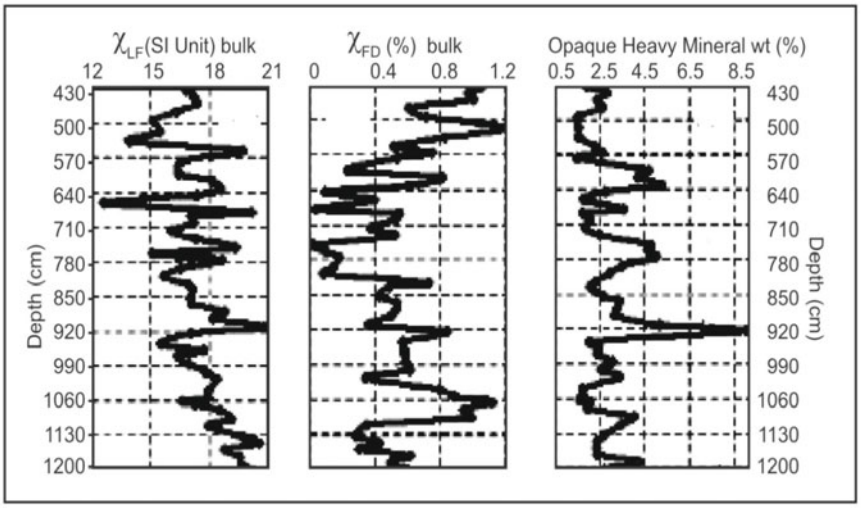

Figure 7.38. Variation of magnetic susceptibility, frequency dependent susceptibility and opaque heavy mineral percentage along depth profile for the sediment sequence at Bhimpura, where the Roman numerals indicate flood events. Simultaneous measurements of χ and its frequency dependence coupled with heavy minerals can be used to identify flood periods and nonflood periods, reflecting indirectly strong and weak monsoon phases (Sant et al., 2006).

The samples of Navlakhi mudflat, whose organic matter was subjected to carbon dating, gave an age of ~11 calibrated ka years before present (cal years BP). A combination of foraminiferal and magnetic analyses was used to reconstruct the depositional environment of clays from a 3.5 m shallow core of the mudflats of the Gulf of Kutch (Fig. 7.39), wherein samples of two levels, viz. 140 cm and 200 cm yielded ^{14}C dates of 9,390±140 years (cal 11,040 to 10,430 years) and 8,720±200 years (cal 10,150 to 9,530 years).

Wet periods of monsoonal reinforcements occurred at the early and middle (°) Holocene, which has been suggested by: (1) overall reduction in magnetic grain size reflected in higher values of ARM/SIRM, (2) low hematite content inferred from high S-ratio, (3) higher (lower) values of S-ratio correlate well with higher (lower) numbers of *Elphidiidae* and *Nonionidae*, which seemed to be governed by the increasing (decreasing) degree of salinity, and (4) increase in percentage abundance of the micro-fauna of *Elphidiidae* and vice versa. The relation of these magnetic parameters to climate change is through discharge variations across time. For example, low variations in the S-ratio, which relates directly to the presence of hematite, indicate changes in fresh water influx in this environmental setup. As this hematite is derived from erosion of oxidized soils of the catchment during drier periods, low values in S-ratio can directly be related to low discharge conditions (weaker monsoons). On the other hand, high S-ratio values reflecting more titanomagnetite in the sediments reveal increased fresh water influx during wet periods of monsoon reinforcement.

IV. Magnetic Susceptibility and Rajasthan Playa Sediments

Playas are enclosed shallow depressions in desert basins, tectonic lows, interdune flats and abandoned channels, which contain deposits and evaporites

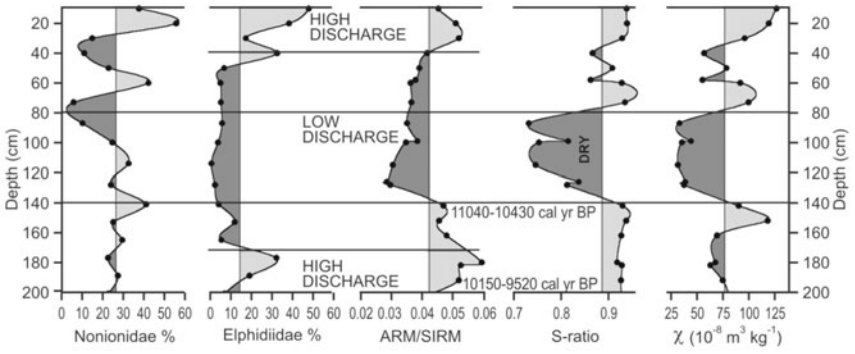

Figure 7.39. Downcore variations of magnetic susceptibility and remanence measurements and their quotients together with foraminiferal from the Navlakhi mudflat core. Interpreted values of low and high discharges are marked across the plots. The study demonstrates magnetic parameters coupled with foraminifera provide useful insights into climate related salinity changes. Note S-ratio together with ARM/SIRM suggests the influence of fresh water resulting in salinity variations (Rajsekhar et al., 2004).

from the impoundment of episodic stream flow or near-surface groundwater. These can be entirely dry or seasonally filled with water, where the sediment load carried into a playa from streams or blown in by wind includes clay, silt and fine grained sand. Evaporation of water from playas leaves exposed surfaces of the resident material, which can be any mix of clay, silt, fine sand and salt. Episodic streams may enter the playa from runoff during or shortly after rainfall in distant watersheds. Water may also appear due to rising groundwater in localities, where the basin floor or a channel intercepts the water table.

The playa sediments carry both the history of past climates and hydrology. In a desert, changes in water level, water chemistry and rate of sedimentation are all controlled by the climate. A dry phase of climate means dessication and shrinkage of the lake leading to increase in salinity. A wet climate leads to more vegetation around the lake filled with water. The pollen of steppe type of vegetation has been reported for Didwana. However, from 8.1 to 6.3 ka and 4.6 to 2.0 ka the landforms were unstable, and the climate was dry and arid, during which maximum influx of sediments took place in the lake.

Bap-Malar and Kanod lakes are in the arid Thar desert of Rajasthan, where climatic records for the past ~12 ka have been preserved. χ values at Kanod and Bap-Malar show progressive decrease down the profile and are interpreted in light of the changing hydrology of the lakes. During periods of high lake levels or rise in groundwater table, sediment composition is governed by the presence of paramagnetic minerals brought into the playa either by eolian or

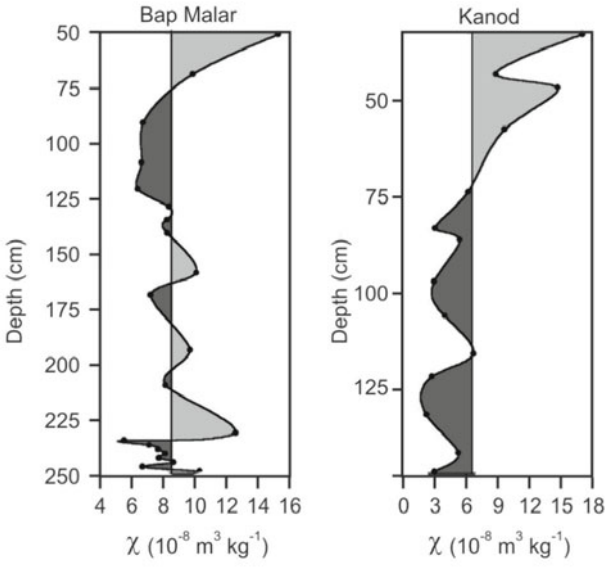

Figure 7.40. Variation in magnetic susceptibility in the Bap Malar and Kanod playa lake sediments. Variations in χ reflect changes in the lake hydrology, leading to dilution of χ through increases in diamagnetic evaporitic minerals. Higher χ values occur when aeolian detrital fluxes increase onto the playa surface (Deotare et al., 2004).

wind activity. When the lake evaporates and groundwater tables go down, the precipitation of evaporites and carbonates suppresses χ. With progressive aridity and simultaneous drying up of the lake, precipitation of evaporite and carbonate minerals decline. Subsequently, eolian sediments rich in hematite deposited onto the lake surface increase χ values.

V. Magnetic Susceptibility, FTIR Record and Civilization Collapse

The world has witnessed gradual as well as abrupt civilizational growth and collapse. The decline has been because of any one or a combination of factors such as war, drought, natural disaster, disease, overpopulation and economic disruption. In India, past settlements and old civilizations occur along most of the lakes and river basins, barring few of the inhospitable terrains. Palaeoclimatic fluctuations are known to coincide with changes in cultural stages in Palaeolithic sites of Rajasthan and Gujarat.

Lothal in Gujarat is a fascinating remnant of ancient Harappan civilization and little is known about the climate that prevailed before, during and at the terminal phase (3.5 ka ago) of this grand culture. Hence, collective proxy studies were carried out to ascertain critical palaeogeographical and palaeoclimatological issues. The magnetic record is jointly interpreted with remote sensing and Fourier transform infrared spectroscopy (FTIR) studies. FTIR was employed to know the relative abundance of carbonate with respect to silicate in order to see the effect of any dilution on the χ values.

Three different levels of χ in the sediment trench record (Fig. 7.41) display changing depositional environments from coastal realm at the lower part to

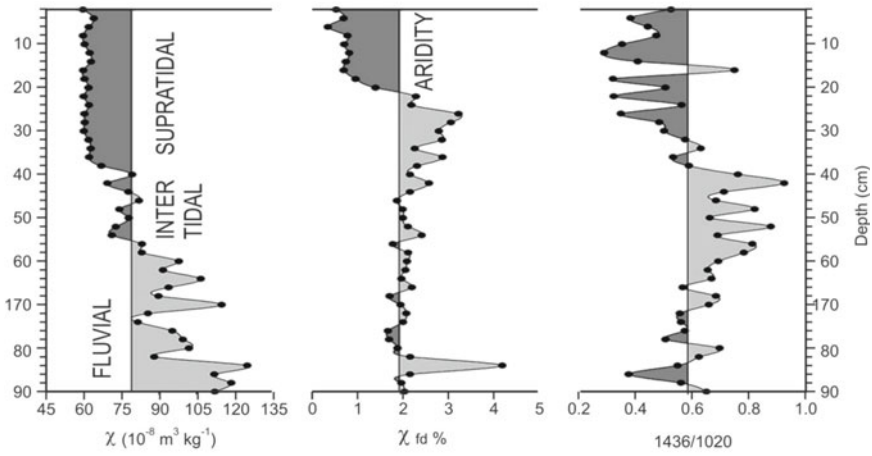

Figure 7.41. Down profile changes in χ and χ_{fd}% compared with variations in relative percentage of carbonate with respect to silica in the sediment. χ and carbonate concentration show fluctuations that are governed by changes in the depositional environment. A marked drop in χ_{fd} is observed towards the top implying a reduction in soil generating processes (Khadkikar and Basavaiah, 2004).

intertidal at the centre, and supratidal at the top. The uppermost part of the sediment record is characterized by low χ. This is not matched with χ_{fd}%, showing high values till ~26 cm after which a fall is observed at 18 cm. This low χ_{fd}% implies reduced monsoon rainfall accompanied by high sea levels witnessing collapse of Harappan civilization. When Lothal was inhabited, the weathering processes in the provenance area were subdued.

VI. Magnetic Susceptibility and Terra Rossae

Late Quaternary aeolinites occur along the coast of Saurashtra in Gujarat, western India. They show a wide array of epikarst and red soil (Terra Rossa) events making them typical formations to study the manner and character of aeolinite weathering under a monsoonal regime (Fig. 7.42). Karst is derived from a German word meaning crag or stone. In geomorphological terms, it refers to limestone terrains, and describes locales with distinctive characteristics

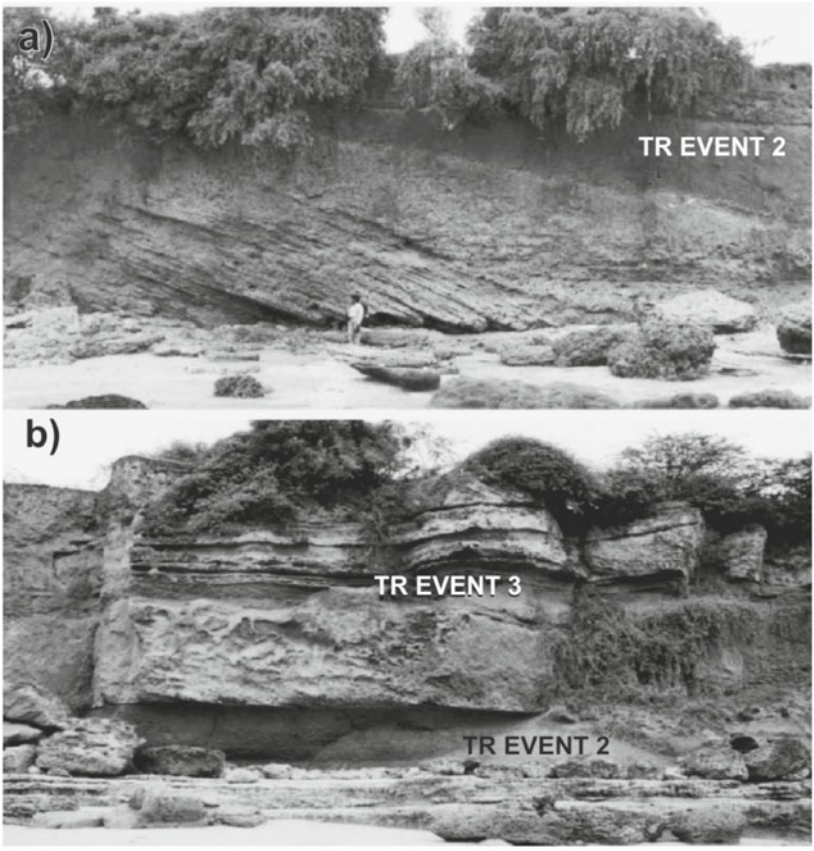

Figure 7.42. Terra Rossae inter-stratified with aeolianites at the classic exposure of Gopinath along with their event stratigraphy and notations (Khadkikar and Basavaiah, 2004).

of relief and drainage arising primarily from a higher degree of rock solubility in natural waters than is found elsewhere. The term also refers to dissolution features found pervasively developed in aeolinites, like in Gujarat. 'Karst' is essentially a variant of solution pipes that are vertically oriented, sometimes interconnected to form honeycomb network or appear as an irregular surface dominated by cavities and channels. Most of the variants of karst are 'epikarst'. These are solution features that have developed near the surface within depths extending to a few metres only. Terra Rossa, on the other hand, are red soils commonly developed on limestones under a Mediterranean type of climate. These are also reported from tropical regions. The Terra Rossa soils are understood to have formed by leaching and residual accumulation of limestone. Alternatively, it has also been suggested that the dust from Sahara gave rise to these soils.

Three Terra Rossae events were observed along the coast of Saurashtra, which placed the age of lower Palaeolithic in western India at ~30 to 100 ka. Of the three Terra Rossae events, event 2 was formed during the last interglacial period and the older event correlates with 170 ka event similar to MIS-3 during which time the Earth entered into interstadial. These Terra Rossae events were formed during periods of interglacial style of climates that were also durations of increased SW Indian monsoon rainfall.

The down-profile changes in χ, χ_{FD} and ARM (Fig. 7.43) are complex, and are related to changes in concentrations of SSD and SP magnetite, siliciclasts, carbonate, and hematite. Seasonal wetting in the monsoon months formed SSD and SP magnetic grains by the breakdown of MD magnetite, whereas formation of hematite was restricted to dry hot summers through oxidation of magnetite. The formation of SSD and SP magnetite and hematite are linked genetically to weathering of the aeolianite that formed Terra Rossa.

VII. Magnetic Susceptibility and Beach Sands

Beaches are by far the most widely distributed of any of the coastal sedimentary environments. The actual shape and orientation of the beach is apparently dependent on a number of variables, including the direction of wave approach, the material comprising the beach, the overall shape and composition of the coast. Beach sediment is the unconsolidated debris produced from the weathering of rocks. Since beaches are prone to erosion or deposition of sediments and are used for recreational purposes, their study forms an important public utility service.

Magnetic proxy measurements can serve as a fast and efficient tool for screening anthropogenic heavy (magnetic) mineral accumulation in soils and sediments. Beach samples from Vengurla (Fig. 7.44) were collected in the three seasons of the year from 2002 to 2005. Magnetic measurements (χ) were carried out to understand sediment movement along the beaches, and to test the validity and efficacy of this technique to collect rapidly and reliably the initial data on sediment movement. The study found that magnetic minerals

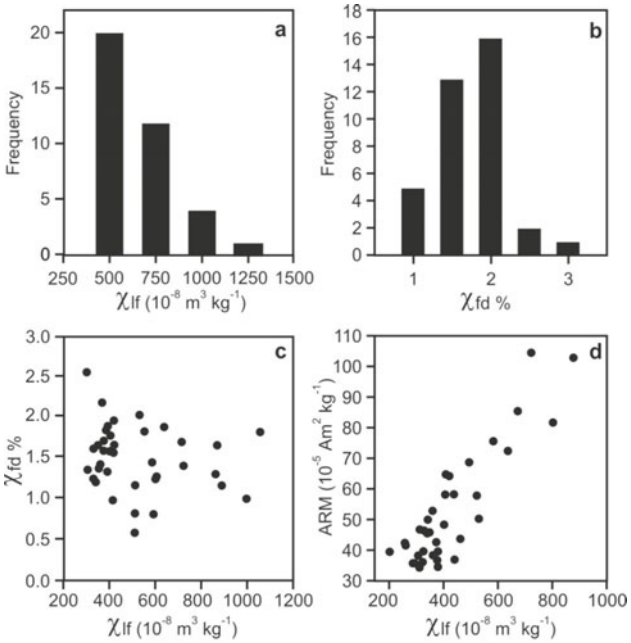

Figure 7.43. Histogram showing the frequency distribution of (a, b) low and frequency-dependent susceptibility (χ_{lf} and χ_{fd}). Both these parameters do not covary as shown in (c). (d) Bivariate plot of ARM and magnetic susceptibility χ_{lf} which shows that they are positively correlated, implying a genetic relationship (Khadkikar and Basavaiah, 2004).

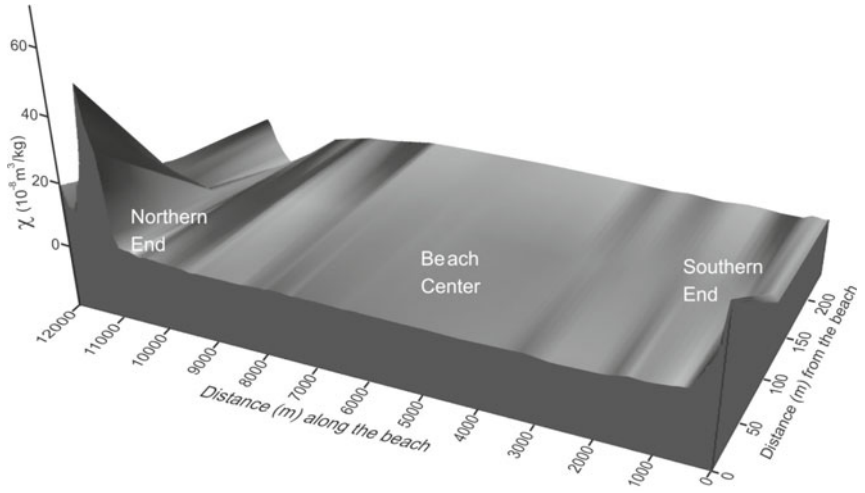

Figure 7.44. Magnetic susceptibility changes delineating magnetic mineralogy and sand migration along beaches of Redi, Aravali and Vengurla, of Sindhudurg district, Maharashtra, India. It can be seen from the diagram the prevalence of magnetic minerals at the extreme ends of the beaches denoting the migration path of beach sediments and the morphotectonic features of longshore currents (Gawali et al, 2010).

across the beach are mostly of ferrimagnetic and antiferromagnetic type concentrated more towards the northern and southern ends of the beaches (Fig. 7.44). But stations situated at the centre of the beaches are distinguished by exclusive presence of antiferromagnetic and/or paramagnetic minerals. The studies also revealed that concentration of magnetic minerals is more during the monsoon season than in pre-monsoon and post-monsoon because of the increased detrital influx from both land and sea. The main source or provenance of these magnetic minerals is the Deccan basalts, laterite and iron ores present along this stretch.

VIII. Magnetic Susceptibility and Himalayan Lake (Vanished) Sediments

The great Himalayan mountain range as a highland emerged by middle to late Miocene (11 to 7.5 Ma); it became a mountain barrier high enough to disrupt W–E flow of winds and push low-pressure area over northern India, which attracted moist summer winds from the Indian ocean. Palaeoclimatically, the uplift of Himalaya and Tibet exerts profound influence on regional and global climate in several ways.

Since the ascent of the Himalayas, the region has undergone several climatic vicissitudes experiencing glaciation for ~18 ka. Such events have devastating effect. For example, the slopes of the Alaknanda valley are loose and fissile phyllitic rocks prone to landslides, which temporarily block the river from a few days to several thousand years. The filled up reservoir is unable to withstand pressure from the stored water causing flash floods in its wake. Landslides of the recent past blocked scores of the Himalayan rivers, inducing scientists to look for evidences of ancient and pre-historical blockades. The presence of ancient river streams and lakes is confirmed by the respective presence of sand and clay/silt at the bottom. Two palaeolakes were thus identified at Goting and Garbayang (Fig. 7.45) in the higher central Himalayas, where sampling was carried out for detailed analyses like mineral magnetics, geochemical and optically stimulated luminescence studies (OSLS).

These palaeolakes contain signatures of glaciation within the timeframe between 40 and 10 ka. The higher central Himalaya is a narrow strip of mountainous terrain between the great Himalayan range and the Indo-Tibetan water divide. Garbayang lies in a transitional zone between dry steppe (Tibetan plateau) and the sub-humid (Himalayan) climate zone. Here the SW monsoon is the dominant source of precipitation which accounts for 80% of the total precipitation, a part of which falls as snow. During Nov to Feb, the westerly disturbances (winter monsoons) contribute the remaining 20% of the precipitation. Goting basin, on the other hand, represents the dry steppe climate of the adjoining Tibetan plateau. At Garbayang, deposition occurred in a proglacial lacustrine environment. These deposits formed in a lake blocked by terminal moraine after the retreat of the main valley glacier. The base of the

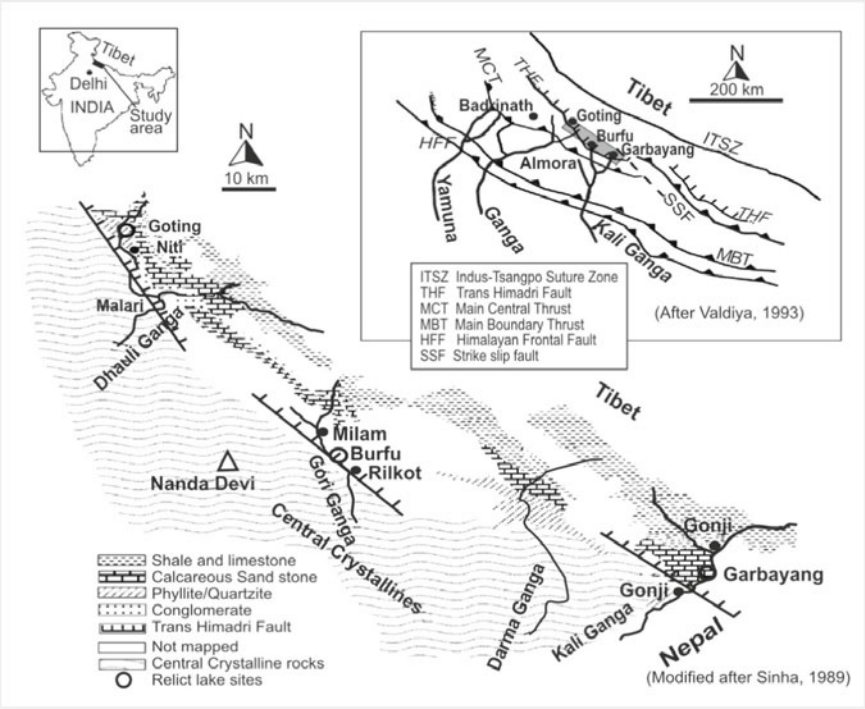

Figure 7.45. Lithology and structure between Garbayang (NE) and Goting (NW). Central crystalline rocks (wavy symbol) are south of the trans-Himadri fault (THF). Open circles are the relict lake locations. An inset indicates a synoptic view of major structures in the region.

palaeolake at Garbayang and Goting has been dated to 20±3 and 29±3 ka, respectively (Fig. 7.46).

Garbayang varve lake deposits: Environmental magnetism can extract valuable insights from physical and biogeochemical lake processes and can characterize lake systems 'prior to' and 'post' significant anthropogenic impacts. Variations in magnetic mineral concentration, grain size and mineralogy are used in the Himalayas to identify changes in environmental conditions that include deglaciation, Younger Dryas cold and arid events during the early and mid Holocene. Younger Dryas represents the 'big freeze' between 12.7 and 11.5 ka. This was a global phenomenon during which time apparently everything remained frozen.

The Swiss launched the first scientific expedition to the remote Himalayas in 1930s, when Heim and Gansser discovered varve-like deposits at Garbayang. Varves (Swedish varv) are fine clays deposited in layers, each representing a year (summer/winter) of glacial melt. Melting of ice increases with the advent of summers, which bring in more detrital input forming thicker layers whereas during winters due to reduced snow melt, the layer of sediments are thinner.

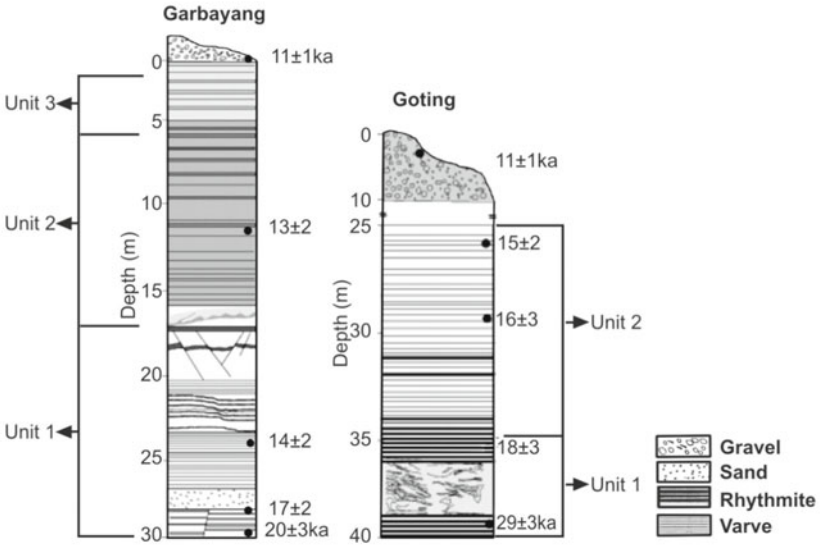

Figure 7.46. Stratigraphy and luminescence chronology of Garbayang and Goting deposits.

One can count such varves with ease and decipher the number of winters and summers the area witnessed in the past.

The Garbayang sediments are equivalent to MIS stage 4 and are estimated to be ~100 m thick. However, the steep cliffs make most of the succession inaccessible and only the top 28 m accessible part is studied. The varves at Garbayang are typical of layered deposition in a placid and calm lake already formed, while the glacier existed (Fig. 7.47). This fact was confirmed by the terminal moraine that proved to be much older than the lake sediments.

Mineral magnetism and palaeoclimate in Garbayang lake deposits: Garbayang deposits reveal high frequency, but low amplitude fluctuations from the base to the top (Fig. 7.48). The provenance of this lake is weakly magnetic precluding the chances of high magnetic material entering the lake. Elemental data was obtained for the upper 8 m of the sequence, which agrees well with the magnetic data (Fig. 7.48) underscoring the immense utility of this technique of being fast, inexpensive and reliable. The salient features of the study are: (1) Dominance of varves and a decline in susceptibility values between 20±3 and ~18±3 ka represent LGM, (2) Magnetic susceptibility and sedimentalogical data suggest that the period between 18±3 and ~13±2 ka witnessed high frequency/low amplitude climatic oscillations, (3) A sudden drop in magnetic susceptibility and elemental concentration of layers dated at 12–11 ka suggests cooling associated with Younger Dryas, and (4) A 1.7 m thick sand body reflects enhanced melt water discharge.

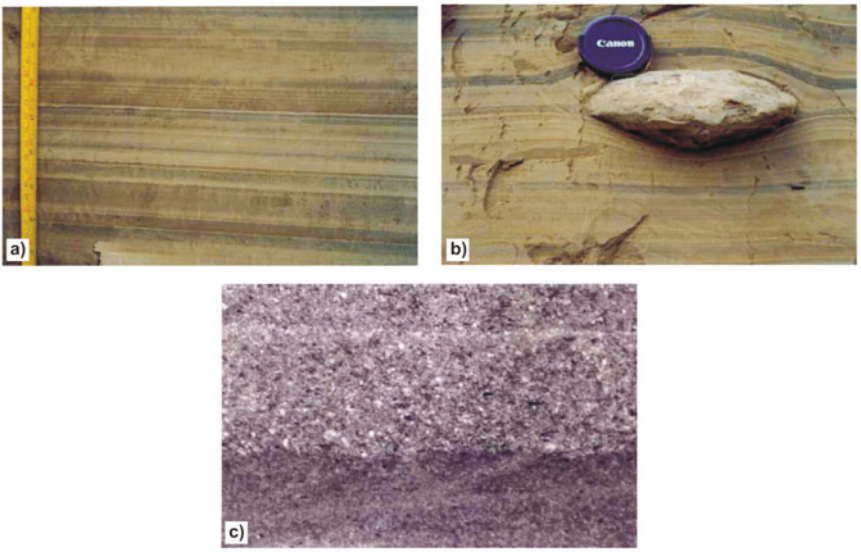

Figure 7.47. (a) Varve like laminations, scale is given alongside. (b) Dropstone (~10 cm horizontal axis) embedded in varve-like laminations. (c) Photomicrograph showing dark winter and light summer lamina, horizontal scale at the bottom is 12 mm (Basavaiah et al., 2004).

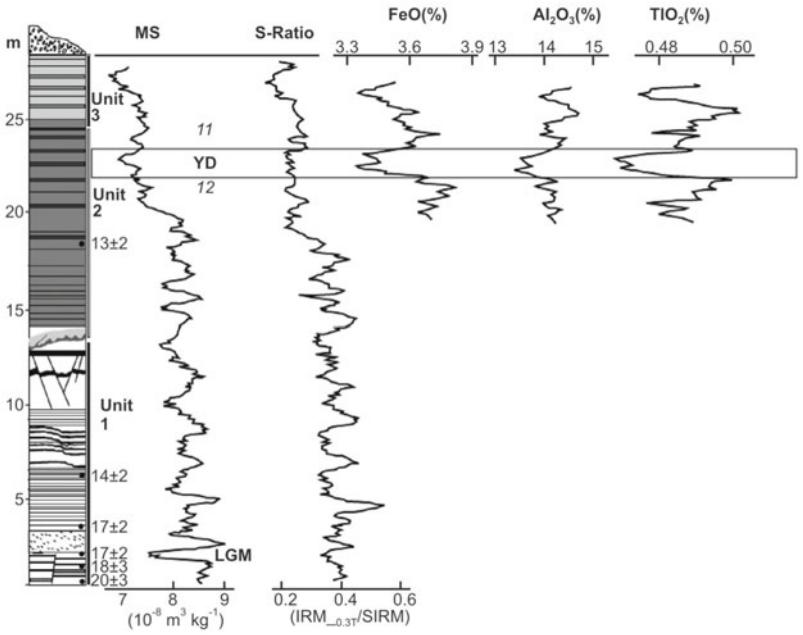

Figure 7.48. Magnetic susceptibility, S-ratio and elemental data plotted against the litholog. Infrared stimulated luminescence (IRSL) ages are shown along side the susceptibility curve. The IRSL ages of 12 ka (22 m height) and 11 ka (25 m height) are interpolated ages (Navin et al., 2004).

Magnetic mineralogy and climate linkages in lake sediments: The property of magnetism is temperature dependent and to exactly identify magnetic minerals following techniques are employed: (i) low and high temperature (–196° to 700°C) dependence of magnetization and magnetic susceptibility, (ii) hysteresis parameters (saturation magnetization M_S, saturation remanence M_{RS}, coercivity remanence H_{CR}, and coercivity H_C) and resistance to AF or thermal demagnetizations. Based on stepwise thermal demagnetization of SIRM, the Himalayan Garbayang lake sediments are found to contain Ti-rich titanomagnetites with varying titanium content and pure hematite (Fig. 7.49a,b). It is suggested that low temperature oxidation (LTO, maghematization) is more advanced in samples (e.g. GB-854 in Fig. 7.49a) of drier phases (decreased rainfall) expressed by alteration (oxidation) of titanium-rich titanomagnetite to hematite. Samples (e.g. GB-906 in Fig. 7.49b) from wetter spells (increased rainfall) show that LTO is less pronounced and titanomagnetites are still preserved. The changes in magnetic mineralogy confirm its suitability in climate related studies.

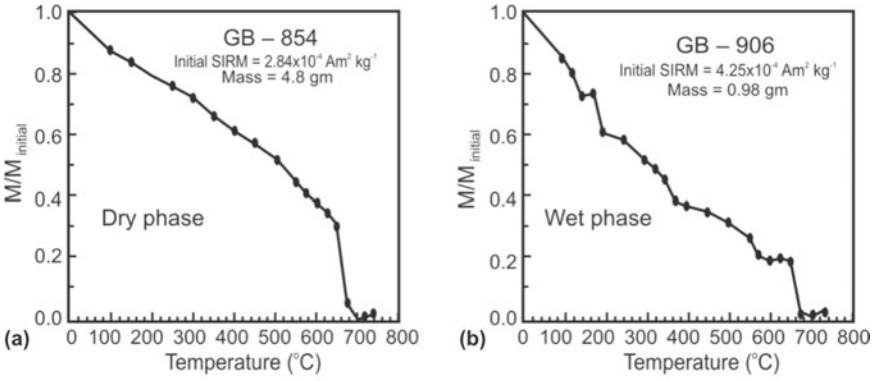

Figure 7.49. Typical thermal demagnetization curves of the normalized SIRM values of the Garbayang lake sediments: (a) GB-854 sample shows a sharp decrease in magnetization at ~675°C suggesting dominance of hematite. (b) Sample GB-906 indicates three magnetic phases, i.e. Ti-rich titanomagnetite, magnetite and hematite (Juyal et al., 2004).

Mineral magnetism and palaeoclimate in Goting lake deposits: Sedimentological evidences indicate the prevalence of two distinct climatic regimes at Goting by infrared stimulated luminescence (IRSL) dating between 29 and 18 ka. The lower unit-I suggests enhanced sediment supply (dominated by titanomagnetite) and higher surface water temperature, whereas the overlying varve dominated unit-II indicates cooler condition punctuated by frequent warm oscillations (Fig. 7.50). The Goting samples are characterized by χ values between ~11 and 17.5 (10^{-8} m^3/kg). Warm condition prevailed with less frequent oscillations between 29 and 18 ka; LGM is identified at ~18 ka (depth 34 m).

IX. Mineral Magnetism and Palaeoclimate in the Himalayan Loess (Silt Deposits)

Loess is a glacial rock flour blown by wind and deposited thousands of miles away from its place of origin. These are homogenous because winds can carry particles of a particular size only. On deposition, the carbonate content binds them together to form huge deposits. Loess sediments are commonly found in China and midwestern USA and are also a hall mark of several European countries. India has very few loess deposits, and the first to identify them was R.K. Pant from Kashmir valley in 1978. Subsequently, in 1984, R.J. Williams and M.F. Clarke reported loess from Sone valley in central India. Pant and his team were lucky to strike loess once again at altitudes ranging from 1800 to 2500 m in the central Himalayas at Dhakuri in Bageshwar district in Pindar river basin and Chopta in Chamoli district in Alaknanda river basin of Uttarakhand (Fig. 7.51).

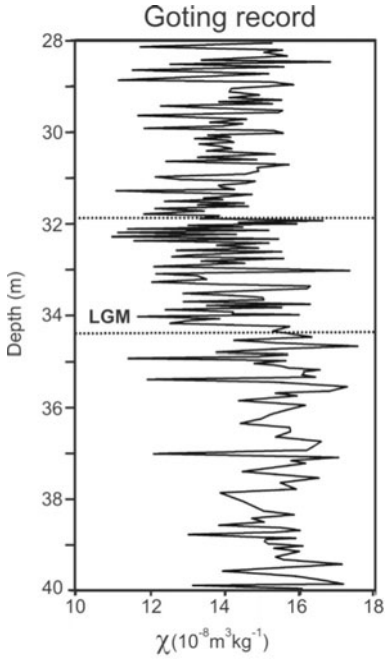

Figure 7.50. Magnetic susceptibility of Goting varve deposits. Note a marked low representing LGM in a saw tooth pattern. LGM - last glacial maximum (Basavaiah et al., 2004).

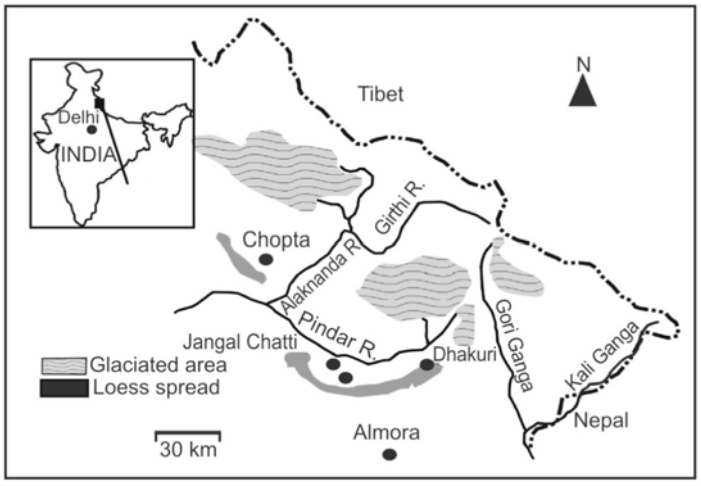

Figure 7.51. Map of the central Himalaya showing distribution of loess deposits south of the glaciated terrain (Pant et al., 2005).

To estimate the age and duration of loess accretion and soil formation episodes, IRSL and ^{14}C techniques were used. IRSL determines the time elapsed since the loess mineral grains were last exposed to sunlight. As the fine sediments carried by the winds are deposited layer after layer, year after year, the sunlight to older sediments becomes dearer. The IRSL ages ranged from 20±4 ka for loess at 200 cm depth and 1±0.3 ka at 20 cm depth (Fig. 7.53). Dhakuri has a higher magnetic content and the anticipated source area is postulated to be a granite terrain. However, granites are poor in Fe content; hence, it is conjectured that they come from a far away place. Some have obtained loess from the sea floor drill-cores. Alternatively, oxidation could have enhanced the magnetic content, as the results suggest. Thermomagnetic χ-T runs between RT and 700°C and unblocking temperatures (SIRM-T) reveal inflection in the heating curves at ~350 and 300°C, which are attributed to the formation and destruction of maghemite due to oxidation (Fig. 7.52). The magnetic properties of the sequences seem to be dominated by magnetite and maghemite in palaeosols, whereas magnetite as well as hematite (with additional maghemite) dominates the loess (Fig. 7.52).

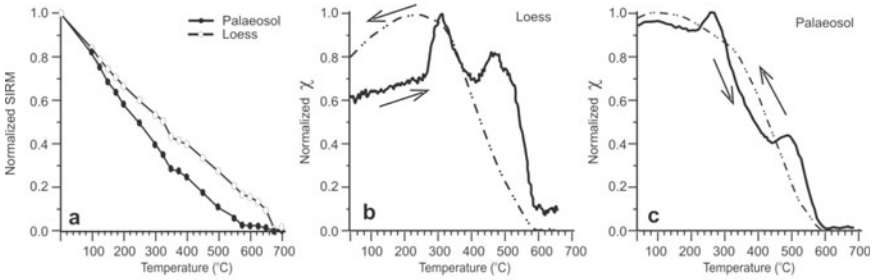

Figure 6.52. (a) Thermal demagnetization of saturation isothermal remanent magnetisation (SIRM) for palaeosol and loess samples. Normalized susceptibility versus temperature curves for loess (b) and palaeosol (c) samples. Thick (broken) lines represent heating (cooling) curves (Pant et al., 2005).

Variations in mineral magnetic properties (Fig. 7.53a-c) are in good agreement with loess stratigraphy, where palaeosols S1 and S2 have higher χ and χ_{FD}% indicating secondary formation of ultrafine grained SP ferrimagnetic minerals (maghemite and possibly magnetite). Lower χ and χ_{FD}% and S-ratio corresponding to loess indicate higher contribution of hematite. Variations in χ are attributed to pedogenic enhancement by inorganic and biogenic processes. Loess accumulation and pedogenesis (soil formation) occur alternatively because loess accumulation is greater during cooler and drier conditions, whereas pedogenesis occurs during wetter conditions. These episodes are interpreted in terms of changes in the strength of the Indian SW monsoon. Thus, magnetic measurements reveal changes in mineralogy and concentration of dominant magnetic minerals between the loess and palaeosols. Geochemistry also corroborates magnetic data (Fig. 7.53d-e).

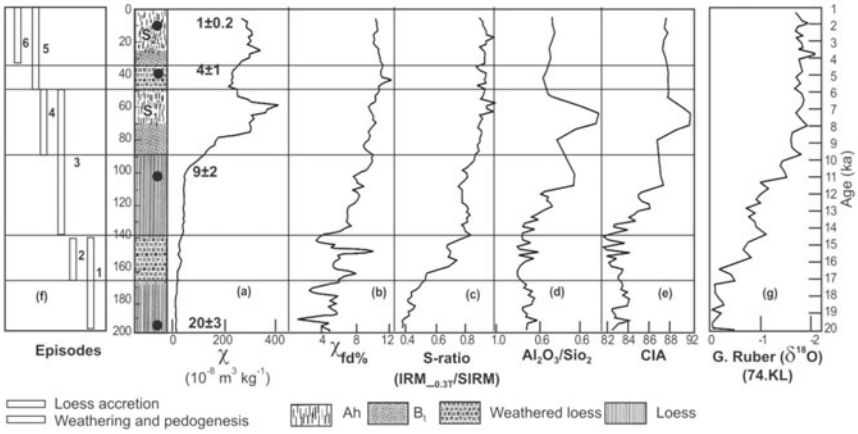

Figure 7.53. Plot of mineral magnetic parameters (a)–(c) of magnetic susceptibility (χ), frequency-dependence susceptibility (χ_{fd}%) and a simplified S-ratio and geochemical data (d)–(e) of Al_2O_3/SiO_2 ratio and chemical index of alteration (CIA). In 2 m loess-palaeosol sequence, six episodes have been identified (f), odd numbers (white vertical bars) represent periods of loess accretion and the even numbers (shaded vertical bars) represent episodes of weathering and pedogenesis. A close correspondence between loess-palaeosol sequence and the oxygen isotopic data (g) obtained on *Globerinoides ruber* from the Arabian Sea (core 74KL, Sirocko, 1996; Pant et al., 2005).

This study allows the following conclusions: (i) loess-palaeosol sequences in the central Himalaya mimic changes in the regional climate including SW monsoon variability over the last 20 ka, (ii) the region experienced a drier and dustier climate from 20 to >15 ka, 12 to 9 ka and 4 to >1 ka, suggesting these to be phases of weaker SW monsoon and (iii) enhanced SW monsoon existed between ~16 and 12 ka and even stronger monsoon conditions existed during 9 to >4 ka, facilitating pedogenesis of loess.

Figure 7.54 reports a synthesis of monsoonal variability in the Indian subcontinent. Loess accretion between 24 and 12 ka is reported from central India, whereas the southern margins of Thar desert experienced enhanced dune building activity during this same period (Fig. 7.54). The period 11 to 7 ka saw the emergence of microlithic culture in the southern margin of Thar desert, and the Ganga plain witnessed channel activity due to the strengthening of the SW monsoon.

7.13 MAGNETOMINERALOGICAL S-RATIO AND PALAEOCLIMATE IN SEDIMENTS

The foregoing sections and case studies prove the effectiveness of mineral magnetic parameters like susceptibility and remanence, revealing climate and environmental change features that are unresponsive to other proxy parameters. Magnetic proxies are very effective in basaltic terrain, especially the S-ratio.

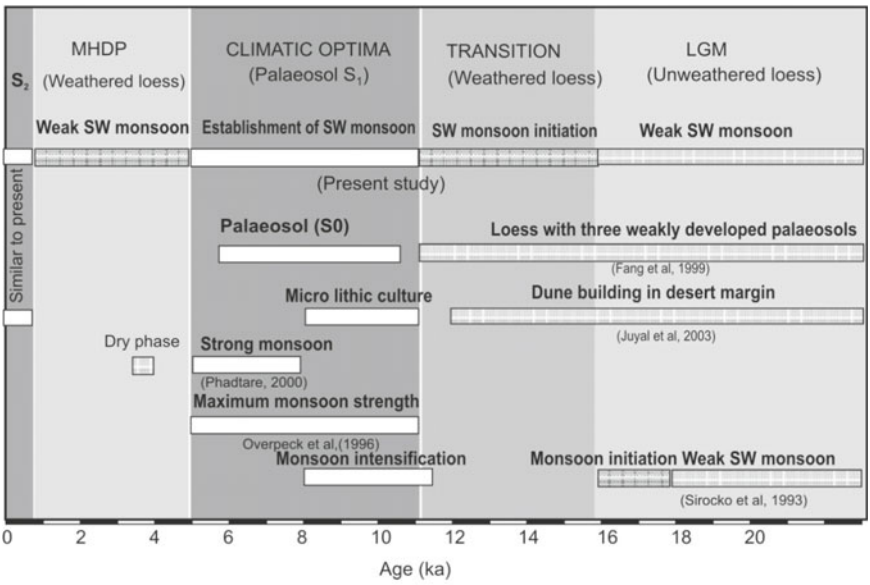

Figure 7.54. Synthesis of marine and terrestrial records of monsoon variability since past 20 ka from Indian sub-continent (*courtesy:* Navin Juyal).

S-ratio is defined as the ratio of laboratory induced backfield IRM and SIRM in fields of 300 mT and 1.5 T, respectively. An example of the use of mineral magnetic lithostratigraphy in late Pleistocene and Holocene studies is shown in Fig. 7.55, where S-ratio is plotted against depth for several sediment cores and profiles covering peninsular and extra-peninsular regions. The mineral magnetic fluctuations of the last 20 ka in S-ratio can be correlated with different environmental (climatic) variations.

High (low) S-ratios occur in warm (wet) sediments indicating higher proportions of 'magnetite' as opposed to 'hematite' minerals in cold (dry) climates. This parameter essentially documents changes in the relative abundance of two ionic states of Fe^{2+} and Fe^{3+}. For example, the oxidation state in magnetite is Fe^{2+}, while that in hematite is Fe^{3+} (also see Fig. 7.49). These oxidation states are primarily governed by weathering and water saturation of soils, which in turn are sensitive to mean annual rainfall. That is, during periods of reduced rainfall, the somewhat weaker magnetic rhombohedral hematite (αFe_2O_3) forms due to oxidation of magnetite (Fe_3O_4) and Ti-rich titanomagnetites. When there is increase in precipitation the opposite is true.

Extensive studies of sedimentary sequence in the Deccan trap region have revealed that S-ratio has a low variation. For example, the S-ratio derived for Godavari (Fig. 7.55) ranges between 0.90 and 0.96 attributed to different stages of oxidation states of (titano)magnetite having varying amounts of Ti oxide. To infer climatic events affecting the entire Indian subcontinent, one need to have composite and multiple maps which can be relied upon more intimately than on single or isolated maps of localized extent (Fig. 7.55). S-ratio has enabled in identifying key events hitherto unreported from the Indian monsoon.

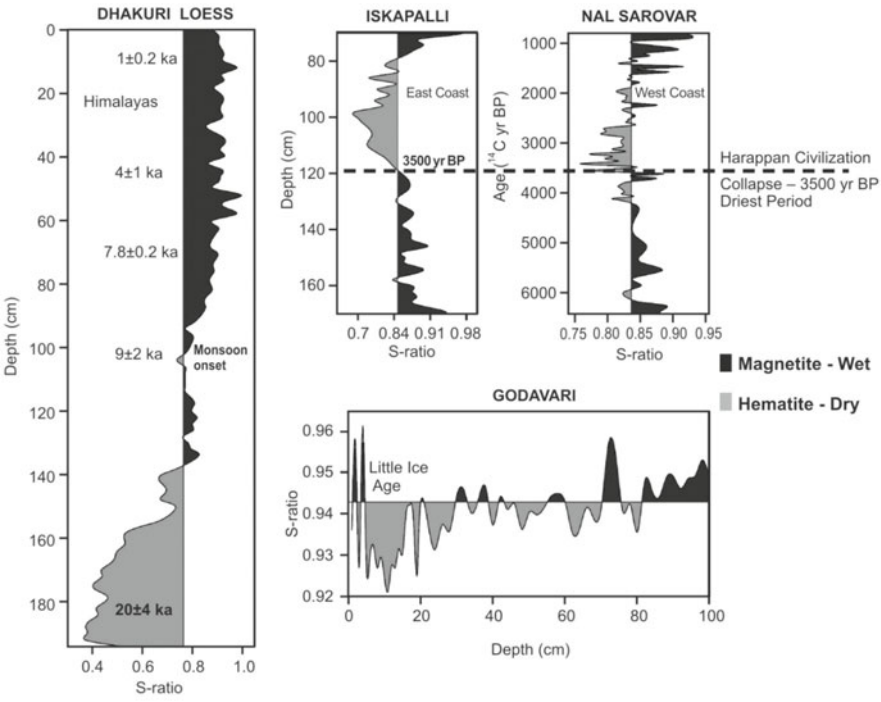

Figure 7.55. The stacked S-ratio as an accurate proxy of palaeomonsoon rainfall. Variation of mineral magnetic S-ratios with depth in sediment cores from the entire Indian subcontinent. High magnetic ratios corresponding to high 'magnetite to haematite' ratios occur in the wetter spell sediments and vice versa. Himalayan Dhakuri loess S-ratio clearly outlines key climatic events over the past 20 ka revealing step-wise improvement in SW monsoon since last glacial maximum, culminating in its establishment around 9 ka (Basavaiah and Khadkikar, 2004).

These include identification of Younger Dryas, YD (11 ka), little ice age, LIA (1780 AD) and reduced monsoon during 4000–3000 cal year BP.

Composite S-ratio map and palaeoclimate: Studies till date establish S-ratio to be an effective tool in decoding the past monsoonal characteristics of the peninsular and to a limited extent, the extra-peninsular region of India. For example, the S-ratio record of Dhakuri loess site in the central higher Himalayas clearly outlines key climatic events over the past 20 ka revealing step-wise improvement in SW monsoon since LGM, culminating into its establishment ~9 ka (Fig. 7.55). The S-ratio trend depicts a prolonged dry spell along the eastern (Iskapalli) and western (Nalsarovar) coast of India at ~3.5 ka back, effectively bringing about the downfall of Harappan civilization (Fig. 7.55). Little ice age from ca. 1400 to 1850 AD is sort of a repetition of the earlier ice ages but with a smaller geographical extent and is identified from the analyses of Godavari mangrove vibra-core samples. Also, a globally known cooler event, the LGM, that occurred ~20 ka ago is identified from Goting/Garbayang

palaeolake sediments and Dhakuri loess sequences (Fig. 7.55). Environmental geomagnetic studies have also identified YD cooling event that occurred ~11 ka back from the Himalayan lake sequences of Garbayang. Since these events are global in nature, it is envisaged that the central higher Himalayan climate was influenced by the northern hemispheric glaciation.

Also, a link between LTO of titanomagnetite and monsoon rainfall is proposed from lake sediment studies of Thar desert playas, Tulsi, Mastani and Nalsarovar. The ability of S-ratio to sensitively documents palaeomonsoonal changes, especially reduction of monsoon rainfall in time with higher latitude climate events of LGM, YD and LIA, imparts a great deal of confidence in establishing its efficacy as an accurate proxy of climate change.

7.14 FUTURE STUDIES

I. Magnetotactic Bacteria

Biogenic processes are an important source of magnetic minerals. Bacterial magnetite (BM) contribution is found in lacustrine, brackish and marine sediments, rivers, salt marshes, ponds, terrestrial soils and stratified ocean waters. For example, the importance of BM contribution in sediment cores can be gauged from the Chatham Rise, SW Pacific Ocean which has documented higher χ and increased concentration of SD magnetic grains for interglacial periods. It is interpreted that low productivity during interglacial periods favoured oxic conditions at the sea bottom for longer periods producing more magnetite, when compared to glacial periods. Small water bodies normally have high nutrient levels and rates of productivity, hence the sediments are commonly organic-rich and reducing. This is usually the case in temperate climate water bodies as well as in saline playas of arid areas. Under such conditions diagenetic destruction of bacterial magnetite is likely. The abundance and distribution of magnetotactic bacteria are dependent on four environmental factors, viz. organic matter, iron, oxygen and sulphide. It is very difficult to identify magnetotactic bacteria or their extracts for the simple reason that they are very tiny and elusive.

The magnetic particles formed by magnetotactic bacteria may contribute significantly to the magnetic properties of sediments. Their presence can be used as an indicator of microaerobic conditions that point to the oxic and anoxic conditions, as well as the EMF direction, intensity and the environment at the time of their existence. Also, any palaeoenvironmental or palaeoclimatic signal that may be encoded by BM is determined by the ecology and subsequent degree of preservation of the fine grained magnetite in the sediments indicating the palaeoecological and palaeoredox conditions. Bacteria that produce equant magnetosomes are abundant under more oxic conditions, while those that produce elongate magnetosomes are more tolerant of less oxic conditions. Some have also found greater abundance of magnetosomes in interglacial sediments, because of thicker oxic zone enabling the magnetite-producing bacteria to colonize for a longer period.

II. Mineral Magnetism and Pollution Studies

All particles are magnetic, though their individual intensity differs considerably. Hence, nearly all atmospheric fall-out dusts, whether of natural or anthropogenic origin, contain magnetic spherule particles. Spherules are formed through transformation of iron impurities within the fossil fuel and appear to be characterized by presence of both magnetite and hematite phases and relatively large (>SP/SD) magnetic grain size. In urban and industrial areas, during combustion of the coal, pyrite may be decomposed into elemental sulphur and pyrrhotite and the latter will further break down into sulphur and iron. Finally, the iron oxidizes to form a microscopic sphere of magnetite. Besides the combustion processes, magnetic particles can also originate from road traffic and also get deposited on the top surface of tree leaves. The distribution of the pollutants depends on the direction and speed of the wind, atmospheric humidity, precipitation, topography and vegetation. It is frequently possible to distinguish between anthropogenic and natural dusts with regard to its origin. The industrial dusts contain magnetic spherules that can be easily identified using thermomagnetic and microscopic analysis. Compared to the magnetic properties of natural dust, industrial dust that includes these magnetite spherules show high values of SIRM/ARM ratio, low levels of frequency dependent χ, low ARM and dissociation from finer, clay sized components of the soil. This provides an effective way to use magnetic methods to identify industrial pollution. Pollution history (back in time) can be revealed from measurements of depth profiles of soils and/or sediments.

III. Secular Variation Master Curves

Characteristic patterns of secular variation changes occur on a regional scale, e.g. on the spatial scale of North America or Europe. These changes can be recorded in rapidly accumulating lake sediments. The technique relies on radiocarbon dating of lake sediments. These enable to date earlier SV changes and can then be applied to other SV records from lake sediments in the same region. It is envisaged to develop dated secular variation 'master curves' for India. Also a study will be made to construct magnetostratigraphy for a wide range of sediment sequences from the Cretaceous through the Quaternary to the recent.

IV. Archaeomagnetism Studies

India has a rich cultural history which extends back more than 4500 years. There are extensive Neolithic and Palaeolithic cultural sites which may extend back more than 100 ka. Magnetostratigraphic studies will be undertaken to better date archaeological sites, especially those with a stratigraphic sequence of several cultural levels. The advantage of archaeomagnetic studies to palaeomagnetism is the addition of new time series of magnetic field variation for the South Asia over the last 4000 years.

V. Palaeoseismological Studies

Mineral magnetic investigations supplemented with particle size analyses will be made towards the study of palaeoseismic record by analyzing stratigraphic sections of fluvio-lacustrine sedimentary sequences. This work is expected to yield useful data on earthquake recurrence intervals and develop quasi-empirical techniques for earthquake predictions.

VI. Lonar Lake Magnetism

Lonar Lake has become a focal point of intense debate regarding its origin (Fig. 7.56a). A section of Earth scientists and geophysicists feel it to have formed by an impact of meteorite while others assign to it a volcanic origin. Both these groups have strong evidences to back their claims. However, the work carried out on Lonar is decades' old and it needs to be revisited equipped with state-of-art equipment and a new thought process (Fig. 7.56b). An integrated approach is required to understand its geomorphological, geological and geophysical characteristics. The entire basaltic terrain is formed by fissure-type volcanic activity and Lonar study is taken up to provide a unique insight into the magmatic extrusion on such a massive scale. Its impact origin provides an opportunity to study extra-terrestrial material enhancing the knowledge about the origin as well as the fundamental understanding of the universe. The planned Mars and Moon expeditions will greatly benefit from these studies.

The Lonar Lake can play a major role in studying the modern and past climatic conditions prevalent in central Indian region. This is the only lake in central India with a long pre-anthropogenic record and therefore essential for documenting the human impact on natural climate change. Further, the crater has accumulated within its lake sediments of ~50 ka. It is thus a rich repository of climatic and environmental change signatures that can be studied to understand the monsoonal pattern. In conclusion, latest developments in sedimentology, mineral magnetism, and geochemistry, especially the use of microfacies analyses, XRF (50-μ resolution) and stable isotope (on microfossils and organic compound specific isotope investigations) researches have made seasonal scale climate reconstruction possible, necessitating the raising up of lake bottom sediment cores from Lonar Lake.

Figure 7.56 (a) The magnificent Lonar Lake. (b) Mini boat and 1.2 m pneumatic Mackereth sampler for recovering under water sedimentary cores from the Lonar Lake.

APPENDIX 7.1

Calculation of Geomagnetic or Palaeomagnetic Pole Position

Suppose that D_m and I_m be the site-mean magnetic field direction which is located at geographic latitude λ_s and geographic longitude Φ_s. Here, D_m and I_m may be direct measurements of the field or may refer to the ancient field recorded by a rock.

Let λ_p and Φ_p be the geographic latitude and longitude respectively of the geomagnetic or palaeomagnetic pole position. From the knowledge of spherical trigonometry the magnetic colatitude p (i.e. the angular distance between site and pole) is

$$p = \cot^{-1}(\tan I_m/2)$$
$$= \tan^{-1}(2/\tan I_m)$$

Since p is the angular distance, it should be positive. If it comes negative, then it should be added with 180°.

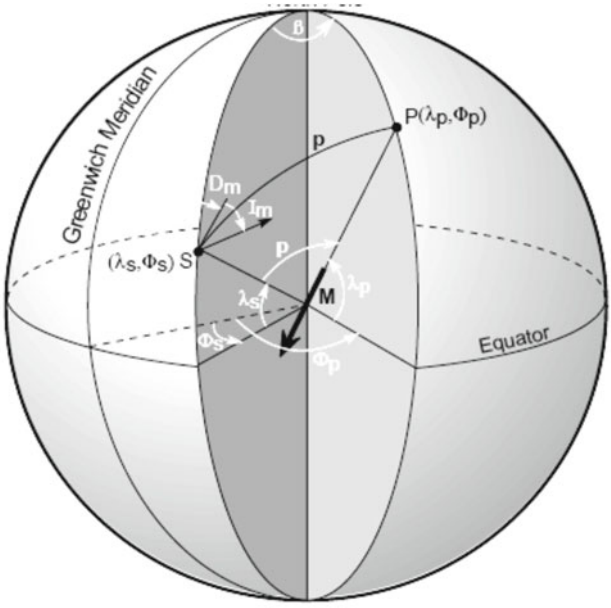

Now pole latitude is given by $\lambda_p = \sin^{-1}(\sin\lambda_s \sin p + \cos\lambda_s \cos p \cos D_m)$

The longitudinal difference between site and pole i.e. $\beta = (\Phi_p - \Phi_s)$ is related as

$$(\Phi_p - \Phi_s) = \sin^{-1}(\sin p \sin D_m/\cos\lambda_p)$$

At this point in the calculation, there are two possibilities for pole longitude.

If $\cos p \geq \sin\lambda_s \sin\lambda_p$

Then $\Phi_p = \Phi_s + \beta$
If $\cos p < \sin \lambda_s \sin \lambda_p$
Then $\Phi_p = \Phi_s + 180° - \beta$

Refer to Table 7.1 for calculation of VGP of site A. Its λ_s and Φ_s are 16.37°N and 73.84°E respectively. The mean characteristic direction i.e. obtained after magnetic cleaning are $D_m = 155.1°$ and $I_m = 48.7°$.

The magnetic colatitude $p = \tan^{-1} (2/\tan I_m)$
$= 60.35°$

Pole latitude $\lambda_p = \sin^{-1} (\sin \lambda_s \cos p + \cos \lambda_s \sin p \cos D_m)$
$= -38.08°$ (i.e. in southern hemisphere)

The longitudinal difference β between the site and pole
$= \sin^{-1} (\sin p \sin D_m / \cos \lambda_p)$
$= 27.67°$

As $\cos p > \sin \lambda_s \sin \lambda_p$, hence $\Phi_p = \Phi_s + \beta = 73.84°$ (E) $+27.67°$ (E) = 101.51° (E)
Since $\lambda_p = -38.08°$ thus gives the position of the pole in the southern hemisphere. Conventionally palaeomagnetist calculates the north geomagnetic or palaeomagnetic pole position. Thus the dipole magnet is rotated by 180° to obtain the north geomagnetic pole.
Thus the pole longitude is

$$\Phi_p = \Phi_p + 180°$$
$$= 101.51° \text{ (E)} + 180°$$
$$= 281.51° \text{ (E)}$$

Thus the VGP of the site A is 38.1° (N) and 281.5° (E).

Palaeomagnetic Data from India

Sl. No.	*Geological formation and locality*	*Age (m. yr)*	*Co-ordinates*		*Sampling details*		*Mean remanents magnetic direction*		*Polarity*	α_{95}	*Palaeolatitude of Nagpur 21°N, 79° E*	*Palaeomagnetic*	
			Lat. (N)	*Long. (E)*	*No. of sites*	*No. of specimens*	*D*	*I*				*Lat.*	*Long.*
1.	Pavagadh acid tuffs	20-35	22° 28′	71° 33′	2	15	355	+17	N	7°	6° 30′N	75°N	89°W
2.	Pavagadh basic	50-60	22° 28′	71° 34′	8	69	351	-16	N	8°	9° S	58°N	91°W
3.	Upper Deccan Traps												
3A	Mahabaleshwar	55-75	17° 55′	73° 38′	7	175	339	-57	N				
3B	Amba	55-75	16° 59′	73° 46′	3	54	355	-26	N				
3C	Nipani	55-75	16° 26′	74° 22′	3	74	338	-32	N				
3D	Gargoti	55-75	16° 19′	74° 10′	2	35	11	-46	N				
3E	Ajra	55-75	16° 3′	74° 3′	1	22	35	-70	N				
3F	Alandi dykes	55-75	16° 34′	73° 35′	2	41	346	-53	N				
3G	Panchmarhi	55-75	16° 27′	78° 26′	2	25	338	-47	N				
3H	Mumbai	55-75	16° 58′	72° 49′	3	71	328	-47	N				
3.	Mean Upper Deccan Traps (8 localities)	55-75			23	497	345	-44	N	10°	25° 30′S	42°N	87°W
4.	Lower Deccan Traps												
4A	Mahabaleswar	70-90	17° 55′	73° 38′	20	339	157	+52	R				
4B	Khandala	70-90	18° 45′	73° 22′	16	233	147	+58	R				
4C	Linga	70-90	21° 58′	78° 55′	4	195	164	+48	R				
4D	Amba	70-90	16° 59′	73° 46′	5	109	144	+60	R				
4E	Nipani	70-90	16° 26′	74° 32′	2	44	168	+60	R				
4F	Neral dykes	70-90	18° 57′	73° 19′	5	65	139	+43	R				
4G	Neral flow	70-90	18° 57′	73° 19′	1	11	148	+40	R				
4H	Alandi	70-90	18° 34′	73° 53′	1	12	141	+66	R				

(*Contd.*)

Palaeomagnetic data from India (*Contd.*)

Sl. No.	*Geological formation and locality*	*Age (m. yr)*	*Co-ordinates*		*Sampling details*		*Mean remanents magnetic direction*		*Polarity*	α_{95}	*Palaeolatitude of Nagpur 21°N, 79° E*	*Palaeomagnetic*	
			Lat. (N)	*Long. (E)*	*No. of sites*	*No. of specimens*	*D*	*I*				*Lat.*	*Long.*
4I	Buldhana	70-90	20° 33′	76° 12′	2	20	149	+53	R				
4J	Panchamarhi	70-90	22° 27′	78° 26′	4	52	156	+50	R				
4K	Kalyan	70-90	19° 13′	73° 07′	1	15	164	+56	R				
4L	Gargoti	70-90	16° 25′	74° 14′	1	28	159	+56	R				
4M	Chincholi	70-90	17° 29′	77° 28′	1	59	153	+62	R				
4N	Gulbarga	70-90	17° 19′	76° 56′	1	69	145	+58	R				
4O	Vikarabad	70-90	17° 22′	77° 30′	1	48	140	+60	R				
4.	Mean Lower Deccan Traps (15 localities)	70-90			65	1299	154	+53	R	10°	30° 30′S	34°N	78°W
5.	Tirupati sandstones												
5A	Janam Peta	90-120	16° 46′	81° 8′	1	94	157	+51	R				
5B	Peddavegi	90-120	16° 48′	81° 8′	1	38	329	-59	N				
5C	Peddavegi	90-120	16° 48′	81° 9′	445	1	26	154	+62	R			
5D	Peddavegi	90-120	16° 49′	81° 13′	1	31	145	+55	R				
5E	Nayanapalli	90-120	16° 50′	81° 12′	1	47	153	+56	R				
5.	Mean Tirupati sandstones (5 localities)				5		153	+56	R	4°	34°S	28°N	73°W
							329	-59	N				
6.	Satyavedu sandstone	90-120	13° 30′	80°	1	13	321	-58	N	4°	33°S	26°N	67°W
7A	Sylhet traps	155-170	25°	91°	-	80	332	-59	N	7°	35° 30′S	16°N	60°W
7B	Sylhet traps	155-170	25°	91°	-	20	243	-60	N	16°			
8.	Rajmahal traps	155-170	25°	87° 51′		120	323	-64	N	4°	44°S	13°N	69°W
9.	Rajmahendari traps												
9A	Rajmahendari traps	155-170	17°	81° 46′	-	30	310	-53	N				
9B	Rajmahendari traps	155-170	17°	81° 46′	1	11	305	-45	N				
9C	Rajmahendari traps	155-170	17°	81° 46′	1	9	305	-44	N				

9.	Mean Rajmahendari traps					50	307	-47	N	4°	25°S	22°N	48°W
10.	Dykes from Palamau Satpura and Surguja												
10A		155-170	23°	83°	6	81	158	+52	R				
10B		155-170	23°	83°	4	59	338	-33	N				
11.	Parsora sandstone	215-230	23° 26′	81° 06′	2	113	318	-40	N	2.5°	23°S	28°N	54°W
12.	Kamthi sandstone												
12A	Jaipuram	245-260	18° 52′	79° 35′	1	55	303	-44	N				
12B	Jaipuram	245-260	18° 52′	79° 35′	1	87	306	-53	N				
12C	Rallapet	245-260	19° 7′	79° 30′	1	65	309	-47	N				
12.	Mean Kamthi sandstone				3	207	306	-50	N	2°	29°S	18°N	53°W
13.	Himgir sandstone	245-260	22°	84°	1	31	332	-44	N	6°	22°S	30°N	58°W
14.	Vindhyan sandstone												
14A	Upper Vindhyan sandstone	540-580	24° 37′	83° 6′	1	143	0	+30	N	6°	13°S	82°N	103°W
14B	Upper Vindhyan sandstone	540-580	24° 37′	83° 6′	1	38	186	-30	R	7°			
15.	Malani Rhyolites	580-735	26°	73°	9	170	353	+56	N	10°	31°S	78°E	45°W
16.	Mundawara complex, basic rocks	650-850	25°	73°	1	25	329	-24	N	21°			
17.	Banded Hematite quartzites, Porkhra	750-950	24°	81°	1	5	270	-12	N	7°	9° 30′S	2°N	3°W
18.	Banded Hematite Jasper, Parkhuri	750-950	24°	81°	1	5	289	-9	N	7°	7°S	15°N	25°W
19.	Bijiwar traps, Gwalior	750-950	26°	78°	11	25	70	+3	R	18°			
20.	Veldurthi Hematite	900-1200	15° 36′	78°	4	170	133	-37	R	14°	24° 30′N	45°N	3°W
21A	Chitloor dyke	1100-1200	14° 36′	79°	1	3	146	+11	R	19°			
21B	Chitloor dyke	1100-1200	14° 36′	79°	1	3	296	-32	N	3°	14°S	20°N	36°W
21C	Chitloor dyke	1100-1200	14° 36′	79°	1	3	264	-29	N	4°	9° 30′N	9°N	25°W
22A	Cuddapah shales	1400-1600	15°	78°	1	5	295	-10	N	5°	2°S	23°N	23°W
22B	Cuddapah sandstone	1400-1600	15°	78°	1	24	294	-6	N	8°		22°N	20°W
23.	Hyderabad dyke		17° 23′	78° 28′	1	26	44	-3	N	5°	3°S	43°N	173°W

APPENDIX 7.3

Palaeo-, Rock- and Environmental Magnetic Parameters

HYSTERESIS PARAMETERS

Instrumentation: Molspin Vibrating Sample Magnetometer (VSM); Princeton Measurements Alternating Gradient Force Magnetometer (AGFM)

Saturation Magnetization M_s [mAm^2kg^{-1}]	Maximum induced magnetization at 1T and is calculated by extrapolating the high field magnetization curve to the y-axis
Saturation Remanent Magnetization M_{rs} [$mAm^2\ kg^{-1}$]	Magnetization retained even after complete removal of magnetic field following magnetization at 1T and in theory the same as SIRM on the Molspin spinner
Coercive Force, H_c [mT]	The backfield that makes magnetization zero
Coercivity of Remanence, H_{cr} [mT]	Measured as larger backfield strength required than H_c to return M_{rs} to zero
Reverse low field (χ_{low}) or initial magnetic susceptibility χ_{in} [$10^{-6}\ m^3kg^{-1}$]	The slope of magnetization curve at the origin of a hysteresis loop within a small magnetic field and is reversible, i.e. no remanence is induced
High field susceptibility χ_{hf} [$10^{-6}\ m^3kg^{-1}$]	Measured as the high-field slope of a hysteresis curve between 800 mT and 1 T. χ_{hf} refers to paramagnetic susceptibility χ_{para} and is used to calculate the ferrimagnetic component χ_{ferri} in the total magnetic susceptibility χ_{total}

MAGNETIC SUSCEPTIBILITY

Instrumentation: MS2 Bartington Susceptibility Meter and Dual Frequency Sensor (noise level $3 \times 10^{-9}\ m^3kg^{-1}$); Agico KLY-2 Kappabridge (noise level $2 \times 10^{-10}\ m^3kg^{-1}$)

Volume Susceptibility κ [dimensionless]	Defined as $\kappa = M/H$, M being volume magnetization induced to intensity of magnetizing field H
Specific susceptibility, χ [$m^3\ kg^{-1}$]	Measured as the ratio of volume susceptibility to density $\chi=\kappa/\rho$

Frequency dependent of susceptibility χ_{fd} [percentage or $m^3\ kg^{-1}$]	Variation in χ between low (0.47 kHz) and high frequencies (4.7 kHz). χ_{fd} indicates viscous grains at the superparamagnetic/stable single-domain boundary

MAGNETIC REMANENCE

Instrumentation: Molspin Spinner Magnetometer (noise level 0.1 × $10^{-5}Am^2kg^{-1}$); Agico JR-6 Spinner Magnetometer; 2G-Enterprises SQUID Magnetometer (for 10 g samples, noise level 3 × $10^{-9}Am^2kg^{-1}$); Magnetic Measurements MMPM9 Pulse magnetizer, Molspin Pulse Magnetizer

Natural Remanent Magnetization NRM [mAm^2kg^{-1}]	Acquired in the Earth's magnetic field either by cooling of a mineral through its Curie (blocking) point, crystal growth through the blocking volume or deposition and 'fixing' of detrital particles
Viscous (time-related) remanent magnetization,VRM [mAm^2kg^{-1}]	Acquired on exposure to a new magnetic field and is time-dependent magnetization unrelated to Earth's magnetic field
Anhysteretic remanent magnetization ARM [$10^{-5}Am^2kg^{-1}$]	An ideal magnetic remanence for being free from hysteresis and is imparted in a peak 100 mT AF that smoothly decreased to zero in a small DC field's presence. ARM allows estimation of concentration and presence of finer ferrimagnetic minerals. For example, SSD particles have high ARM intensities per unit mass compared to MD particles
Susceptibility of ARM, χ_{ARM}[m^3kg^{-1}]	Normalized ARM for the strength of the steady field
Isothermal remanent magnetization IRMs [$10^{-5}\ Am^2kg^{-1}$]	Acquired in different DC forward and back fields (10 mT to 2 T or even up to 9 T) at a given temperature, commonly at room temperature
Saturation isothermal remanent magnetization SIRM [$10^{-5}Am^2kg^{-1}$]	Measured as the highest volume of magnetic remanence that can be produced in a sample by application of a very high field (usually >1 T). SIRM relates to both mineral type and concentration
'Soft' IRM, IRM_s [Units are same as for SIRM]	Remanent magnetization after a magnetization either in a relatively low forward field of 20 mT, 30 mT, 40 mT or 50 mT or reverse fields 'back IRMs'
'Hard' IRM, IRM_h [Units are same as for SIRM]	Difference between SIRM and IRM measured after magnetization in a field of 300 mT or difference between SIRM and IRMs in a reverse field of 300 mT, i.e. HIRM = SIRM-IRM_{-300mT}

(*Contd.*)

Palaeo-, rock- and environmental magnetic parameters (*Contd.*)

USEFUL PERCENTAGES AND QUOTIENTS (RATIOS): INTERPRETATION OF RESULTS	
χ_{fd}[%]	~10% or 5-10% would indicate a large fine viscous (magnetite) component of SP range
SIRM/χ	Useful to distinguish between different types of magnetic behaviour. For example, if both χ and SIRM are low, but SIRM/χ is relatively high, there may be a large amount of hematite. If χ is positive but there is little or no remanence, then the magnetic minerals in the sample will probably be mostly paramagnetic minerals
SIRM/χ; ARM/χ & ARM/SIRM	High SIRM/χ, ARM/χ and ARM/SIRM values denote significant SSD (magnetite) grains
ARM/SIRM	Low ARM/SIRM values indicate a large MD (magnetite) component
Backfield IRM/SIRM or S-ratio;	S-ratio defined here as $IRM_{-0.3T}$/SIRM recognizes samples with hematite to magnetite proportions
High field remanence HIRM	because ferrimagnets are expected to saturate in fields below 0.1 T. Larger high field remanences, HIRM are due to proportionally high imperfect antiferromagnetic components such as hematite and goethite
M_{rs}/M_s ratio	Indicator of magnetization state of a sample; ratio values of 0.5 represent SSD grains; less than 0.1 for MD and still lesser values for SP grains.
H_{cr}/H_c ratio	Provides magnetization state of a sample; uniaxial SSD grains have ratio of 1.09, MD grains around 4.0 and SP grains in excess of 10.0